UNIVERSIDADE ESTADUAL PAULISTA

"Júlio de Mesquita Filho"

INSTITUTO DE BIOCIÊNCIAS DE BOTUCATU

IDENTIDADE MOLECULAR DE BIOMATERIAIS APLICADOS EM ODONTOLOGIA

Fábio José Barbosa Bezerra

Tese apresentada ao Instituto de Biociências, *Campus* de Botucatu, UNESP, para obtenção do título de Doutor pelo Programa de Pós-Graduação em Biotecnologia.

Willian Fernando Zambuzzi

BOTUCATU – SP

2018

UNIVERSIDADE ESTADUAL PAULISTA

"Júlio de Mesquita Filho"

INSTITUTO DE BIOCIÊNCIAS DE BOTUCATU

IDENTIDADE MOLECULAR DE BIOMATERIAIS APLICADOS EM ODONTOLOGIA

Fábio José Barbosa Bezerra

Tese apresentada ao Instituto de Biociências, *Campus* de Botucatu, UNESP, para obtenção do título de Doutor pelo Programa de Pós-Graduação em Biotecnologia.

Willian Fernando Zambuzzi

BOTUCATU – SP
2018

FICHA CATALOGRÁFICA ELABORADA PELA SEÇÃO TÉC. AQUIS. TRATAMENTO DA INFORM.
DIVISÃO TÉCNICA DE BIBLIOTECA E DOCUMENTAÇÃO - CÂMPUS DE BOTUCATU - UNESP
BIBLIOTECÁRIA RESPONSÁVEL: ROSANGELA APARECIDA LOBO-CRB 8/7500

Bezerra, Fábio José Barbosa.
Identidade molecular de biomateriais aplicados em odontologia / Fábio José Barbosa Bezerra. - Botucatu, 2018

Tese (doutorado) - Universidade Estadual Paulista "Júlio de Mesquita Filho", Instituto de Biociências de Botucatu
Orientador: Willian Fernando Zambuzzi
Capes: 90300009

1. Biotecnologia. 2. Nanotecnologia. 3. Durapatita. 4. Implantes artificiais. 5. Transdução de sinais.

Palavras-chave: Biotecnologia; Hidroxiapatita; Implantes; Nanotecnologia; Transdução de Sinal.

Agradecimentos

Ao Instituto de Biociências de Botucatu – UNESP, seu corpo doscente e funcionários pela oportunidade de aprender em um ambiente de excelência acadêmica e científica, composto por pessoas com ideais educacionais exemplares;

Ao Coordenador e Professores do Curso de Doutorado em Biotecnologia do IBB – UNESP, que através do seu conhecimento, paixão pelo ensino e simplicidade, nos apresentaram novos caminhos e possibilidades, renovando o eterno desafio e a beleza do aprendizado constante;

Ao **LaBIO** – Laboratório de Bioensaios e Dinâmica Celular – e meus colegas de pós-graduação: Célio Fernandes, Marcel Ferreira, Denise Andia, Nilson Cruz, Rodrigo Silva, Amanda Andrade, Thais Pinto, Maiara do Carmos, Georgia Feltran, Mariana Rossi, Pedro Padilha e Anderson Gomes. Muito obrigado pela amizade, parceria e competência. Desejo sucesso pleno em suas carreiras!

A S.I.N. Sistema de Implantes, pela doação das amostras utilizadas em nossas pesquisas;

Ao meu Orientador, Prof. Dr. Willian Fernando Zambuzzi, por seu conhecimento ímpar, brilhantismo e simplicidade grandiosa. Vim em busca de um método, encontrei um amigo e com esta tese concretizo um grande sonho. Sem palavras para lhe agradecer!

A minha esposa Ana Paula e filhos, Lucas e Maria Clara, por serem a razão, o exemplo e a síntese do amor que me impulsiona a cada dia.

À FAPESP (2014/22689-3).

A DEUS – por tudo!

Resumo

Diferentes biomateriais são sugeridos como alternativas biomédicas, porém pouco se sabe sobre os mecanismos moleculares envolvidos com sua interface com as células do hospedeiro. Uma vez que as vias de sinalização intracelular são preditivos da qualidade da interação entre a célula e a superfície do biomaterial, este estudo avaliou o comportamento de células pré-osteoblásticas em resposta a variações nano topográficas na superfície de titânio, ligas de Cobalto-cromo (CoCr) e zircônia (ZrO_2), explorando mecanismos metabólicos desencadeados por cadeias de fosforilação em cascata e correlacionando-os à variações morfológicas destas células durante eventos de adesão e diferenciação celulares. Em relação ao titânio, mostramos que a superfície modificada com nano-hidroxiapatita (nHA) desempenhou melhor resultado quanto ao espraiamento celular e posteriormente diferenciação, demonstrando que esta superfície promove uma rede de sinalização intracelular necessária para a adaptação celular sobre superfícies de Ti. Em relação aos mecanismos moleculares que regem a resposta ao CoCr, mostramos que este afeta diferencialmente fibroblastos e osteoblastos, mostrando ativação diferencial do gene integrina ß1 e proteínas como FAK, Src, Rac e Cofilina, além de níveis diferenciais de fosforilação de CDK2, Mapk-Erk e Mapk-p38. Posteriormente, mostramos que modulações importantes foram desencadeadas pela Zircônia. Durante os mecanismos de adesão celular, houve uma significante diminuição na atividade de PP2A, garantindo níveis elevados de fosforilação de Mapk-p38. Além disso, mostramos que a zircônia estabelece mecanismo importante de reprogramação de genes envolvidos com o rearranjo da matriz extracelular (ECM), modulando genes como a matriz metaloproteinases (MMPs) e seus inibidores teciduais (TIMPs e RECK). Em síntese, esta tese traz um repertório importante dos mecanismos de transdução de sinais disparados por osteoblastos e, eventualmente, fibroblastos, além da reprogramação gênica envolvida neste processo. De um modo geral, nosso trabalho traz com detalhes mecanismos metabólicos envolvidos com o fenótipo de osteoblastos em resposta a diferentes materiais aplicados em odontologia, buscando enriquecer a identidade molecular destes biomateriais.

Unitermos: Biotecnologia; Nanotecnologia; Hidroxiapatita; Cobalto; Cromo; Zircônia; Implantes, Osteoblastos, Adesão, Transdução de Sinal.

ABSTRACT

Several biomaterials are suggested as biomedical alternatives, but little is known about the molecular mechanisms involved with their interface with the host cells. Since intracellular signaling pathways are proposed to predict the quality of cell-surface relationship, this study addressed pre-osteoblast behavior in response to topographic variations in the titanium (Ti) surface, Cobalt-chromium alloys (CoCr) and Zirconia (ZrO_2), exploring the metabolic mechanisms related to the phosphorylation cascade and correlating with cell morphological changes related with adhesion and differentiation events. In relation to titanium, the surfaces modified by the nano-hidroxiapatite (nHA) showed better results for cell spreading and later differentiation when compared to the other groups, demonstrating that this surface promotes an intra-cellular signaling pathway necessary to the cell-surface adaptation. Regarding the molecular mechanisms involved in the CoCr responses, we have shown that it affects fibroblasts and osteoblasts in different ways related to the gene integrin ß1 and proteins such as FAK, Src, Rac and Coffilin, as well as, different levels of CDK2, Mapk-Erk and Mapk-p38 phosphorilation. Lately, our results showed important modulations up-regulated by Zirconia. During the mechanisms of cellular adhesion there was a significant minimization in the PP2A activity, garanteeing high levels of Mapk-p38 phosphorilation. Beyond that, we showed that the zirconia stablishes an important mechanism to reprograme the genes involved in the extracellular matrix (ECM) new arrangement, modulating genes such as the metalloproteases matrix (MMPs) and its tissue inhibitors (TIMPs and RECK). In general, this thesis brings a repertory of important signal transduction mechanisms up-regulated by osteoblasts and eventually fibroblasts, as well as, the gene reprogramming related to this process. Altogether our results describes in details the metabolic mechanisms involved in the osteoblasts phenotype in response to different biomaterials used in dentistry.

Key words: Biotechnology; Nanotechnology; Hydroxyapatite; Cobalt; Chromium; Zirconia; Implants; Osteoblasts; Adhesion; Signal Transduction.

SUMÁRIO

LISTA DE FIGURAS

Capítulo 1:

Capítulo 2:

Capítulo 3:

Capítulo 4:

Capítulo 5:

LISTA DE TABELAS

Capítulo 2:

Capítulo 3:

Capítulo 5:

LISTA DE ABREVIAÇÕES

AFM – Atomic Force Microscopy
AKT – Protein Kinase B
ALP – Alkaline Phosphatase
Bax – Apoptosis Regulator
Bcl2 – Apoptosis Regulator
CDK2 – Cyclin Dependent Kinase 2
cDNA – Complementary DNA
Co – Cobalt
Cr – Chromium
DAE – Dual Acid Etched
ECL - Enhanced ChemiLuminescence
ECM – Extracellular Matrix
EDX – Energy Dispersive X-Ray
Erk – Extracellular Signal-Regulated Kinase
FAK – Focal Adhesion Kinase
FBS – Fetal Bovine Serum
GADPH – Glyceraldehyde 3-phosphate dhydrogenase
GFAAS - Graphite Furnace Atomic Absorption Spectrometry
HA – Hidroxiapatite
IL – Interleucin
JNK – C-Jun N-terminal Kinase
Mac – Machined (for implants surfaces)
MAPK – Mitogen-Activated Protein Kinase
MMP – Matrix Metalloproteinase
nHA – hidroxiapatite-blasted surface
OCN – Osteocalcin
OPN – Osteopontin
OTX – Osterix
PKB – Protein Kinase B
pNPP – *p*-Nitrophenyl Phosphate
PP1 - 1-(1,1-dimethylethyl)-3-(4-methylphenyl)-1H-pyrazolo[3,4-d]pyrimidin-4-amine
PP2A – Protein Phosphatase 2A
Pre-Ob – pre-Osteoblasts
PTP – Protein Tyrosine Phosphatase
PVDF – Polyvinylidene difluoride
qPCR – Quantitative polymerase chain reaction
RECK – Reversion-Inducing- Cysteine-Rich Protein with Kazal Motifis
ROS – Reactive Oxygen Scpecies
RUNX2 – Runt-Related Transcription Factor 2
SDS PAGE – Sodium Sodecyl Sulfate Polyacrylamide Gel Electrophoresis

SEM – Scanning Electron Microscopy
Ser/Thr – Serine/Threonine
Src – Proto-oncogene tyrosine-protein kinase - similar to the v-Src gene of Rous sarcoma virus
TBS - Tris-buffered saline
Ti – Titanium
TIMP - Tissue Inhibitor of Matrix Metalloproteinases
TNFα – Tumor Necrosis Factor Alpha
v/v – volume / volume
w/v – weight / volume
wDAE – With Dual Acid Etched
woDAE – Without Dual Acid Etched
ZrO_2 – Zirconia
αMEM – Alpha Minimum Essential Media

Capítulo 1

INTRODUÇÃO

Nas últimas décadas, os implantes osseointegráveis têm sido amplamente utilizados em Odontologia para restaurar o edentulismo total, parcial ou unitário (Sohrabi et al., 2012), impactando na qualidade de vida de um número crescente de pacientes em todos os continentes. Embora a pesquisa sobre macro-geometrias, materiais e técnicas de implantes dentários tenha aumentado nos últimos anos e espera-se expandir no futuro, ainda há muito trabalho envolvido no uso de melhores biomateriais, geometrias de implantes, modificação e funcionalização de superfícies para melhorar os resultados a longo prazo do tratamento (revisado em Gaviria et al , 2014), sobretudo nos casos com maior risco de tratamento, como os casos complexos, pacientes com alterações sistêmicas e com potencial de resposta cicatricial comprometia. Para aumentar a taxa de sucesso dos implantes dentários, pesquisas tem focado no melhor conhecimento e controle das propriedades da superfície, como topografia, rugosidade e nano-ativação, assim como a resposta gerada pela interação do biomaterial com o meio em nível molecular e celular (Martinez et al., 2017; Rossi et al., 2017, Fernandes et al., 2017).

Especificamente, os recursos em nível micrométrico são incluídos para melhorar a Osseointegração ou contato direto do osso ao implante (Di Liddo et al., 2014; Salou et al., 2015), sendo que superfícies moderadamente rugosas (1,0 a 2,0 micrômetros) têm demonstrado resultados cicatriciais superiores quando comparadas as superfícies minimamente rugosas (0,5 a 1,0 micrômetros) ou rugosas (superior a 2,0 micrômetros) (Wennerberg A e Abrektsson T. 2009; Rosa et al., 2013). A nanotopografia sugere ser muito importante para os estágios iniciais do processo de Osseointegração, regulando os mecanismos de forforilação e adsorção proteica (Zambuzzi et al., 2014; Bezerra et al., 2017) além de aumentar a neoformação óssea in vivo (Barkarmo et al., 2014b). Ademais, sabe-se que as superfícies nanotexturizadas não só melhoram a formação óssea, mas também fortalecem as suas propriedades biomecânicas (Jimbo et al., 2012).

Dentre os desafios encontrados na área da Osseointegração aplicada a Odontologia podem ser destacados os tratamentos de alta complexidade, onde usualmente há maior risco para o sucesso do tratamento devido a resposta cicatricial comprometida do hospedeiro, quer seja por limitações sistêmicas ou locais (Agarwal R, Garcia A. 2015). De acordo com este cenário, promover estímulos positivos para aprimorar a resposta cicatricial óssea é vital para o sucesso do tratamento, sendo que o conhecimento aprofundado da resposta biológica circundante ao material implantado é fundamental, uma vez que a superfície é o primeiro componente a interagir com o hospedeiro (Gemini-Piperni et al., 2014a; Gemini-Piperni et al., 2014b; Henkel et al., 2013).

O processo de Osseoitegração usualmente é avaliado por seu resultado clínico que acontece em fase cicatricial tardia, sendo que a mineralização óssea é precedida por uma cadeia de eventos moleculares, celulares e teciduais que impactarão de forma significativa na previsibilidade e qualidade da resposta do meio ao biomaterial implantado (Rosa et al., 2013). O primeiro passo nesta resposta aos implantes envolve a adsorção de proteínas específicas, lipídios, açúcar e íons, estabelecendo um revestimento orgânico responsável por orientar o desempenho celular circundante levando à ativação de genes específicos. Embora as estruturas nanométricas sejam fatores potenciais para a Osseointegração, as interações interfaciais detalhadas com células osteogênicas não foram totalmente abordadas.

Para entender essas interações, nosso grupo tem explorado a investigação de sinalização celular (Bertazzo et al., 2010a; Bertazzo et al., 2010b; Fernandes et al., 2014; Gemini-Piperni et al., 2014a; Zambuzzi et al., 2011a; Zambuzzi et al., 2011b; Zambuzzi et al., 2012, Rossi et al., 2017, Fernandes et al., 2017), concentrando-nos na investigação do mecanismo molecular que regula a adesão de osteoblastos em diferentes superfícies de biomateriais para estabelecer um mapa de sinalização de proteínas capaz de orientar o desenvolvimento de novos materiais biomédicos, como a sinalização de Erk MAPK e o envolvimento FAK/Src. A sinalização Erk MAPK desempenha papéis críticos no desenvolvimento esquelético (Hu et al., 2015; Jiang et al., 2015), sendo seu eixo Ras / Raf / Mek / Erk ativado por vários estímulos em células eucarióticas, transduzindo sinais extracelulares para o interior das células e coordenando respostas celulares

específicas (Asati et al., 2016). Além disso, as ativações de *Focal Adhesion Kinase* (FAK) e Src estão envolvidas na sinalização celular após a ativação da integrina e são sugeridas como biomarcadores da interface célula/biomaterial (**Figura 1**).

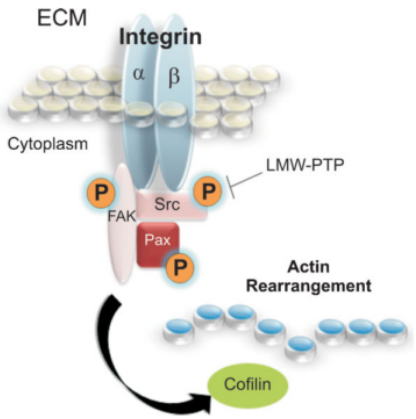

Figura 1 - Mecanismos intracelulares decorrentes da adesão celular. Integrinas ligam o meio extracelular com o citoesqueleto da célula. Após captar sinais extracelulares as integrinas mobilizaram móleculas de sinalização para o ponto de adesão focal. O balanço da fosforilação de FAK, Src e paxilina e, ao final desta cascata, a cofilina levara um sinal intracelular que será responsavel pelo rearranjo dos filamentos de actina. Estas alterações do citoesqueleto são responsáveis por adaptações celulares a superfícies diferentes. Fonte: Zambuzzi et al., 2011.

Ainda em relação às pesquisas na área de desenvolvimento de biomaterias com aplicação medico-odontológicos e, somando-se a sua importância no cenário econômico e social da União, ainda faltam alternativas à pesquisa com animais que tragam respostas rápidas ao setor produtivo, sobretudo quanto aos aspectos que regem a biocompatibilidade desses materiais. Poucas são as metodologias de análise capazes de analisar e ranquear novos materiais a partir de ensaios *in vitro* ou *in silico*. Consequentemente, universidades e empresas recorrem, quase sempre, a testes convencionais fazendo uso de modelos animais, comprometendo avanços necessários nesta área. Uma vez que as vias de sinalização intracelular são capazes de prever a qualidade da interação celular, este estudo teve como objetivo avaliar o comportamento celular quando interagindo com diferentes superfícies nanoestruturadas de titânio, além de explorar estas interações com ligas de Cobalto-

Cromo (CoCr) e Zircônia, os quais estão apresentados nesta tese em Capítulos, incluídos a seguir.

CAPÍTULO 2

NANO HYDROXYAPATITE-BLASTED TITANIUM SURFACE AFFECTS PRE-OSTEOBLAST MORPHOLOGY BY MODULATING CRITICAL INTRACELLULAR PATHWAYS

Fábio BEZERRA[1], Marcel R. FERREIRA[1], Giselle N. Fontes[2], Célio Jr da Costa FERNANDES[1]; Denise C. Andia[3], Nilson C. Cruz[4], Rodrigo A. da SILVA[1]; Willian F. ZAMBUZZI[1,‡]

[1]Dept. of Chemistry and Biochemistry, Bioscience Institute, State University of São Paulo – UNESP, *campus* Botucatu, Botucatu, São Paulo, Brazil;
[2]Laboratory of Microscopy Applied to Life Science - LAMAV, Directory of Metrology Applied to Life Science - Dimav, National Institute of Metrology Quality and Technology - INMETRO, Duque de Caxias, RJ, Brazil
[3]Faculdade de Odontologia – Área de Pesquisa em Epigenética, Universidade Paulista, UNIP, São Paulo/SP, Brasil.
[4]Laboratório de Plasmas Tecnológicos; Instituto de Ciência e Tecnologia, Universidade Estadual Paulista, Sorocaba - SP; 18087-180,

Bezerra F, Ferreira MR, Fontes GN, da Costa Fernandes CJ, Andia DC, Cruz NC, da Silva RA, Zambuzzi WF. Nano hydroxyapatite-blasted titanium surface affects pre-osteoblast morphology by modulating critical intracellular pathways. **Biotechnol Bioeng.** 2017 Aug;114(8):1888-1898.

ABSTRACT

Since intracellular signalling pathways are proposed to predict the quality of cell-surface relationship, this study addressed pre-osteoblast behaviour in response to nano hydroxyapatite (HA)-blasted titanium (Ti) surface by exploring critical intracellular pathways and pre-osteoblast morphological change. Physicochemical properties were evaluated by atomic force microscopy and wettability considering water contact angle of three differently texturized Ti surfaces: Machined (Mac), Dual acid-etching (DAE) and nano hydroxyapatite-blasted (nHA). The results revealed critical differences in surface topography, impacting the water contact angle and later the osteoblast performance. In order to evaluate the effect of those topographical characteristics on biological responses, we have seeded pre-osteoblast cells on the Ti discs for up to 4 hours and subjected the cultures to biological analysis. Firstly, we have observed pre-osteoblasts morphological changes resulting from the interaction with the Ti texturized surfaces whereas the cells cultured on nHA presented a more advanced spreading process when compared with the cells cultured on the other surfaces. These results argued us for analysing the molecular machinery and thus, we have shown that nHA promoted a lower Bax/Bcl2 ratio, suggesting an interesting anti-apoptotic effect, maybe explained by the fact that HA is a natural element present in bone composition. Thereafter, we investigated the potential effect of those surfaces on promoting pre-osteoblast adhesion and survival signalling by performing crystal violet and immunoblotting approaches, respectively. Our results showed that nHA promoted a higher pre-osteoblast adhesion supported by up-modulating FAK and Src activations, both signalling transducers involved during eukaryotic cell adhesion. Also, we have shown Ras-Erk stimulation by the all evaluated surfaces. Finally, we showed that all Ti-texturing surfaces were able to promote osteoblast differentiation up to 10 days, when alkaline phosphatase (ALP) activity and osteogenic transcription factors were up-modulated. Altogether, our results showed for the first time that nano hydroxyapatite-blasted titanium surface promotes crucial intracellular signalling network responsible for cell adapting on the Ti-surface.

Key words: Biotechnology; Nanotechnology; Hydroxyapatite; Implants; Osteoblast; Adhesion; Signal Transduction.

INTRODUCTION

Over the last decades endosseous implants have been widely used for restoring edentulism (Sohrabi et al., 2012), impacting patients' quality of life. Although research on dental implant designs, materials and techniques has increased in the past few years and is expected to expand in the future, there is still a lot of work involved in the use of better biomaterials, implant design, surface modification and functionalization of surfaces to improve the long-term outcomes of the treatment (reviewed in Gaviria et al , 2014). In order to increase the success rate of dental implants, research has been focused on the control of surface properties such as topography and roughness. Specifically, micro-level features are included to impart osseointegration or direct bone to implant contact at the micro level (Di Liddo et al., 2014; Salou et al., 2015). Nanotopography has been suggested decisive for early osseointegration (Zambuzzi et al., 2014), which enhance new bone formation in vivo (Barkarmo et al., 2014b). In addition, it is known that nanotextured surfaces not only enhance bone formation but also strengthen biomechanical properties (Jimbo et al., 2012).

Surrounding biological response to implanted material is mediated by the interaction of the implant through its surface and in order to further improve the treatment success, modifications on implants surfaces have been extensively proposed since it is the first component to interact with the host (Gemini-Piperni et al., 2014a; Gemini-Piperni et al., 2014b; Henkel et al., 2013). The first step in this response to implants involves the adsorption of specific proteins, lipids, sugar, and ions, establishing an organic coating responsible to guide surrounding cell performance leading to activation of specific genes. Although nanoscaled structures are enhancing factors for osseointegration, the detailed interfacial interactions with osteogenic cells have not been fully addressed. In order to understand such interactions, we have explored cell signalling investigation (Bertazzo et al., 2010a; Bertazzo et al., 2010b; Fernandes et al., 2014; Gemini-Piperni et al., 2014a; Zambuzzi et al., 2011a; Zambuzzi et al., 2011b; Zambuzzi et al., 2012).

In this work, we focused on investigating the molecular mechanism governing osteoblast adhesion on different biotechnologically modified surfaces in order to establish a map of signalling proteins able to guide the development of novel biomedical materials, such as Erk MAPK signalling and FAK/Src involvement. Erk MAPK

signalling plays critical roles in skeletal development (Hu et al., 2015; Jiang et al., 2015). Ras/Raf/Mek/Erk axis signaling is activated by various stimuli in eukaryotic cells, transduces extracellular signals into cells and coordinates cellular responses (Asati et al., 2016). In addition, Focal Adhesion Kinase (FAK) and Src activations are involved in the cell signalling upon the integrin activation and have been suggested as biomarkers of cell-biomaterial interface (Bergeron et al., 2016; Cavagis et al., 2014; Zambuzzi et al., 2014).

Since intracellular signalling pathways are able to predict the quality of cell interaction, this study aimed to evaluate the pre-osteoblast behaviour on nano hydroxyapatite-blasted titanium surface by exploring critical intracellular signal pathways. Briefly, our results showed for the first time that nano hydroxyapatite-blasted titanium surface promotes a better nano-environment for cell adapting by up-regulating crucial intracellular signalling network.

MATERIAL AND METHODS

Materials

Three different titanium surfaces (discs) were evaluated in this study: Machined (Mac; control), Dual Acid-Etched (DEA), and acid-etched nanoHA-blasted (nHA). All materials were sterilized by exposure to Gamma irradiation and donated by S.I.N. – Sistema Nacional de Implantes (São Paulo, SP, Brazil). HA nanocrystalline synthesis and titanium modification: samples were surface modified with hydroxyapatite (HA) using the Promimic HAnano-method, a detailed description can be found elsewhere (Gottlander et al., 1997; Meirelles et al., 2008). Briefly, the samples were dipped into a stable particle suspension containing 10 nm in diameter HA particles followed by a heat treatment at 550 ^{o}C for 5 min in nitrogen atmosphere. The surfactant-mediated process allows better control of the chemical composition of the coating (Meirelles et al., 2008). Antibodies: Phospho-MEK1/2 (Ser221) (166F8) Rabbit mAb #2338; Phospho-p44/42 MAPK (Erk1/2) (Thr202/Tyr204) Antibody #9101; Phospho-FAK (Tyr397) (D20B1) Rabbit mAb #8556; Phospho-Src Family (Tyr416) (D49G4) Rabbit mAb #6943; Bax (D3R2M) Rabbit mAb (Rodent Preferred) #14796; BCL2L10 Antibody #3869; β-Actin (8H10D10) Mouse mAb #3700 were purchased from Cell Signaling Technology, Inc. (MA, USA).

Surface's characterization of the materials

Atomic force microscopy (AFM)

AFM analyses were performed in order to probe Ti-modified surfaces. In this technique, the AFM tip acts as a "nano profilometer", being able to generate information on the micro and nano dimensional aspects of the surface (x, y and z axis). Images were acquired via the equipment Bioscope Catalyst (Bruker Coorp), and AFM cantilevers also from Bruker ("RTESPA", k = 20 to 80 N/m) were used. The equipment worked under intermittent contact mode and images were taken from 3 different samples (Machined, Double-Acid Etching and nano Hydroxyapatite) and 3 different regions on each sample (border, middle and opposite border). Scans of 3.3 x 3.3 μm^2 were taken to check homogeneity.

Water contact angle

An automated goniometer (Ramé Hart, 100-00) has been used to evaluate water wettability and free surface energy through contact angle measurements. Deionized water and diiodomethane have been used as probe liquids and the presented results correspond to the average of 10 measurements.

Cell culture and cytotoxicity assay

MC3T3-E1 (subclone 4), mouse pre-osteoblastic cells, was used in this study. Cells were cultured in alfa-MEM supplemented with 10% of fetal bovine serum (FBS) at 37°C and 5% CO_2. Sub-confluent passages were tripsinized and used in all experiments. For cell viability assay, sterile titanium discs with different texturized surfaces were transferred to Petri dishes containing culture media (α-MEM). After 24 h incubation at 37°C, conditioned medium was collected and tested for cell viability profile. $50x10^4$ cells/mL was seeded in 96-well dish plates and after 24 hours at sub-confluent stage they were incubated for 24 h with those conditioned medium (n=6). An internal control was assayed by keeping the cells exposed solely to conventional culture medium (control). After 24 h, cell viability was evaluated by using MTT assay (Mossman, 1983), a

colorimetric method (Synergy II; BioTek Instruments, USA). The concentration of Formazan directly indicated the viability of cells.

Cell adhesion assay

Pre-osteoblast cells were treated with conditioned medium for 24 hours. Thereafter, the cells were trypsinized, counted and then re-seeded at 5×10^4 cells/mL in 24-well culture plates for 4 h. Briefly, adherent cells were rinsed in warm PBS and fixed in absolute ethanol-glacial acetic acid (3:1; v/v) for 10 min at room temperature and air-dried. The adherent cells were stained with 0.1% crystal violet (w/v) for 10 min at room temperature. Excess dye was removed by decantation and washed twice with distilled water. The dye was extracted with 10% acetic acid (v/v), and the optical density measured at 550 nm using a microplate reader (Biotek Co., Winooski, VT). Data from each experiment were analysed with six observations in each group.

Scanning Electron Microscopy (SEM)

Pre-osteoblasts were seeded on different titanium surfaces at the density of 5×10^4 cells/disc. After 4 h, cells were fixed with 2.5% of glutaraldehyde in 0.1 M phosphate buffer pH 7.3 for 24 h. They were immersed in osmium tetroxide 0.5% for 40 minutes, dehydrated through a series of alcohols, dried at critical point, and finally metallized. Samples were studied using a Quanta 200 - FEI Company scanning electron microscope at an accelerating voltage of 12.5 kV. EDX analyses were performed with 20 kV to evaluate the x-ray characteristics of Ca and Ti in the samples.

Immunoblotting

Cells were directly cultured on different texturized titanium surfaces and after 4 hours they were lysated [Lysis Cocktail (50 mM Tris [tris(hydroxymethyl)aminomethane]–HCl [pH 7.4], 1% Tween 20, 0.25% sodium deoxycholate, 150 mM NaCl, 1 mM EGTA (ethylene glycol tetraacetic acid), 1 mM *O*-Vanadate, 1 mM NaF, and protease inhibitors [1 µg/mL aprotinin, 10 µg/mL leupeptin, and 1 mM 4-(2-amino-ethyl)-benzolsulfonyl-fluorid-hydrochloride])] for 2 h on ice in order to obtain protein extracts. After clearing by centrifugation, the protein concentration was determined using Lowry method. An equal volume of 2x sodium dodecyl sulfate (SDS) gel loading buffer (100 mM Tris-HCl

[pH 6.8], 200mM dithiothreitol [DTT], 4% SDS, 0.1% bromophenol blue, and 20% glycerol) was added to samples and boiled for 5 minutes. Proteins extracts were resolved by SDS-PAGE (10 or 12%) and transferred to PVDF membranes (Bio-Rad, Hercules, CA, USA). Membranes were blocked with either 1% fat-free dried milk or bovine serum albumin (2.5%) in Tris-buffered saline (TBS)–Tween 20 (0.05%) and incubated overnight at 4° C with appropriate primary antibody at 1:1000 dilutions. After washing in TBS-Tween 20 (0.05%), membranes were incubated with horseradish peroxidase-conjugated anti-rabbit, anti-goat or anti-mouse IgGs antibodies, at 1:2000 dilutions, in blocking buffer for 1 hour. Thereafter, for detecting the bands we have used enhance chemiluminescence (ECL).

Quantitative PCR assay (qPCR)

Total RNA was extracted from cells with Ambion TRIzol Reagent (Life Sciences - Fisher Scientific Inc, Walthan, MA, USA) and treated with DNase I (Invitrogen, Carlsband, CA, USA). cDNA synthesis was performed with High Capacity cDNA Reverse Transcription Kit (Applied Biosystems, Foster City, CA) according to the manufacturer's instructions. qPCR was carried out in a total of 10 µl, containing PowerUp™ SYBR™ Green Master Mix 2x (5 µl) (Applied Biosystems, Foster City, CA), 0,4 µM of each primer, 50 ng of cDNA and nuclease free H_2O. Results were expressed as relative amounts of the target gene using β-actin as inner reference gene, using the cycle threshold (Ct) method. Primers and details are described in **Table 1**.

Alkaline phosphatase (ALP) activity

MC3T3-E1 pre-osteoblastic cells in suspension (75×10^3 cells/mL) were seeded in 6-wells dish plate (polystyrene group) or Ti-discs (test's groups) until 85–90% of confluence. Thereafter, the cells were stimulated to differentiate by remaining then under differentiation medium containing ascorbic acid (50 µg/mL) and β-glycerophosphate (10 mM) during 10 days. Thereafter, the adherent cells were rinsed with ice-cold PBS and incubated for 30 minutes at room temperature with ALP assay buffer (100 mM of Tris-HCl, pH 9.0, 1 mM of $MgCl_2$) containing 1% Triton X-100. The cell extracts were removed from dishes, centrifuged, and used for the enzyme assay. The ALP activity was determined using 5 mM of pNPP as substrate. One unit of enzyme activity was defined

as the amount of enzyme that converted 1 µmol of substrate to product per minute. Protein concentrations were determined by the Lowry method.

Table 1. Expression primers sequences and PCR cycle conditions.

Gene	Primer	5'-3' Sequence	Reactions Condicition
RUNX2	Forward Reverse	GGA CGA GGC AAG AGT TTC A TGG TGC AGA GTT CAG GGA G	95°C - 3s; 55°C - 8s; 72°C - 20s
Osteocalcin (OCN)	Forward Reverse	AGA CTC CGG CGC TAC CTT CTC GTC ACA AGC AGG GTT AAG	95°C - 3s; 55°C - 8s; 72°C - 20s
Osterix (OTX)	Forward Reverse	CCC TTC CCT CAC TCA TTT CC CAA CCG CCT TGG GCT TAT	95°C - 5s; 56°C - 10s; 72°C - 15s
b-actin	Forward Reverse	TCT TGG GTA TGG AAT CCT GTG AGG TCT TTA CGG ATG TCA ACG	95°C - 3s; 55°C - 8s; 72°C - 20s

Statistical analysis

Mean values and standard deviation obtained for each test were calculated, and one-way ANOVA was performed (alpha error type set to 0.05) when adequate, with Bonferroni corrected post-test, or non-parametric analysis, using GraphPad Prysm 5 (GraphPad Software, USA).

RESULTS

Firstly, the surfaces were subjected to methodologies for evaluating surface properties. Atomic force micrographs showed that there is a significant difference among the titanium-texturized surfaces evaluated in this study. The nano-scaled topography promoted by blasting HA on the surfaces was confirmed by AFM (**Fig.1**). In addition, the topography modifications influenced the total surface energy and they were decisive to wettability, significantly impacting water contact angle (**Table 2**).

Table 2. Wettability and Energy characteristics

	Angle				
	Water	**Diiodomethane**	**Total Surface Energy**	**Polar Component**	**Dispersive Component**
Mac	81.41 ± 0.01	41.21 ± 0.01	47.53 ± 0.01	7.92 ± 0.00	39.60 ± 0.00
DAE	97.18 ± 0.01	52.84 ± 0.00	36.79 ±	2.78 ±	34.01 ±
nHA	40.95 ± 0.02	39.51 ± 0.01	67.70 ± 0.01	27.32 ± 0.01	40.38 ± 0.00

Mac: Machined; DAE: double-acid etching; nHA: nano hydroxyapatite-blasted surface.

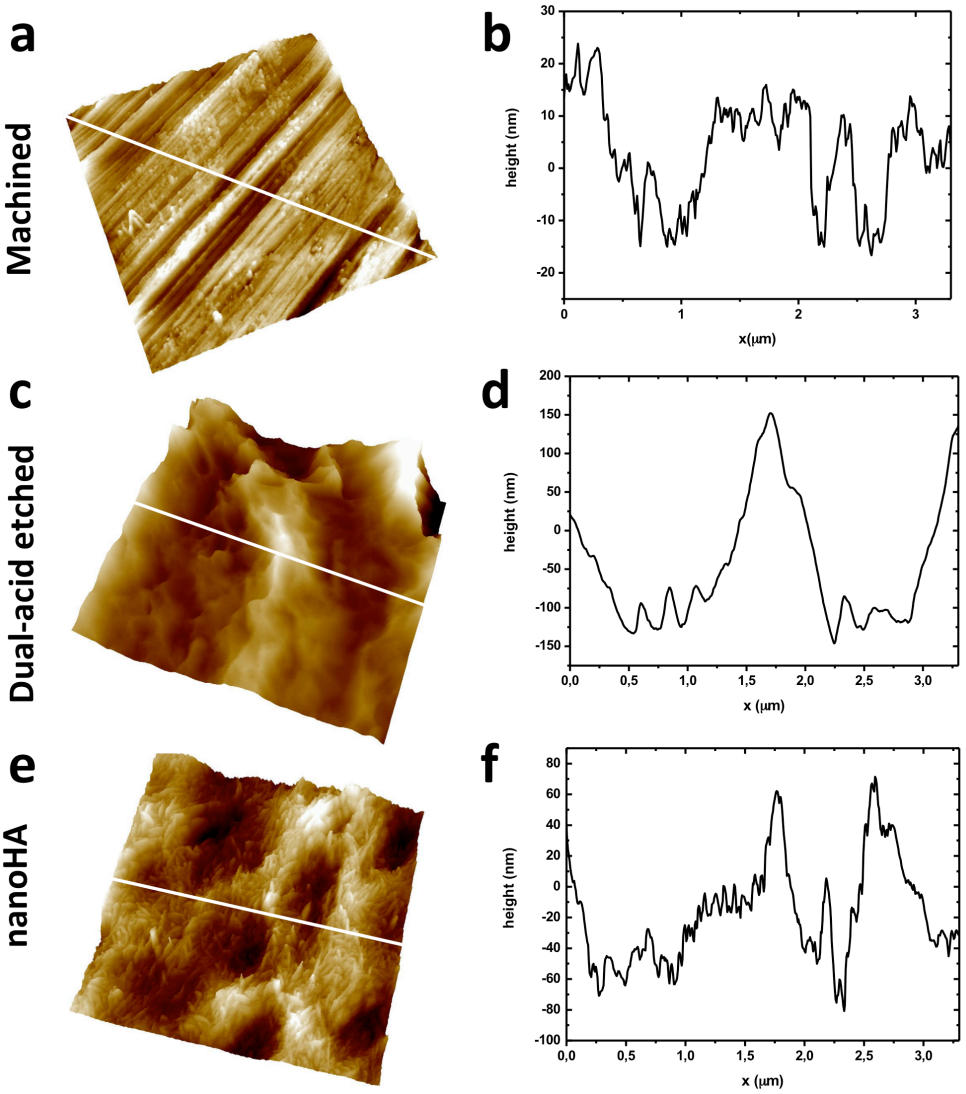

Fig.1. Atomic force micrographs reveal the topography of Ti-texturing surfaces. AFM analysis infer on topography height and three dimensional perspective image showing a 3x3 μm² field representative from Ti-texturing surfaces: Mac (**a**); DAE (**c**); nHA (**e**). Lateral profiles taken from the pre-selected line are displayed on images (**b,d,f**). From these images it is possible to infer a sample roughness ranging from units to hundreds of nanometers. It is possible to verify a fine (nanometeric) roughness

covering the surface of nHA and going along with the micrometric roughness promoted by the acid etching treatment.

Pre-osteoblast morphological changes are dependent on titanium surface texturing.

Pre-osteoblast cells were seeded on Mac and nHA Ti-discs and immediately after 4 hours, the Ti discs were subjected to Scanning Electron Microscopy (SEM) in order to evaluate pre-osteoblast morphological changes. Comparing the morphological changes, it is clear that nHA promoted a better environment to trigger cell spreading while at the same time pre-osteoblast cultured on machined Ti-surface preserved the round up cells morphology (**Fig.2**). Thereafter, these findings were validated by EDX analysis, where we can check the distribution of Carbon (**Fig. 3b, e**) and Titanium (**Fig. 3c, f**) over the electron-micrographs. Note that the peak of carbon is coincident with the cell localization on the micrograph (**Fig. 3b, e**).

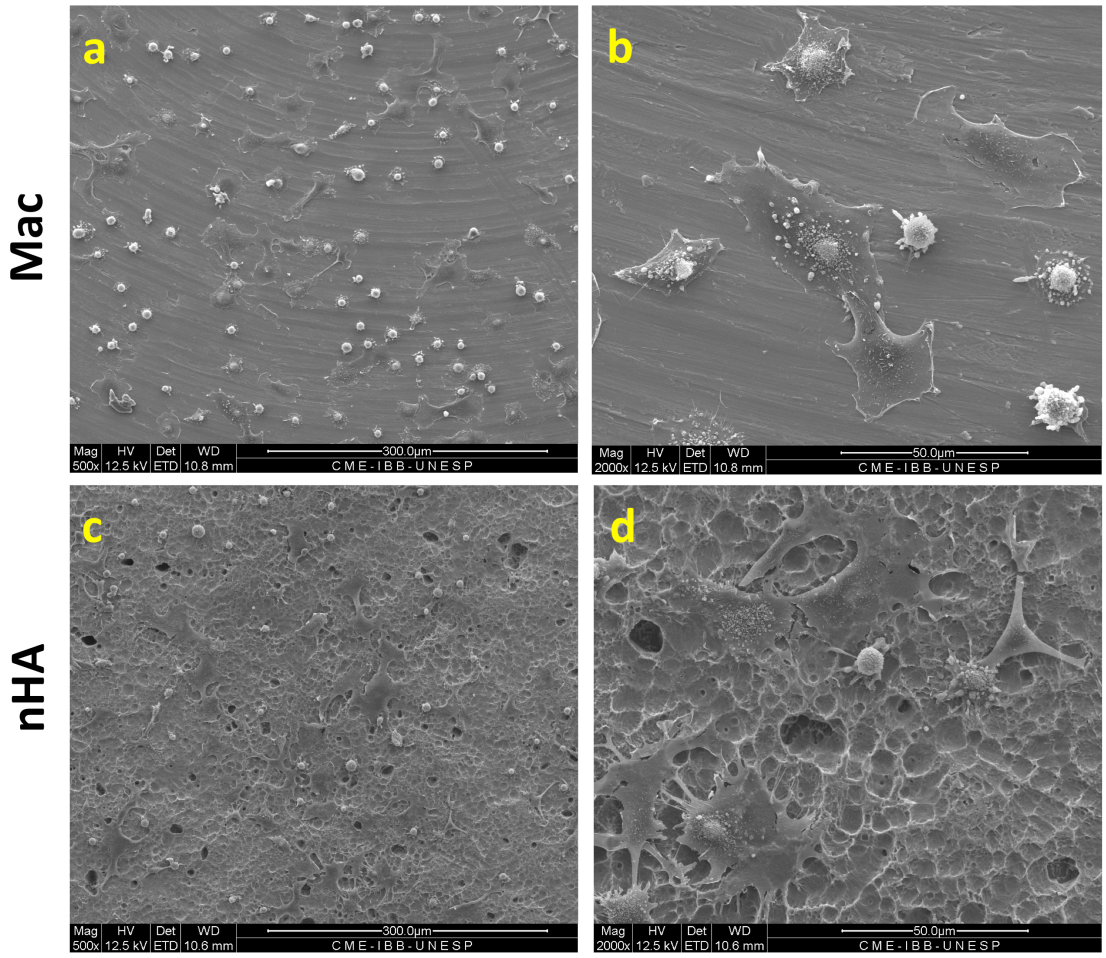

Fig.2. Scanning Electron Microscopy reveals pre-osteoblast morphological changes dependent on titanium-texturing surfaces. Pre-osteoblast cells were seeded in 2 different titanium-texturing surfaces: control (Machined) and nano HA-blasted titanium surfaces up to 4h. Different magnifications (500x and 2000x) were used to obtain SEM images of each group. It is clear to observe that pre-osteoblast cells interacting with nHA surfaces presented a more advanced spreading process when compared to those cultured on machined surfaces (control).

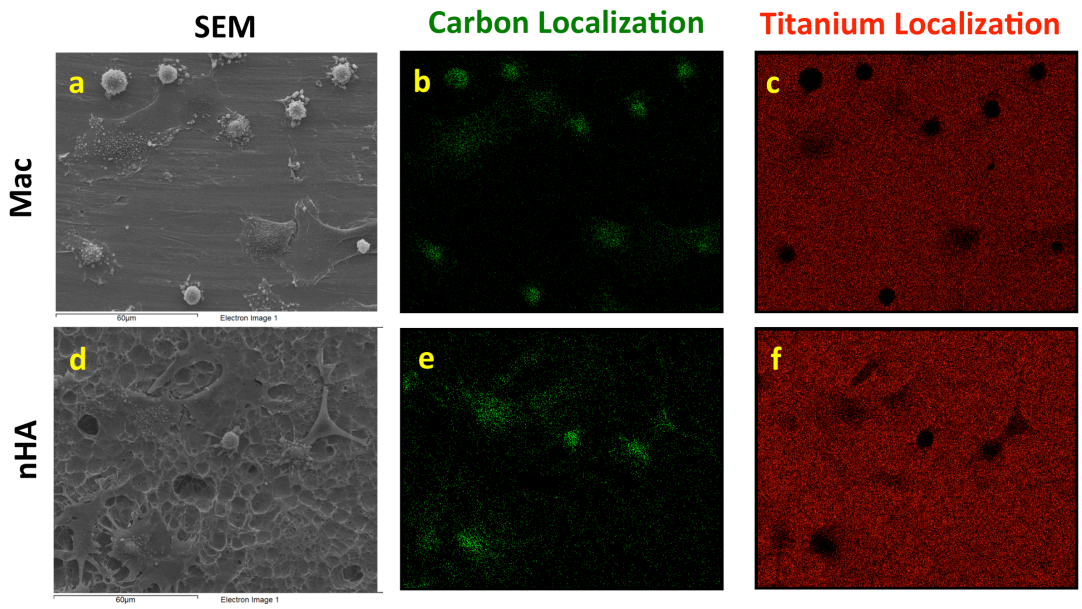

Fig.3. SEM-associated EDX approach validates cell behaviour on different Ti modified surfaces. EDX analyses were performed with 20 kV to detect x-ray characteristic of carbon and titanium containing onto the samples. It can be observed carbon elements identification was coincident with the adherent cells, while titanium elements was also identified on whole sample. Importantly, nano hydroxyapatite-blasted titanium surfaces (nHA) presented a more dispersed carbon distribution coincident with more spreading cells. The differences in the carbon distribution on both evaluated surfaces emphasize the difference in early cell behaviour on each surface.

Osteoblast adhesion signalling is finely modulated by nHA-modified surface.

Firstly, we evaluated the ability of the surfaces to promote osteoblast adhesion by performing violet crystal assay. Our result showed that DAE and nHA promoted significant increase of osteoblast adhesion when compared with their immediate control (Mac) (**Fig. 4a**). As adsorbed protein as a coating in the Ti discs surfaces could affect cell adhesion, we investigated protein concentration forming a thin film on the Ti Surfaces. In fact, **Fig. 4b** shows that protein concentration profile on Ti-surfaces was variable, suggesting that nHA seems to adsorb more protein from serum.

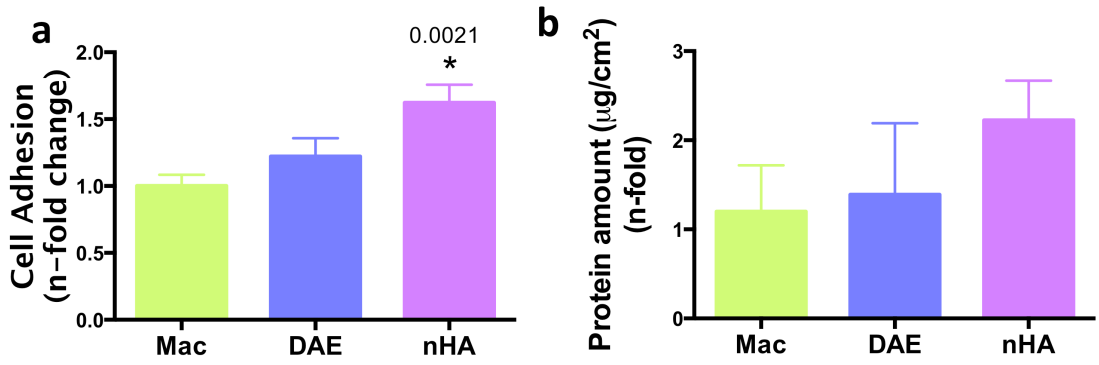

Fig.4. Cell adhesion on Ti-texturing surfaces is mediated by early protein adsorption from medium. a. Firstly, pre-osteoblast cells were treated with conditioned medium from the different Ti-texturing surfaces (conditioned medium was prepared as recommended by ISO 10993-12). After 24h of treating, the pre-osteoblasts were trypsinized and counted by using a haematological chamber. The same amount of cells was seeded and 4h later, the adherent cells were stained with Violet Crystal as mentioned in M&M in details. The results show that pre-osteoblast has a more influence of nHA on cell adhesion performance (*p<0.0021, n=12); **b.** Ti-texturing discs was maintained emerged on cell culture containing FBS 10% up to 24 hours. Thereafter, the adsorbed protein on titanium discs was gently 3x rinsed in 1mL PBS and thereafter the adsorbed protein was mechanically scraped in 500μL of PBS. These samples were used to measure the amount of protein by using Lowry method at absorbance 570 nm (n=6). Briefly, the results showed there is an influence of Ti-texturing surfaces on protein coating, however it did not express significance among the groups here evaluated. **Note:** Machined (Mac; control); 2. Dual Acid-Etched (DAE), and Dual Acid-Etched nano HA-blasted (nHA).

This result prompted us to analyse signaling protein involved with cell adhesion. In this sense, we have evaluated the phosphorylation of both FAK (Y397) and Src (Y416). Both proteins were increased in response to DAE and nHA (**Fig. 5**), corroborant with the profile of cell adhesion (**Fig. 4a**). The **Fig.5a** presents representative blots obtained in this work, while **Figs.5b-c** shows a densitometry analysis.

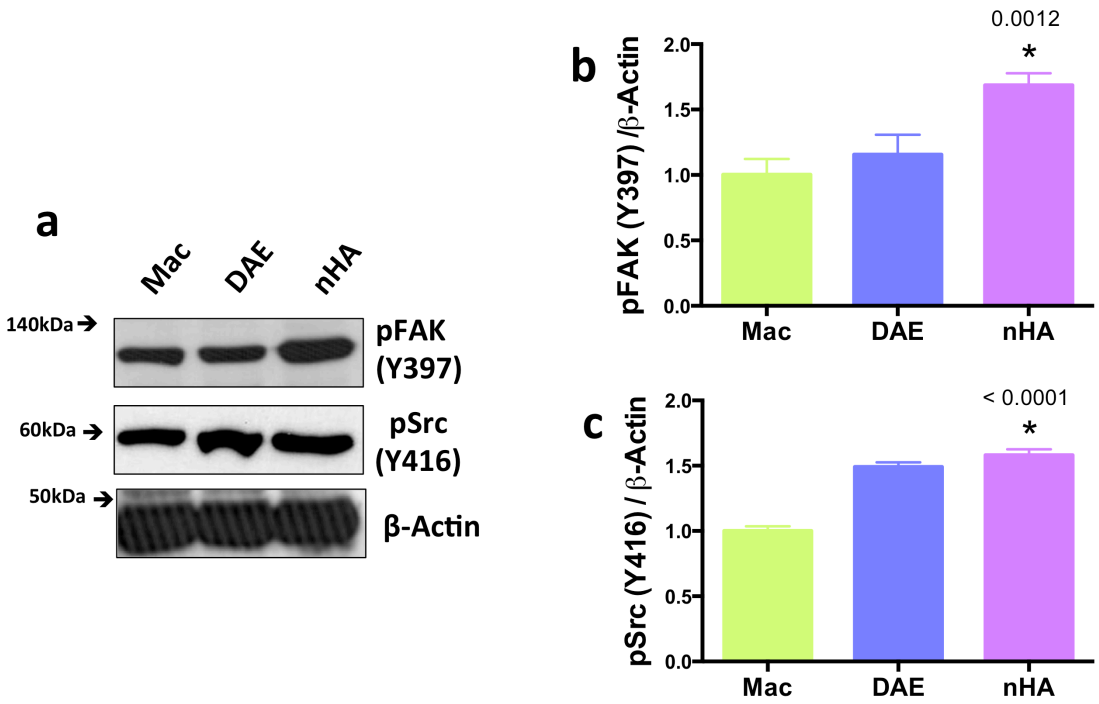

Fig.5. Both FAK and Src phophorylations are differentially required in response to nano hydroxyapatite-blasted surface. a. To assess signalling proteins involved in early osteoblast response to titanium, we checked the phosphorylation profile of proteins related to focal adhesion components [**b:** Src (Y416) and **c:** FAK (Y925, Y397)]; pre-osteoblasts cells were seeded on Ti-texturing surfaces and after 4h the samples were collected to perform immunoblotting approach. Both FAK and Src have been activated by all Ti-texturing surfaces evaluated in this study, it was clear that nHA provoked a bigger phosphorylation of both FAK and Src when compared with others. Also, all western-blotting panels showed in this work were normalized with ß-actin expression, here considered as a housekeeping control. Note: Machined (Mac; control); 2. Dual Acid-Etched (DEA), and acid-etched nano-HA-blasted (nHA). **Note:** significances were considered when *p<0.001, n=3.

Nano HA-blasted titanium surface promotes anti-apoptotic signalling.

In order to understand the osteoblast performance on titanium surfaces, we also studied cell viability. Our result shows that both DAE and nHA did not interfere on osteoblast viability when compared to the immediate control group, the machined surface (**Fig. 6a**). Thereafter, we investigated if titanium surfaces triggered cell death signalling by evaluating the Bax/Bcl2 ratio. Our results showed that Bax and Bcl2 expressions (**Fig. 6b**) were thinly modulated when osteoblast were cultured on titanium surfaces; however, the Bax/Bcl2 ratio decreased (**Fig. 6e**) in those evaluated groups, mainly in response to nHA surfaces. All western-blotting panels showed in this work

were normalized with ß-actin expression, here considered as a housekeeping control (**Figs. 6c,d**).

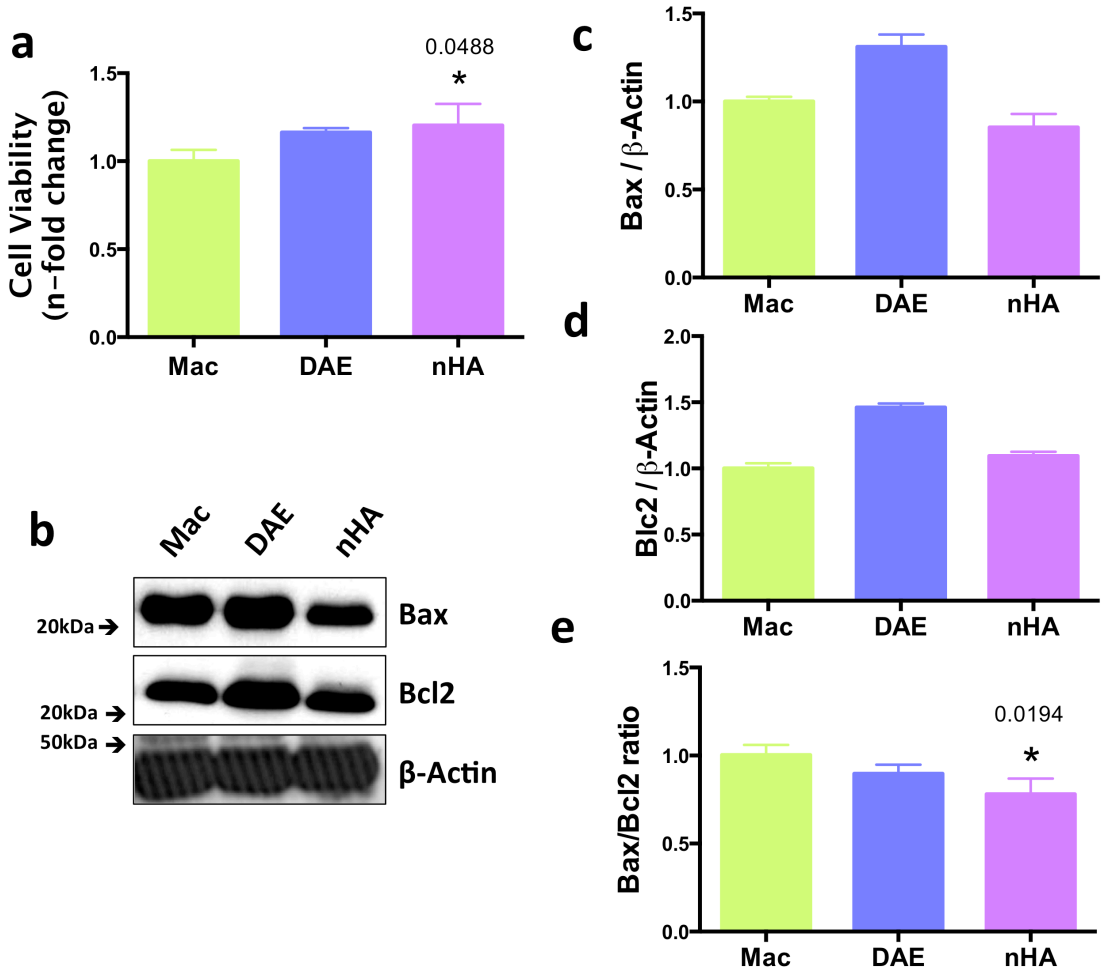

Fig.6. Ti-texturing surfaces decrease pre-osteoblasts anti-apoptotic signalling. a. Cytotoxic effects of Ti-texturing surfaces were measured by mitochondrial dehydrogenase activity (MTT assay) represented as a percentage of control (tissue plastic) cell viability. * means statistically significant differences between groups (*p<0.05; n=12). In order to validate this result, pre-osteoblasts were cultured on different Ti-modified surfaces during 24 hours and thereafter the cell lysate was collected to evaluate Bax and Bcl2 expressions (**b**), when ß-actin expression was used as housekeeping control (**b**). Letters "**c**" and "**d**" bring a densitometries of the bands of Bax and Bcl2, respectively (n=3). In addition, Bax/Bcl2 ratio was determined in order to estimate anti- or pro-apoptotic signalling. The letter e shows that Ti-modified surfaces promote anti-apoptotic signalling (* p<0.0194), when we stated that Bax/Bcl2 ratio was decreased in comparison to Mac. **Note:** Machined (Mac; control); 2. Dual Acid-Etched (DEA), and acid-etched nano-HA-blasted (nHA).

Titanium-texturing surfaces promote osteoblast survival/proliferation signalling.

Later, pre-osteoblasts were cultured on the different titanium-modified surfaces for 4 hours and the biological samples collected to evaluate cell signalling responsible to cell survival and proliferation and in this sense we have checked Ras-Raf-Mek-p42/44 mapk signalling. Our results showed that Ras-Raf-Mek- p42/44 mapk signalling was involved (**Fig. 7a**) in response to titanium surfaces, involving the phosphorylation of MEK. It is important to mention that texture modified DAE and nHA promoted a significant increase of Raf (**Fig. 7c**), suggesting this protein involvement with other signalling pathway. Also, all western-blotting panels showed in this work were normalized with ß-actin expression, here considered as a housekeeping control (**Figs. 7b-e**).

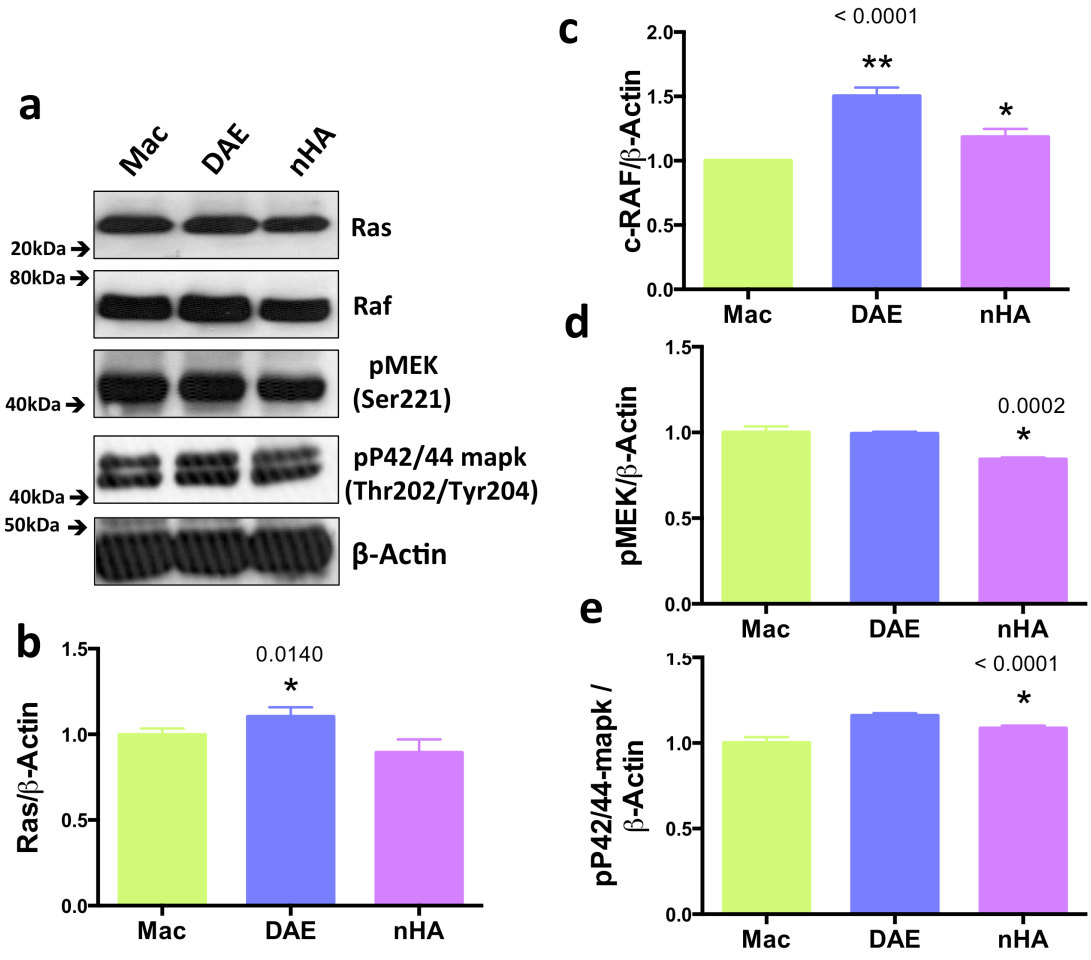

Fig.7. Ti-texturing surfaces promote osteoblast Ras-Erk signalling. Pre-osteoblasts were cultured on the different Ti-texturing surfaces and after 24 hours they were lysed in order to estimate Ras-Erk axis signalling by performing western-blotting approach. **a.** Representative blots of Ras, Raf, pMEK (Ser221) e pP42/44-mapk (Thr202/Tyr204). Graphs were built from 3 independent sets of results and obtained from band

densitometry (**b-e**). All bars representing groups was normalized using ß-actin expression average. In graphs, *means significant differences ($p<0.05$; n=3).

Titanium-texturing surfaces promote late osteoblast differentiation.

The osteoblast differentiation was evaluated by investigating osteogenic signal transducers as RUNX2 and OSTERIX, Osteocalcin by qPCR and ALP activity by biochemical dosages, as described in Zambuzzi et al. (2014). For this purpose, we decided to evaluate both direct and indirect effect of the Ti modified surfaces on the osteoblast differentiation, where in the indirect manner the cells were treated with the conditioned medium from the titanium samples (**Fig.8a**) while in the direct manner the cells were grown directly on the top of discs (**Fig.8e**). Both osteogenic transcription factors, RUNX2 (**Fig.8b,f**) and OSTERIX (**Fig.8c,g**), were up-modulated by the DAE and nHA, independently of the manner, direct or indirectly. However, the nHA stimulated even more RUNX2 transcripts at the direct interaction (**Fig.8f**). Osteocalcin was not significantly modulated (**Fig.8d,h**), maybe because it is a late osteoblast differentiation biomarker and we subjected the osteoblast to the discs up to 10 days. Finally, our results showed that all of the 3 texturized Ti surfaces stimulated ALP activity in osteoblast cultured on them for 10 days (**Fig. 8**); with nHA provoking a significant increase, when considered $p<0.05$ (*).

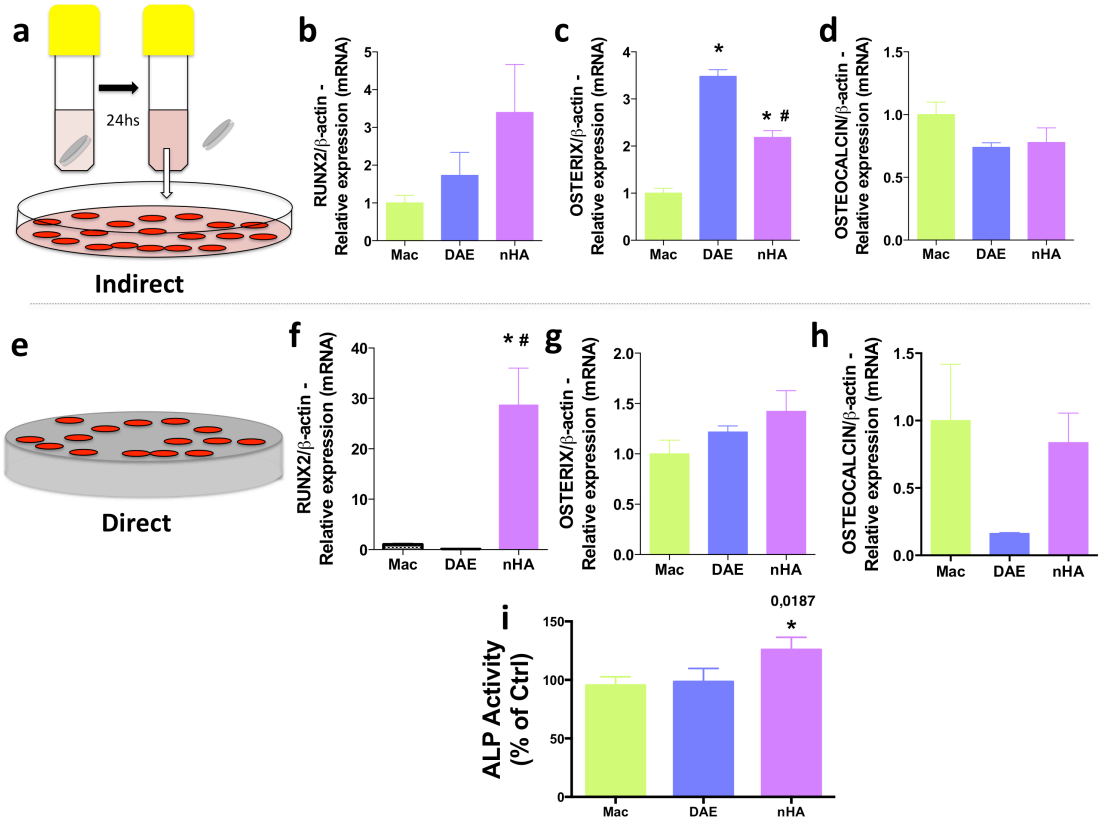

Fig.8. Ti-texturing surfaces promote pre-osteoblast differentiation up to 10 days. **"a,e"** schematization of the experiment, when pre-osteoblast cells subjected for direct (**b-d**) or indirect (**f-h**) responses in order to understand the osteogenic performance in response to the Ti-texturized surfaces (**i**). After 10 days, the cells were scraped allowing osteogenic transcripts (RUNX2, OSTERIX and OSTEOCALCIN) and Alkaline Phosphatase (ALP) as it was measured by Zambuzzi et al. (2014). Briefly, we have shown that all Ti-texturing surfaces evaluated promoted ALP activity, mainly pronounced by nHA surfaces. To note: *, # mean significances between the groups.

Altogether, our results showed that different titanium surface texturing promoted crucial intracellular signalling pathways, mainly responsible for cell adhesion and proliferation. In this sense, **Fig. 9** summarizes the mainly signalling network involved with cell adaptation and performance on titanium surfaces evaluated in this study and we suggest that those proteins are biomarkers of this event.

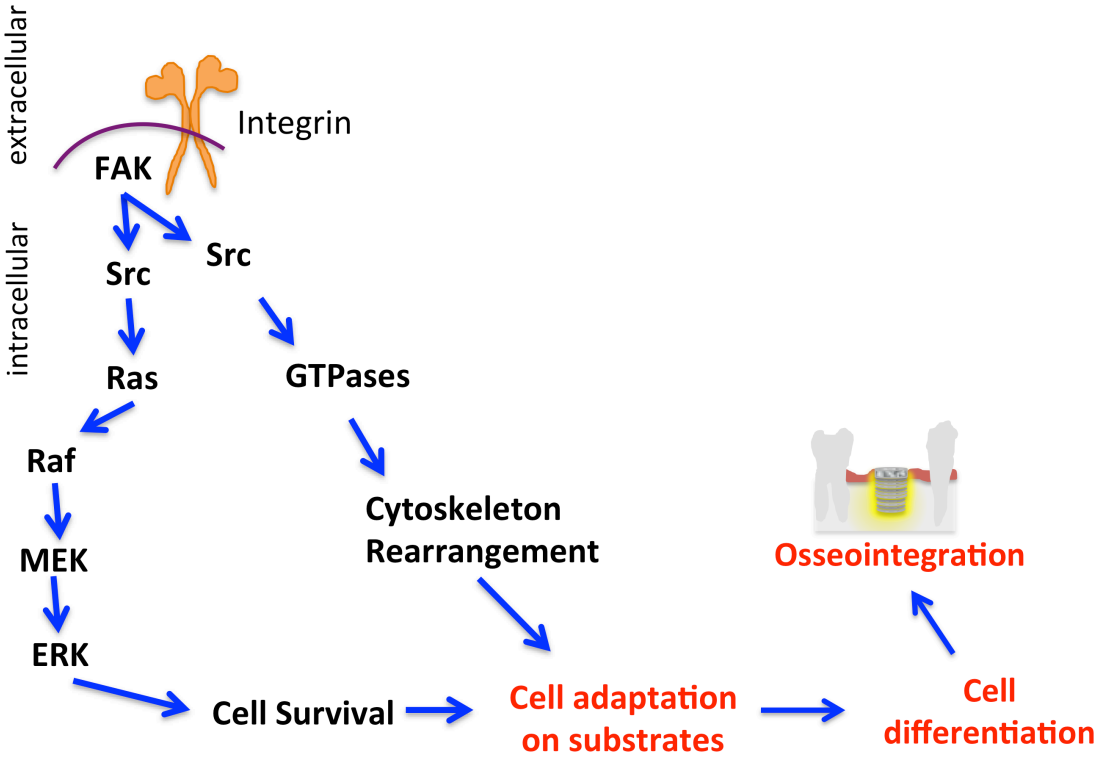

Fig.9. Schematization of signalling proteins proposed in this work. Upon integrin activation there is a recruitment of Focal Adhesion Kinase (FAK), a cytoplasmic protein-tyrosine kinase, and creating a phosphotyrosine docking site for members of the Src family of cytoplasmic tyrosine kinases. We suggest these signalling proteins as biomolecules able to promote cytoskeleton rearrangement necessary during osteoblast adaptation on substrate. Thereafter, Ras-Raf-MEK-ERK cascade couples signals from cell surface receptors to transcription factors, which regulate prevention of apoptosis and induction of cell cycle progression. Altogether, these molecules seem to being responsible to govern osteoblast adaptation on titanium-texturing surfaces.

DISCUSSION

Biotechnology approaches for modification of implant surfaces have been identified as an important strategy to reduce the rehabilitation time of patients suffering edentulism (Dang et al., 2016; Sohrabi et al., 2012). In this sense, the development of novel bio-functionalizing surfaces on titanium alloys has been proved to be fundamental for enhancing osteoprogenitor cells performance and thus accelerating bone neo-formation surrounding implanted devices, positively impacting implant osteointegration (Kulkarni et al., 2015; Longo et al., 2016). In this sense, our group has been devoted to investigate the cell signalling mechanisms involved in the response to different biomaterials (Gemini-Piperni et al., 2014a; Gemini-Piperni et al.,

2014b; Zambuzzi et al., 2014) in order to mine intracellular biomarkers related to this scenario. In this context, we have proposed the importance of Src and FAK involvement as signalling proteins identifying texturing of substrate surfaces (Zambuzzi et al., 2009; Zambuzzi et al., 2010). We have also discussed in this regard that cellular attack is a very important early biological event responsible for integrating implanted devices to whole bone. In addition, we have also considered the protein coating on implants previous to cell attachment. To address this issue, we have shown that different texturized titanium surfaces provide differential protein adsorption, mainly related to surface roughness (Zambuzzi et al., 2014). Our results are in agreement with our previously published data, when nano-HA-blasted titanium surface adsorbs a higher concentration of serum proteins than others. Generally speaking, however, this coating of proteins on implantable surface promotes a bio-functionalizing environment able to guide cell adaptation at early interaction by activating intracellular mechanisms to induce either acceptance or rejection of the implant by determining which and how many cells will populate the surface (Barkarmo et al., 2014a; Kulkarni et al., 2015).

Physicochemical properties of the surface, such as wettability (evaluated by water contact angle) and surface topography (evaluated by Atomic Force Microscopy), interferes profoundly cell adhesion, spreading, proliferation and late differentiation. Owing to a hierarchical sequence of biological surroundings to implantable devices, water contact initiates a complex time-line favouring or not the tissue repair. Surface wettability drives the adsorption of proteins, establishing a biological coating and impacting late cell interaction. Our results showed that there is a significant difference on the topography of the titanium surfaces evaluated in this study and it reflected on the wettability. It is usually reported that cell adhesion requires a moderate hydrophilicity but cell performance is negatively modulated when the material becomes very hydrophilic.

To note, during eukaryotic cell adhesion, both FAK and Src proteins are responsible for modulating intracellular mechanisms to control cell interaction/matrix upon integrin activation (Barkarmo et al., 2014b; Zambuzzi et al., 2014). We have recently shown that intracellular mechanisms via activation of integrin/FAK/Src pathway promote the rearrangement of cytoskeleton rearrangement and it seems decisive for cell adapting on different surface roughness by determining cell

morphology. In this work, we showed that pre-osteoblasts cultured on different texturized Ti surfaces promoted profound morphological changes, here analysed by SEM. Briefly, our electron micrographs showed that pre-osteoblasts cultured on nHA present a more immediate spreading than when on machined surfaces (control surface). This finding is in agreement with Gaviria et al. (2014) that proposed that roughed surfaces produce cells orientation and guide their locomotion affecting cell shape and function (Gaviria et al., 2014). In addition, we also validated these results with EDX approach by co-localizing carbon and titanium. Importantly, the observed morphological changes were accompanied by the activations of both FAK and Src, analysed here by phosphorylation sites of both signalling proteins. Thus, we believe that these morphological changes during cell adaptation are a FAK and Src-dependent manner, as already reported previously for osteoblasts adhesion on polystyrene surfaces (Zambuzzi et al., 2009). At this point, we believe that FAK and Src recognize physicochemical properties of the surfaces and they are considered as interesting biomarkers of cell-surface interactions.

Later, we have shown that critical to cell survival (Ras/Raf /MEK/Erk) was required in pre-osteoblasts cultured on Ti texturized surfaces for 4 hours of adhesion, mainly in osteoblasts cultured on nHA surfaces. Another important point to discuss was the influence of nHA on promoting osteoblast differentiation by significantly up-regulating classical biomarkers as RUNX2 and Alkaline phosphatase activity when pre-osteoblast were grown directly on titanium discs. These characteristics influence the biological response to implantable devices by accelerating tissue healing and later osseointegration (Dang et al., 2016; Longo et al., 2016). Regarding biofunctionalizing nHA surface, the intimate mixture of the coating components allows lower processing temperatures preventing undesired phase transitions and a high homogeneity of the film is expected (Gottlander et al., 1997; Meirelles et al., 2008).

Altogether our results showed for the first time that nano-hydroxyapatite-blasted titanium surface clearly promotes an ideal environment for pre-osteoblast performance by activating crucial signalling network. In general, we have stated that understanding intracellular signalling involved on the mechanisms of osteoblast adhesion, proliferation, and differentiation on implantable devices is fundamental for

the successful design of novel bioengineered materials, potentially decreasing the repair time, thereby allowing faster patient rehabilitation.

ACKNOWLEDGEMENTS

We would like to thank FAPESP (Proc. Nrs. 2014/22689-3, 2015/03639-8) and CNPq (Proc. Nr. 301966/2015-0) for the financial support and Prof. Margarida Juri Saeki for the S.E.M. images acquirement. Also, we would like to thank to Electron Microscopy Center, IBB, UNESP, Botucatu – SP, Brazil.

COMPETING FINANCIAL INTERESTS

The authors declare no competing financial interests.

REFERENCES

Asati V, Mahapatra DK, Bharti SK. 2016. PI3K/Akt/mTOR and Ras/Raf/MEK/ERK signaling pathways inhibitors as anticancer agents: Structural and pharmacological perspectives. Journal Article. *Eur. J. Med. Chem.* **109**:314–341.

Barkarmo S, Andersson M, Currie F, Kjellin P, Jimbo R, Johansson CB, Stenport V. 2014a. Enhanced bone healing around nanohydroxyapatite-coated polyetheretherketone implants: An experimental study in rabbit bone. *J. Biomater. Appl.* **29**:737–47.

Barkarmo S, Andersson M, Currie F, Kjellin P, Jimbo R, Johansson CB, Stenport V. 2014b. Enhanced bone healing around nanohydroxyapatite-coated polyetheretherketone implants: An experimental study in rabbit bone. Journal Article, Research Support, Non-U.S. Gov't. *J. Biomater. Appl.* **29**:737–747.

Bergeron JJM, Di Guglielmo GM, Dahan S, Dominguez M, Posner BI. 2016. Spatial and Temporal Regulation of Receptor Tyrosine Kinase Activation and Intracellular Signal Transduction. JOURNAL ARTICLE. *Annu. Rev. Biochem.*

Bertazzo S, Zambuzzi WF, Campos DDP, Ferreira C V, Bertran CA. 2010a. A simple method for enhancing cell adhesion to hydroxyapatite surface. Journal Article, Research Support, Non-U.S. Gov't. *Clin. Oral Implants Res.* **21**:1411–1413.

Bertazzo S, Zambuzzi WF, Campos DDP, Ogeda TL, Ferreira C V, Bertran CA. 2010b. Hydroxyapatite surface solubility and effect on cell adhesion. *Colloids Surfaces B Biointerfaces* **78**:177–184. http://www.sciencedirect.com/science/article/pii/S0927776510001153.

Cavagis A, Takamori E, Granjeiro J, Oliveira R, Ferreira C, Peppelenbosch M, Zambuzzi W. 2014. TNFalpha contributes for attenuating both Y397FAK and Y416Src phosphorylations in osteoblasts. Journal Article, Research Support, Non-U.S. Gov't. *Oral Dis.* **20**:780–786.

Dang Y, Zhang L, Song W, Chang B, Han T, Zhang Y, Zhao L. 2016. In vivo osseointegration of Ti implants with a strontium-containing nanotubular coating. Journal Article. *Int. J. Nanomedicine* **11**:1003–1011.

Di Liddo R, Paganin P, Lora S, Dalzoppo D, Giraudo C, Miotto D, Tasso A, Barbon S, Artico M, Bianchi E, Parnigotto PP, Conconi MT, Grandi C. 2014. Poly-epsilon-caprolactone composite scaffolds for bone repair. Journal Article. *Int. J. Mol. Med.* **34**:1537–1546.

Fernandes GVO, Cavagis ADM, Ferreira C V, Olej B, Leao M de S, Yano CL, Peppelenbosch M, Granjeiro JM, Zambuzzi WF. 2014. Osteoblast adhesion dynamics: a possible role for ROS and LMW-PTP. Journal Article, Research Support, Non-U.S. Gov't. *J. Cell. Biochem.* **115**:1063–1069.

Gaviria L, Salcido JP, Guda T, Ong JL. 2014. Current trends in dental implants. Journal Article, Review. *J. Korean Assoc. Oral Maxillofac. Surg.* **40**:50–60.

Gemini-Piperni S, Milani R, Bertazzo S, Peppelenbosch M, Takamori ER, Granjeiro JM, Ferreira C V, Teti A, Zambuzzi W. 2014a. Kinome profiling of osteoblasts on hydroxyapatite opens new avenues on biomaterial cell signaling. Journal Article, Research Support, Non-U.S. Gov't. *Biotechnol. Bioeng.* **111**:1900–1905.

Gemini-Piperni S, Takamori ER, Sartoretto SC, Paiva KBS, Granjeiro JM, de Oliveira RC, Zambuzzi WF. 2014b. Cellular behavior as a dynamic field for exploring bone bioengineering: a closer look at cell-biomaterial interface. Journal Article, Research Support, Non-U.S. Gov't, Review. *Arch. Biochem. Biophys.* **561**:88–98.

Gottlander M, Johansson CB, Wennerberg A, Albrektsson T, Radin S, Ducheyne P. 1997. Bone tissue reactions to an electrophor- etically applied calcium phosphate coating. *Biomaterials*. **18**:551–557.

Henkel J, Woodruff M, Epari D, Steck R, Glatt V, Dickinson I, Choong P, Schuetz M, Hutmacher D. 2013. Bone Regeneration Based on Tissue Engineering Conceptions – A 21st Century Perspective. *Bone Res.* **1**:216–248. http://dx.doi.org/10.4248/BR201303002.

Hu N, Feng C, Jiang Y, Miao Q, Liu H. 2015. Regulative Effect of Mir-205 on Osteogenic Differentiation of Bone Mesenchymal Stem Cells (BMSCs): Possible Role of SATB2/Runx2 and ERK/MAPK Pathway. Journal Article, Research Support, Non-U.S. Gov't. *Int. J. Mol. Sci.* **16**:10491–10506.

Jiang T, Guo L, Ni S, Zhao Y. 2015. Upregulation of cell proliferation via Shc and ERK1/2 MAPK signaling in SaOS-2 osteoblasts grown on magnesium alloy surface coating with tricalcium phosphate. Journal Article, Research Support, Non-U.S. Gov't. *J. Mater. Sci. Mater. Med.* **26**:158.

Jimbo R, Coelho PG, Bryington M, Baldassarri M, Tovar N, Currie F, Hayashi M, Janal MN, Andersson M, Ono D, Vandeweghe S, Wennerberg A. 2012. Nano hydroxyapatite-coated implants improve bone nanomechanical properties. Comparative Study, Journal Article, Research Support, Non-U.S. Gov't. *J. Dent. Res.* **91**:1172–1177.

Kulkarni M, Mazare A, Gongadze E, Perutkova \v{S}., Kralj-Igli\v{c} V, Milo\v{s}ev I,

Schmuki P, Igli\v{c} A, Mozeti\v{c} M. 2015. Titanium nanostructures for biomedical applications. *Nanotechnology* **26**:62002 (1-18).

Kjellin P, Andersson M. 2006. SE-0401524-4, assignee. Synthetic nano-sized crystalline calcium phosphate and method of production patent SE527610.

Longo G, Ioannidu CA, Scotto d'Abusco A, Superti F, Misiano C, Zanoni R, Politi L, Mazzola L, Iosi F, Mura F, Scandurra R. 2016. Improving Osteoblast Response In Vitro by a Nanostructured Thin Film with Titanium Carbide and Titanium Oxides Clustered around Graphitic Carbon. Journal Article. *PLoS One* **11**:e0152566.

Meirelles L, Arvidsson A, Andersson M, Kjellin P, Albrektsson T, Wennerberg A. 2008. Nano hydroxyapatite structures influence early bone formation. *J. Biomed. Mater. Res. A*. **87**:299-307.

Salou L, Hoornaert A, Stanovici J, Briand S, Louarn G, Layrolle P. 2015. Comparative bone tissue integration of nanostructured and microroughened dental implants. Journal Article, Research Support, Non-U.S. Gov't. *Nanomedicine (Lond).* **10**:741–751.

Sohrabi K, Mushantat A, Esfandiari S, Feine J. 2012. How successful are small-diameter implants ? A literature review.

Zambuzzi WF, Fernandes GVO, Iano FG, Fernandes M da S, Granjeiro JM, Oliveira RC. 2012. Exploring anorganic bovine bone granules as osteoblast carriers for bone bioengineering: A study in rat critical-size calvarial defects. *Braz. Dent. J.* **23**:315–321.

Zambuzzi WF, Milani R, Teti A. 2010. Expanding the role of Src and protein-tyrosine phosphatases balance in modulating osteoblast metabolism: Lessons from mice. *Biochimie* **92**:327–332. http://dx.doi.org/10.1016/j.biochi.2010.01.002.

Zambuzzi WF, Bonfante EA, Jimbo R, Hayashi M, Andersson M, Alves G, Takamori ER, Beltrao PJ, Coelho PG, Granjeiro JM. 2014. Nanometer scale titanium surface texturing are detected by signaling pathways involving transient FAK and Src activations. Journal Article, Research Support, Non-U.S. Gov't. *PLoS One* **9**:e95662.

Zambuzzi WF, Coelho PG, Alves GG, Granjeiro JM. 2011a. Intracellular signal transduction as a factor in the development of "smart" biomaterials for bone tissue engineering. Journal Article, Review. *Biotechnol. Bioeng.* **108**:1246–1250.

Zambuzzi WF, Ferreira C V, Granjeiro JM, Aoyama H. 2011b. Biological behavior of pre-osteoblasts on natural hydroxyapatite: a study of signaling molecules from attachment to differentiation. Journal Article, Research Support, Non-U.S. Gov't. *J. Biomed. Mater. Res. A* **97**:193–200.

Zambuzzi WF, Bruni-Cardoso A, Granjeiro JM, Peppelenbosch MP, De Carvalho HF, Aoyama H, Ferreira CV. 2009. On the road to understanding of the osteoblast adhesion: Cytoskeleton organization is rearranged by distinct signaling pathways. *J. Cell. Biochem.* **108**:134–144.

Capítulo 3

NANO HYDROXYAPATITE-BLASTED TITANIUM SURFACE CREATES A BIOINTERFACE ABLE TO GOVERN SRC-DEPENDENT OSTEOBLAST METABOLISM AS PREREQUISITE TO ECM REMODELING

Célio J. C. Fernandes[1*]; Fábio Bezerra[1*]; Marcel R. Ferreira[1*]; Amanda F. C. Andrade; Thais Silva Pinto[1]; Willian F. Zambuzzi[1,2,‡]

[1]Dept. of Chemistry and Biochemistry, Bioscience Institute, State University of São Paulo – UNESP, *campus* Botucatu, Botucatu, São Paulo, Brazil.
[2]Electron Microscopy Center, IBB, UNESP, Botucatu – SP, Brazil.

Fernandes, CJ; Bezerra, F; Ferreira, MR; Andrade, AFC; Pinto, TS; Zambuzzi WF. Nano hydroxyapatite-blasted titanium surface creates a biointerface able to govern Src-dependent osteoblast metabolism as prerequisite to ECM remodeling. **Colloids Surf B Biointerfaces.** 2018 Mar 1;163:321-328.

ABSTRACT

Over the last several years, we have focused on the importance of intracellular signaling pathways in dynamically governing the biointerface between pre-osteoblast and surface of biomaterial. Thus, this study investigates the molecular hallmarks involved in the pre-osteoblast relationship with different topography considering Machined (Mc), Dual Acid-Etching (DAE), and nano hydroxyapatite-blasted (nHA) groups. There was substantial differences in topography of titanium surface, considering Atomic Force Microscopy and water contact angle (Mc=81.41 ± 0.01; DAE=97.18 ± 0.01; nHA=40.95 ± 0.02). Later, to investigate their topography differences on biological responses, pre-osteoblast was seeded on the different surfaces and biological samples were collected after 24 hours (to consider adhesion signaling) and 10 days (to consider differentiation signaling). Preliminary results evidenced significant differences in morphological changes of pre-osteoblasts mainly resulting from the interaction with the DAE and nHA, distinguishing cellular adaptation. These results pushed us to analyze activation of specific genes by exploring qPCR technology. In sequence, we showed that Src performs crucial roles during cell adhesion and later differentiation of the pre-osteoblast in relationship with titanium-based biomaterials, as our results confirmed strong feedback of the Src activity on the integrin-based pathway, because integrin-ß1 (~5-fold changes), FAK (~12-fold changes), and Src (~3.5-fold changes) were significantly up-expressed when Src was chemically inhibited by PP1 (5 µM). Moreover, ECM-related genes were rigorously reprogrammed in response to the different surfaces, resulting on Matrix Metalloproteinase (MMP) activities concomitant to a significant decrease of MMP inhibitors. In parallel, we showed PP1-based Src inhibition promotes a significant increase of MMP activity. Taking all our results into account, we showed for the first time nano hydroxyapatite-blasted titanium surface creates a biointerface able to govern Src-dependent osteoblast metabolism as pre-requisite to ECM remodeling

Key words: Biointerfaces; Biotechnology; Nanotechnology; Hydroxyapatite; Implants; Osteoblast; Adhesion; Signal Transduction.

1. Introduction

Biomedical implants are one of the most common therapies used in case of bone lesions. Although several materials have been considered to produce these metallic devices, titanium is considered the gold standard [1]. Mechanistically, the success of the therapy using these biomaterials can be evaluated by the profile of osteointegration promoted by the osteoprogenitor cells in response to them. It is known that the physico-chemical properties of the biomaterial surfaces decisively trigger biological phenomena able to modulate cellular response and later impact the time and quality of osseointegration [2–4]. Therefore, a special look at cellular transducers that govern cell-biomaterial response becomes necessary.

Intracellular signaling pathways triggered upon integrin activation are classical biomarkers of the eukaryotic cell adhesion, and focal adhesion kinase (FAK) and product of the transforming gene of Rous sarcoma virus, Src, are important intracellular proteins to link integrin activation with cytoskeleton rearrangement [5–7]. In detail, integrins are transmembrane proteins responsible for cell anchoring in substrata, such as extracellular matrix components [8]. When activated, integrins recruit FAK and Src molecules leading to a specific intracellular pathway culmination in different responses such as cytoskeletal rearrangement, cell proliferation, motility, differentiation, and survival, as discussed elsewhere [9]. Thus, understanding the biomaterial biointerface able to favor cell interactions is an interesting strategy to contribute to biomedical engineering and biotechnological business.

It is already known that for a complete biomaterial osseointegration a well-orchestrated ECM remodeling peri-implant is necessary [10,11]. As important proteases in this context, matrix metalloproteinases (MMPs) are proteins responsible for degradation of the ECM components and are fundamental for adequate remodeling [12]. On the other hand, tissue inhibitor of matrix metalloproteinases (TIMP's) and reversion-inducing cysteine rich protein with Kazal motifs (RECK) are important modulators of MMP activities, and are required to orchestrate ECM remodeling [13,14].

Summarizing, we investigated the molecular hallmarks involved with the pre-osteoblast relationship with different topography considering Machined (Mc), Dual acid-etching (DAE), and nano hydroxyapatite-blasted (nHA) groups. We showed Src

performs crucial roles during cell adhesion and later differentiation of the pre-osteoblast in relationship with titanium-based biomaterials, because our results confirmed a strong feedback of the Src activity on the integrin-based pathway as integrin-ß1 (~5-fold changes), FAK (~12-fold changes), and Src (~3,5-fold changes) were significantly up-expressed when Src was chemically inhibited by PP1. Moreover, ECM remodeling-related genes were rigorously reprogrammed in response to the different surfaces, resulting on Matrix Metalloproteinase (MMPs) activities inverse to Src expression, suggesting Src as a suppressor of MMP processing.

2. Material and methods

Materials

Three different titanium surfaces (discs) were investigated in this study, distinguishing by the surface properties, called Machined (Mc; control), Dual Acid-Etched (DAE), and acid-etched nanoHA-blasted (nHA). The nHA was obtained by using the Promimic HAnano-method, a detailed description can be found elsewhere [15–17]. Briefly, the samples were dipped into a stable particle suspension containing 10 nm in diameter HA particles followed by a heat treatment at 550 °C for 5 min in nitrogen atmosphere. The surfactant-mediated process allows better control of the chemical composition of the coating [16]. The primers used in this study were purchased from Exxtend company (Campinas, São Paulo, Brazil). The antibodies were purchased from Cell Signalling Technology (Boston, MA, USA). All the titanium materials were sterilized by exposure to Gamma irradiation and donated by S.I.N. – Sistema Nacional de Implantes (São Paulo, SP, Brazil).

Surface characterization of the materials

Atomic force microscopy (AFM)

Ti-modified surfaces were first processed by AFM, in which AFM tip acts as a "nano profilometer" and is able to generate information on the micro and nano-dimensional aspects of the surface (x, y, and z axis). The images were acquired by using Bioscope Catalyst (Bruker Coorp) equipment, and AFM cantilevers, also from Bruker, ("RTESPA", k = 20 to 80 N/m) were used. The equipment worked in intermittent contact mode and

images were taken from 3 different samples (Machined, Double-Acid Etched, and nano Hydroxyapatite) and 3 different regions on each sample (border, middle, and opposite border). Scans of 3.3 x 3.3 μm^2 were taken to check homogeneity.

Water contact angle

An automated goniometer (Ramé Hart, 100-00) was used to evaluate water wettability through contact angle measurements. Deionized water and diiodomethane were used as probe liquids and the presented results correspond to the average of 10 measurements.

Cell culture

MC3T3-E1 (subclone 4), mouse pre-osteoblastic cells, was used in this study. Pre-osteoblasts were cultured in α-MEM supplemented with 10% Fetal Bovine Serum (FBS) at 37 °C and 5% CO_2. Sub-confluent passages were tripsinized and used in all experiments. For the collect samples, the cells were seeded on the titanium surfaces (direct contact) or treated with the titanium-enriched medium (prepared according to the ISO 10993: 2016) up to 24 hours (for the adhesion evaluation) and up to 14 days (for the osteogenic phenotype). During this time, the cells were maintained at 37 °C in conditioned medium. The culture medium was changed every 3 days to provide an adequate concentration of nutrients to the cells. To understand whether Src was affecting the feedback of adhesion-related genes, pre-osteoblast was treated up to 24 hours with PP1 (5 μM), when the total RNA and protein extract were collected.

The efficiency of PP1 was determined by immunoblotting. Briefly, the cells were lysed (50 mM Tris [tris(hydroxymethyl)aminomethane]–HCl [pH 7.4], 1% (vol/vol) Tween 20, 0.25% sodium deoxycholate, 150 mM NaCl, 1 mM EGTA (ethylene glycol tetraacetic acid), 1 mM *O*-Vanadate, 1 mM NaF, plus protease inhibitors [1 μg/mL aprotinin, 10 μg/mL leupeptin, and 1 mM 4-(2-amino-ethyl)-benzolsulfonyl-fluor-hydrochloride] and kept on ice for 2 h. After clearing the lysate by centrifugation, the amount of protein obtained was determined using Lowry's method. Afterwards, an equal volume of 2x sodium dodecyl sulfate (SDS) gel loading buffer (100 mM Tris-HCl [pH 6.8], 200 mM dithiothreitol [DTT], 4% SDS, 0.1% bromophenol blue, and 20%

glycerol) was added to samples, which were then boiled for 5 min. Proteins were resolved by SDS-polyacrylamide gel electrophoresis (SDS-PAGE) and transferred to PVDF membranes. Then, membranes were blocked with either 1% fat-free dried milk or bovine serum albumen (2.5%) in 1x Tris-buffered saline (TBS)–Tween 20 (0.05%, vol/vol) and incubated overnight at 4 °C with appropriate primary antibody at 1:1000 dilutions. After washing in 3x TBS-Tween 20, membranes were incubated with horseradish peroxidase-conjugated anti-rabbit IgGs antibodies, at 1:2000 dilutions (in all immunoblotting assays), in blocking buffer for 1 h. After washing in 3x TBS, the detection was performed by using enhanced chemiluminescence (ECL) [29].

Scanning Electron Microscopy (SEM)

Pre-osteoblasts were seeded on different titanium surfaces at the density of 5×10^4 cells/disc. After 4 h, cells were fixed with 2.5% of glutaraldehyde in 0.1 M phosphate buffer pH 7.3 for 24 h. They were immersed in osmium tetroxide 0.5% for 40 min, dehydrated with a series of alcohols, dried at a critical point, and finally metallized. Samples were studied using a Quanta 200 - FEI Company scanning electron microscope at an accelerating voltage of 12.5 kV.

Quantitative PCR assay (qPCR)

Cells were directly cultured on different texturized titanium surfaces and after 24 hours or 14 days, the total RNA was extracted from cells with Ambion TRIzol Reagent (Life Sciences - Fisher Scientific Inc, Walthan, MA, USA) and treated with DNase I (Invitrogen, Carlsband, CA, USA). cDNA synthesis was performed with High Capacity cDNA Reverse Transcription Kit (Applied Biosystems, Foster City, CA, USA) according to the manufacturer's instructions. qPCR was carried out in a total of 10 µl, containing PowerUp™ SYBR™ Green Master Mix 2x (5 µl) (Applied Biosystems, Foster City, CA, USA), 0.4 µM of each primer, 50 ng of cDNA and nuclease free H_2O. Results were expressed as relative amounts of the target gene using β-actin as inner reference gene (housekeeping gene), using the cycle threshold (Ct) method. Primers and details are described in **Table 1**.

Table 1. Expression primers sequences and qPCR cycle conditions.

Gene	Primer	5'-3' Sequence	Reactions Condition
MMP2	Forward	AACTTTGAGAAGGATGGCAAGT	95°C – 15min; 95°C – 15s; 60°C - 30s; 72°C - 20s
	Reverse	TGCCACCCATGGTAAACAA	
MMP9	Forward	TGTGCCCTGGAACTCACACGAC	95°C – 15min; 95°C – 15s; 60°C - 30s; 72°C - 20s
	Reverse	ACGTCGTCCACCTGGTTCACCT	
TIMP1	Forward	ATCCTCTTGTTGCTATCACTG	95°C – 15min; 95°C – 15s; 60°C - 30s; 72°C - 20s
	Reverse	GGTCTCGTTGATTTCTGGG	
TIMP2	Forward	GCAACAGGCGTTTTGCAATG	95°C – 15min; 95°C – 15s; 60°C - 30s; 72°C - 20s
	Reverse	CGGAATCCACCTCCTTCTCG	
RECK	Forward	CCTCAGTGAGCACAGTTCAGA	95°C – 15min; 95°C – 15s; 60°C - 30s; 72°C - 20s
	Reverse	CCTGTGGCATCCACGAAACT	
FAK	Forward	TCC ACC AAA GAA ACC ACC TC	95°C – 15min; 95°C – 15s; 60°C - 30s; 72°C - 20s
	Reverse	ACG GCT TGA CAC CCT CAT T	
Src	Forward	TCGTGAGGGAGAGTGAGAC	95°C – 15min; 95°C – 15s; 60°C - 30s; 72°C - 20s
	Reverse	GCGGGAGGTGATGTAGAAAC	
Integrin β1	Forward	TATCCTCCTGAGCGCCTTT	95°C – 15min; 95°C – 15s; 60°C - 30s; 72°C - 20s
	Reverse	TGGCCTTTTGAAGAATCCAA	
β-actin	Forward	TCTTGGGTATGGAATCCTGTG	95°C – 15min; 95°C – 15s; 60°C - 30s; 72°C - 20s
	Reverse	AGGTCTTTACGGATGTCAACG	

Activities of MMP were determined by a gelatin proteolysis-based zymography

The proteolytic activities of MMP-2 and MMP-9 in conditioned medium were assayed by gelatin-based zymography, widely used for this end. Conditioned medium was collected in response to the titanium surfaces or by cells in response to PP1 (5 μM), and later it was clarified by centrifugation 13,200 × g for 15 min at 4 °C, and stored at −20 °C. Samples were quantified using the Lowry protein assay (Lowry et al., 1956) and diluted in non-reducing buffer (0.1 M Tris–HCl, pH 6.8, 20% (v/v) glycerol, 1% (w/v) SDS, and 0.001% (w/v) bromophenol blue). Equal amounts of protein (75 μg) were loaded onto SDS–polyacrylamide gel (10% (w/v)) and 4% (w/v) gelatin. MMPs renaturation was performed in 2% (v/v) Triton X-100 for 40 min followed by incubation in incubation buffer [50 mM Tris–HCl and 10 mM CaCl2 (pH 7.4)] at 37 °C for 18 h. Afterwards, gels were stained with 0.5% (w/v) coomassie blue G 250 for 30 min, washed in a 30% (v/v) methanol and 10% (v/v) glacial acetic acid solution and then analyzed using ImageJ software.

Statistical analysis

Mean values and standard deviation obtained for each test were calculated, and one-way ANOVA was performed (alpha error type set to 0.05) when appropriate, with Bonferroni corrected post-test, or non-parametric analysis, using GraphPad Prysm 5 (GraphPad Software, USA).

3. Results

As reported previously elsewhere [17], there are considerable differences in the topography of the titanium-based surfaces evaluated in this study, mainly documented by atomic force microscopy (insert in **Fig. 1**). The topography modifications were decisive for wettability, which significantly impacts water contact angle (Mc=81.41 ± 0.01; DAE=97.18 ± 0.01; nHA=40.95 ± 0.02).

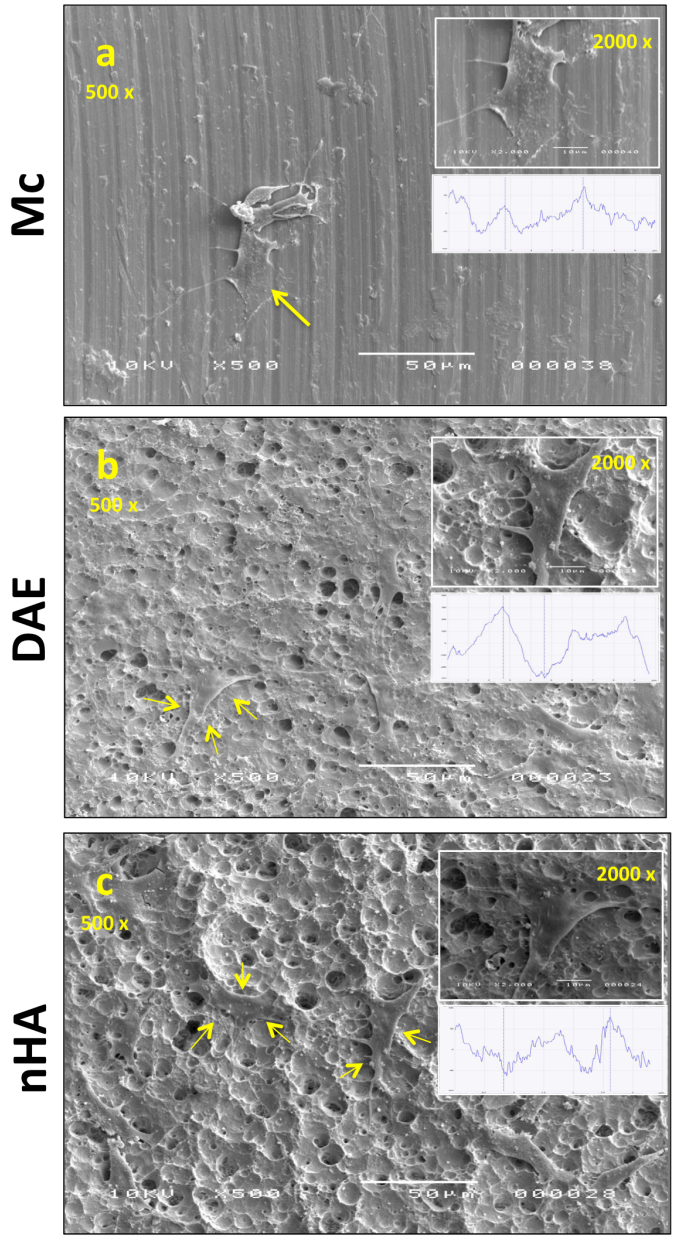

Fig.1. Ti-texturing surface properties and their impact on morphological changes of pre-osteoblast. The titanium topographies were investigated by atomic force microscopy (AFM; three-dimensional perspective image showing a 3×3 µm 2-field representation of Ti-texturing surfaces: Mc; DAE; and nHA). A fine roughness (nanometric scale) covers the surface of nHA and goes along with the micrometric roughness promoted by the dual acid-etching treatment (inserts in **a**; **b**; **c**). Thereafter, pre-osteoblasts were seed on the surfaces and 24 hours after seeding, the cell

morphology was acquired by Scanning Electron Microscopy (yellow arrows; **b**,**d**,**f**). Note the significant differences in cell behavior on those titanium-texturized surfaces.

Biointerface between pre-osteoblast and titanium-modified surfaces requires reprogramming of dynamic adhesion-related genes

Thereafter, we started with the biological characterization by seeding pre-osteoblast on all of those surfaces and after 24 hours of seeding. The pre-osteoblast morphology was evaluated to predict the quality of the pre-osteoblast/surface interactions (**Fig.1b;d;f**). Pre-osteoblast performed better on DAE or nHA at this stage, as they completely spread on the both surfaces (**Fig.1d;f**). To investigate whether the integrin-downstream pathway (**Fig.2a**) was required, the pre-osteoblast was seed on the surfaces, and 24 hours later the biological samples were harvested in order to study specific genes. Curiously, there was a significant decrease on the integrin-ß1 expression in response to DAE and nHA (**Fig.2b**). A similar profile was also found for FAK and Src genes (**Fig.2c,d**). Elsewhere, we reported a significant activation of Src and FAK in response to the same surfaces [17] and suggested the down-modulation of those genes might be regulated by a negative feedback. To validate this hypothesis, we treated the pre-osteoblast with a well-documented Src inhibitor (PP1), which promoted a significant down-regulation of Src at Y416 (**Fig.2e**). Our results confirmed a strong feedback of the Src activity on the integrin-based pathway, because integrin-ß1 (~5-fold changes), FAK (~12-fold changes), and Src (~3.5-fold changes) were significantly up-expressed when Src was chemically inhibited (**Fig.2f-h**). Here, cells not treated with PP1, but with vehicle, were considered the control.

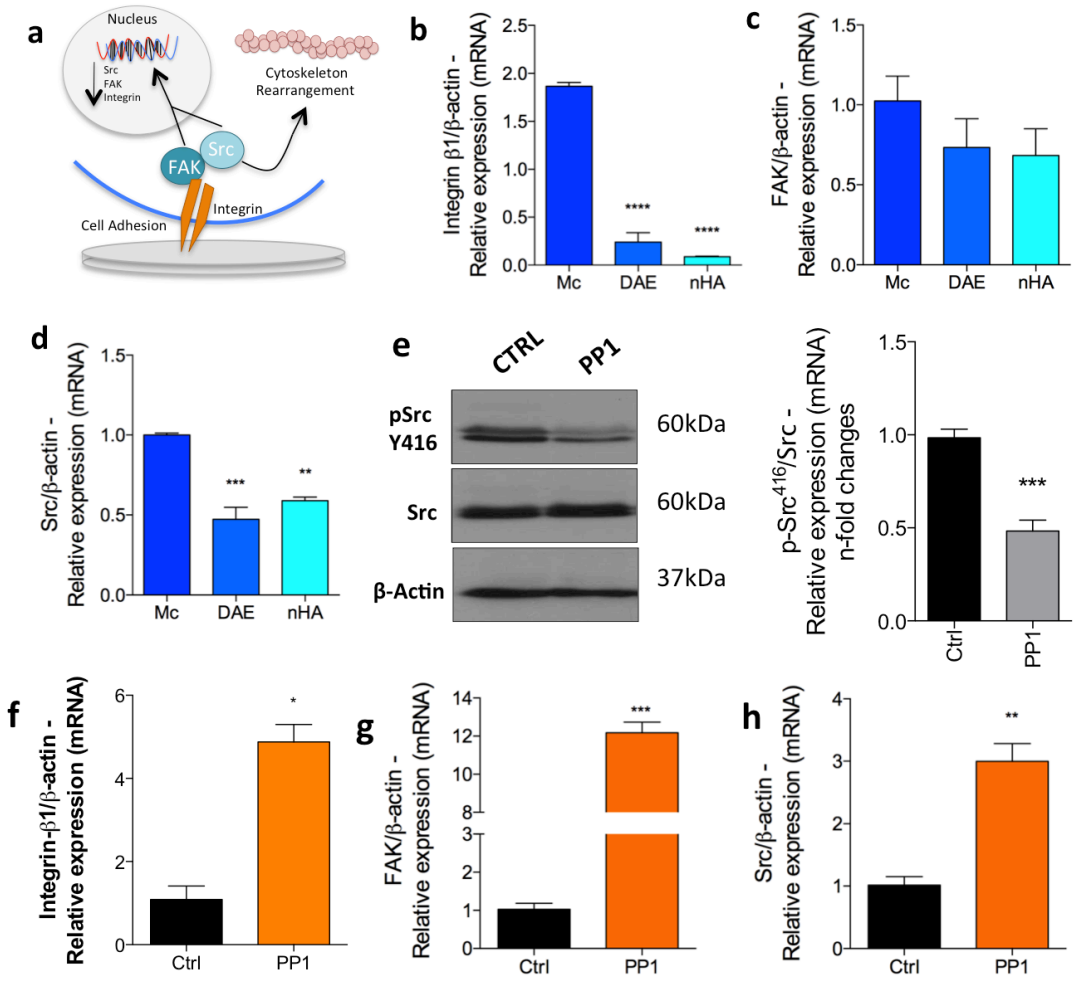

Fig. 2. Biointerface between pre-osteoblast and titanium-modified surfaces requires reprogramming of dynamic adhesion-related genes. a. Schematic depiction of the intracellular pathway evaluated in this study. Cells were seeded on different Ti-related surfaces. After 24 hours the total mRNA was collected and adhesion-related genes evaluated. Note the decrease of integrin-B1 (**b**), FAK (**c**) and Src (**d**). Previously, we reported the relevance of Src and FAK activations in response to titanium, and suggested a negative feedback, down-modulating both genes. To validate this hypothesis, we treated the pre-osteoblast with a well-documented Src inhibitor-PP1 (5 μM). We validated the effect of PP1 by reporting a down-phosphorylation of Src at Y416 (**e**). The Src activity is dependent on modulating integrin-B1 (**f**), FAK (**g**), and Src (**h**). All of those gene activations were evaluated by qPCR. The differences were significant when $p<0.05$.

Titanium-modified surfaces differentially orchestrate ECM remodeling-related genes

The titanium-related surfaces modulated the cell morphology and adhesion up to 24 hours; therefore, we decided to explore their relationship with the surfaces. MMPs and TIMPs were significantly involved in the establishment of the adequate

biointerface for the osteoblast phenotype (**Fig.3a-e**). Our results found increasing of MMP activities in response to both DAE and nHA (**Fig.3f-j**), and this biological effect is guaranteed by the significant decrease of tissue-inhibitor matrix metaloproteinases: TIMP1, TIMP2, and RECK (**Fig.3c-e,** respectively). As suggested previously for osteoblast adhesion, when MMPs-2 and -9 activities increase in the extracellular compartment, ECM remodeling-related genes seems to establish negative feedback on their respective MMP gene activation because both of them significantly decreased in response to DAE and nHA.

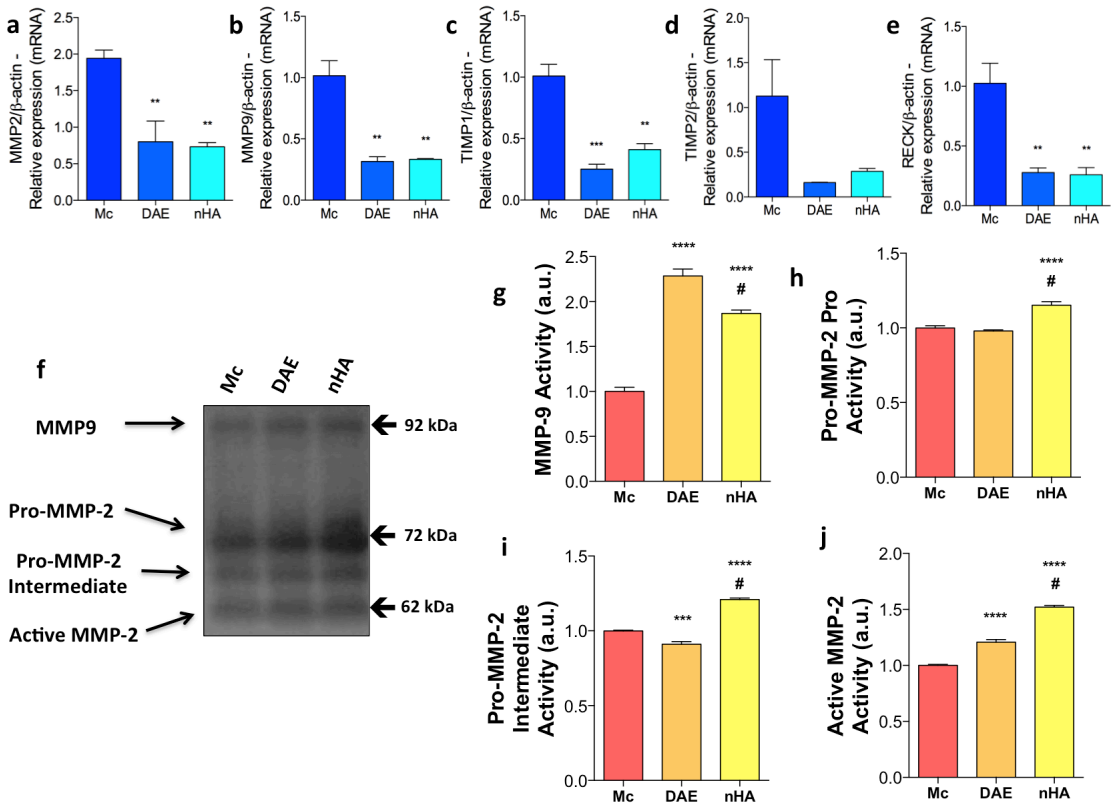

Fig. 3. Titanium-modified surfaces differentially orchestrate ECM remodeling-related genes. First, we investigated whether the titanium-texturized surfaces were also able to modulate MMP expressions, and found a down-regulation of both MMP-2 (**a**) and MMP-9 (**b**), although there is an increase on the both MMP activities (**f-j**). Then, we evaluated matrix metaloproteinase inhibitors - TIMPs -1, -2, and RECK - and all of those genes were down-modulated (**c**, **d**, and **e**, respectively), with the profile of the activation very similar between DAE and nHA. The differences were significant when $p<0.05$.

Src and ECM remodeling-related genes are hallmarks of direct and indirect effects of titanium-modified surfaces on pre-osteoblast behavior during osteogenic phenotype

In bone, it has been reported that ECM remodeling and Src are decisive during osteoblast differentiation [18,19]. Previously, we showed titanium-modified surfaces stimulate osteoblast differentiation in a direct contact manner. By exploring the same biological model (**Fig.4a**), we found here a significant increase of Src gene expression (**Fig.4b**), suggesting a direct feedback of the Src activity, which decreased as a pre-requisite for osteogenic phenotype [20]. On the other hand, in an indirect contact manner, Src gene expression significantly decreased in response to DAE and nHA (**Fig.4c**). Next, we investigated ECM-related gene MMPs and their tissue inhibitors in both direct and indirect manner up to 14 days *in vitro* (**Fig.4**). Curiously, all of the genes investigated were significantly up-modulated in response to DAE and nHA in a direct contact manner – specifically, MMP-2 and MMP-9 were up-modulated ~4 and ~10-fold changes, respectively, in response to DAE (**Fig.4d,e**) and ~2 and ~2.5-fold changes, respectively, in response to nHA (**Fig.4d,e**); while TIMP1 had ~10 and ~2.5-fold changes, in response to DAE (**Fig.4f**) and nHA (**Fig.4f**), respectively. TIMP2 had ~20 and ~10-fold changes, in response to DAE and nHA (**Fig.4g**), respectively. In addition, RECK, a membrane GPI-anchored protein, increased ~2.5-fold changes in response to DAE (**Fig.4h**), while it significantly decreased in response to nHA (**Fig.4h**). All of these analyses were made in comparison with Machined (Mc) surfaces.

Considering the indirect contact, we also found a decreased expression of the gene MMP-2 in response to both DAE and nHA, when compared with Mc (**Fig.4i**). In addition, modulation of MMP-9 depended on material properties; significantly increased (~2-fold changes) in response to DAE and significantly decreased in response to nHA (**Fig.4j**). TIMP1 slightly but not significantly increased (**Fig.4k**). However, TIMP2 was significantly up-modulated, reaching 20-fold change in response to DAE, and had an almost 10-fold increased in response to nHA (**Fig.4l**); while RECK was significantly decreased (**Fig.4m**).

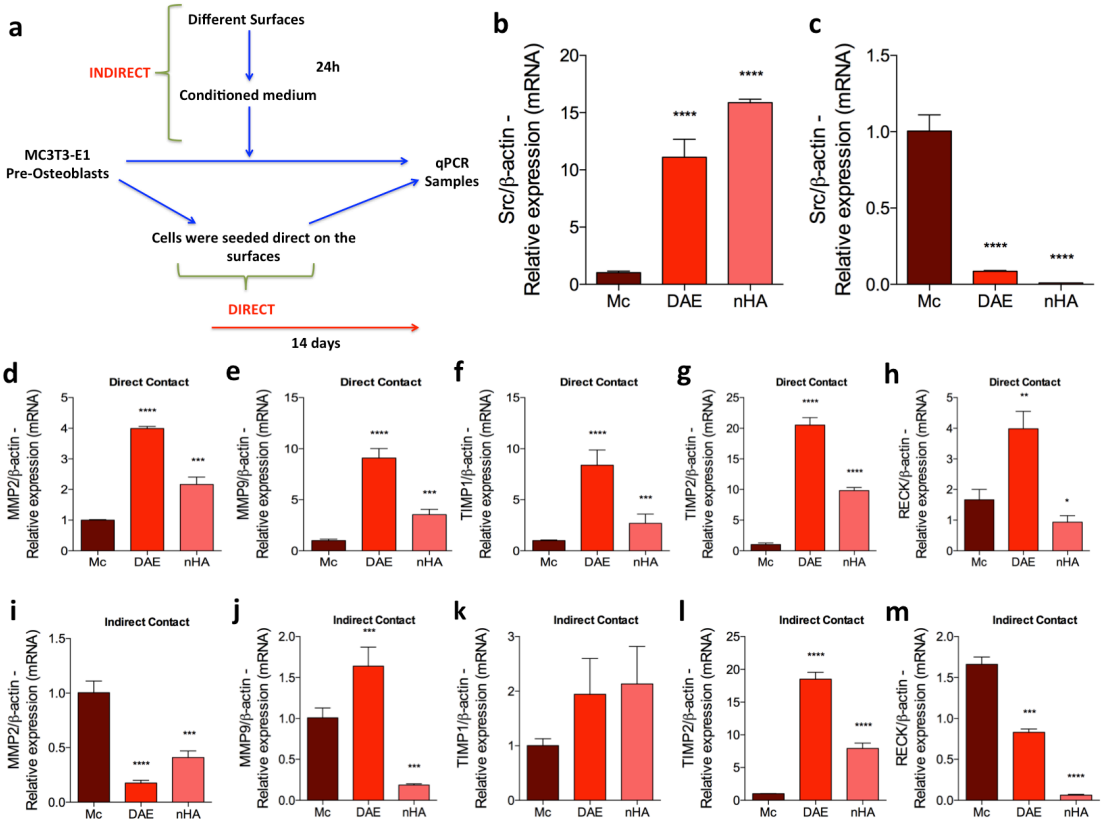

Fig 4. ECM remodeling-related genes and Src reprogramming are hallmarks of direct and indirect effects of titanium-modified surfaces on pre-osteoblast behavior. We focused on understanding the effect of the direct or indirect strategies on ECM-related genes and Src gene reprograming up to 14 days (**a**). Curiously there was an inverse behavior of Src gene activation: when direct contact promoted an increase of the gene expression (**b**), it significantly decreased (**c**) in a titanium-enriched medium (indirect way). We also investigated whether ECM remodeling-related genes were modulated and found a similar profile in the direct contact among the groups; it increased in response to DAE, for all genes investigated (**d-h**), while nHA stimulated an increase in comparison with Mc. With indirect contact, when titanium-enriched medium was considered, the response is even more dynamic; nHA stimulated an increase of TIMPs-1 and -2 (**k,l**), while MMP expression decreased (**i,j**) and RECK was down-regulated in response to both DAE and nHA (**m**). The differences were significant when $p<0.05$.

Importantly, we showed that PP1-inhibition of Src promoted a significant increase of both MMP expression (**Fig.5a,b)** and activity (**Fig.5c,f**).

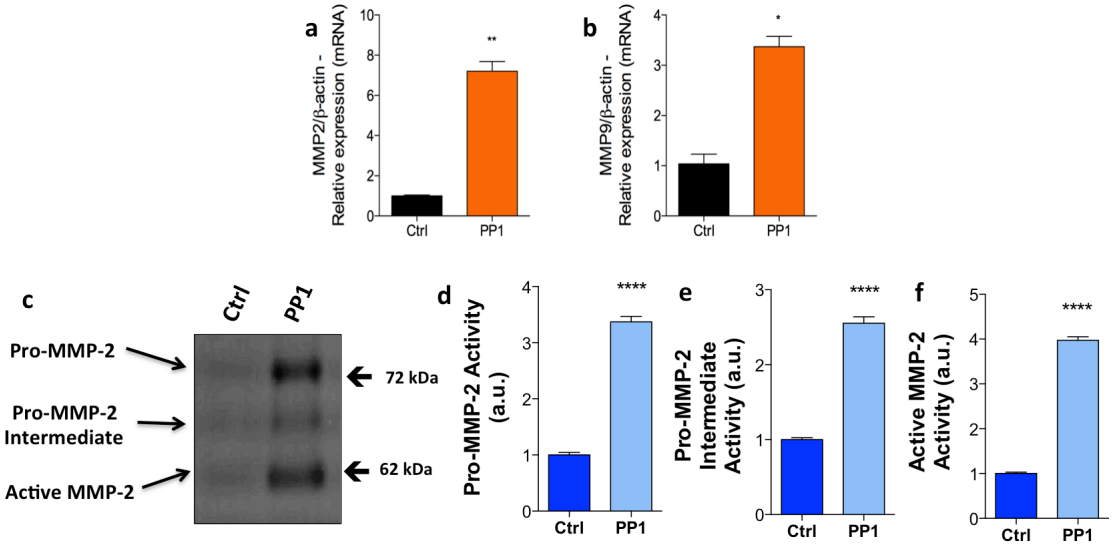

Fig 5. Src is a suppressor gene of MMP expression and activities. To analyze whether Src was able to modulate MMP processing, we subjected pre-osteoblast to PP1 (5 μM) for 24 hours and later the zymography was resolved by using the conditioned medium and the cell lysate used to evaluate gene expression. We found that PP1 promoted an increase of both expression (**a,b**) and activities (**c-f**). The differences were significant when $p<0.05$.

4. Discussion

Over the last 10 years, we have searched for alternative methods to understand the molecular biocompatibility of gold-standard biomaterials to guide biomedical engineering and reduce the number of experimental animals. In this sense, we have proposed cell signaling as a dynamic field to be considered [21,22]. In this work, three different surfaces were assayed: Machined (Mc), Dual acid-etching (DAE), and nano hydroxyapatite-blasted (nHA) groups. The nHA was obtained by adsorbing nanometer-scaled hydroxyapatite on the DAE-modified titanium surfaces [17,23]. First, the topography differences were characterized by atomic force microscopy and corroborated with those obtained previously by Bezerra et al. (2017). Thereafter, we investigated whether the topography could modulate pre-osteoblast morphological changes. The pre-osteoblast performed better on the nHA surfaces, maybe because this surface had a higher hydrophilicity than others, indicated by its smaller water contact angle. Another point to consider is the capacity of titanium-texturized surfaces

to adsorb serum protein, which is able to cause profound cell metabolic changes, as suggested by Zambuzzi's group [22,24].

In sequence, we investigated the molecular fingerprint of the biointerfaces promoted by titanium-modified surfaces, mainly related to cell adhesion (24 hours) and differentiation (10 days). The adhesion-related gene reprogramming revealed a significant decrease in integrin and Src expression in response to DAE and nHA. A reasonable explanation is that Src activity is significantly required during osteoblast adhesion on those surfaces and results in a negative feedback on Src expression. To obtain a better understanding of the participation of Src in this process, pre-osteoblasts were treated up to 24 h with PP1, a chemical Src-inhibitor, and the gene expression of integrin, FAK, and Src were reevaluated. The significant increase of the Integrin, FAK, and Src expression by chemically Src-inhibited pre-osteoblasts validated our hypothesis. In addition, as integrin and FAK are required for later Src activation, this increase in gene expression can be understood as a compensation mechanism for the maintenance of intracellular Src levels, because Src governs important intracellular pathways in osteoblast metabolism [7,20,25]. In addition, ECM remodeling-related genes were also evaluated. Our data showed that MMP activity is a titanium surface-dependent, where nHA stimulated higher MMP-2 and -9 activities of the released MMPs by activate osteoblasts, while their genes were down-regulated in response to both DAE and nHA. According to the same reasonable explanation used earlier, the high activity of MMP might promote a compensation feedback decreasing both MMP transcripts evaluated by qPCR technology. TIMPs were also down-regulated, favoring MMP activity presented. A possible mechanism suggests the involvement of integrin-dependent Src function during osteoblast adhesion, which can be considered a prerequisite to ECM-related genes.

Later, to analyze the possible involvement of Src and ECM remodeling process during the osteogenic phenotype acquisition, pre-osteoblastic cells were maintained in culture up to 10 days using two experimental strategies, direct and indirect contact. Src expression was higher in response to osteoblast under a direct adhesion on the titanium than those cells grown in a titanium-enriched medium, in indirect contact. Elsewhere we showed that titanium-based dental implants release considerable titanium amount when incubated in cell medium up to 24 hours in CO_2 incubator [23]. This titanium-

enriched medium promotes a considerable increase on Reactive Oxygen Species (ROS), culminating on phosphorylation balance governed by the decrease of the PTP activities (since PTPs have cysteine in the enzymatic active-site and cys-residue is very sensitive to oxidation) [23,26–28]. In addition, Fernandes et al. [26] found that ROS production is necessary during the first hours of pre-osteoblast adhesion and it guaranteed FAK and Src phosphorylations as an immediate consequence of the PTP oxidation.

In addition, we have proposed Src as indispensable transducers for osteoblast metabolism, governing their differentiation and osteogenic phenotype [7]. Previously, we found that Src activity decreases significantly (decrease of phosphoY416 and increase of phosphor-Y527) during osteoblast differentiation. Since osteoblast differentiation requires Src inhibition and nHA promotes osteoblast differentiation [17], we suggested the up-expression of the Src was due to compensation feedback, as reported earlier for Src during osteoblast adhesion (up to 24 hours) and MMPs. Importantly, we demonstrated that Src is necessary to govern cytoskeletal remodeling during osteoblast morphological changes [29].

Altogether these results demonstrate the crucial role of intracellular Src in ECM remodeling, and maybe a prerequisite to processing MMP. Thus, it is clear that Src performs a distinct role during osteoblast adhesion and differentiation.

5. Conclusion

This study showed that the molecular hallmarks involved with the pre-osteoblast relationship with different topography-based biointerface can govern Src-dependent osteoblast metabolism as a pre-requisite to ECM remodeling.

Acknowledgements

We would like to thank FAPESP (grant 2014/22689-3) and CNPq (Proc. Nr. 301966/2015-0) for the financial support. The authors are grateful to Dr. Giselle N. Fontes for her technical assistance with the AFM images and SIN Implants Co.

Competing financial interests

The authors declare no competing financial interests.

References

[1] K. Hamad, M. Kon, T. Hanawa, K. Yokoyama, Y. Miyamoto, K. Asaoka, Hydrothermal modification of titanium surface in calcium solutions., Biomaterials. 23 (2002) 2265–2272.

[2] P.G. Coelho, R. Jimbo, Osseointegration of metallic devices: current trends based on implant hardware design., Arch. Biochem. Biophys. 561 (2014) 99–108. doi:10.1016/j.abb.2014.06.033.

[3] Y. Dang, L. Zhang, W. Song, B. Chang, T. Han, Y. Zhang, L. Zhao, In vivo osseointegration of Ti implants with a strontium-containing nanotubular coating., Int. J. Nanomedicine. 11 (2016) 1003–1011. doi:10.2147/IJN.S102552.

[4] P. Trisi, M. Berardini, A. Falco, E. Sandrini, M.P. Vulpiani, A New Highly Hydrophilic Electrochemical Implant Titanium Surface: A Histological and Biomechanical In Vivo Study., Implant Dent. (2017). doi:10.1097/ID.0000000000000605.

[5] X.-Q. Fang, X.-F. Liu, L. Yao, C.-Q. Chen, J.-F. Lin, Z.-D. Gu, P.-H. Ni, X.-M. Zheng, Q.-S. Fan, Focal adhesion kinase regulates the phosphorylation protein tyrosine phosphatase-alpha at Tyr789 in breast cancer cells., Mol. Med. Rep. 11 (2015) 4303–4308. doi:10.3892/mmr.2015.3262.

[6] L. Chen, K. Shi, C.E. Frary, N. Ditzel, H. Hu, W. Qiu, M. Kassem, Inhibiting actin depolymerization enhances osteoblast differentiation and bone formation in human stromal stem cells., Stem Cell Res. 15 (2015) 281–289. doi:10.1016/j.scr.2015.06.009.

[7] W.F. Zambuzzi, R. Milani, A. Teti, Expanding the role of Src and protein-tyrosine phosphatases balance in modulating osteoblast metabolism: lessons from mice., Biochimie. 92 (2010) 327–332. doi:10.1016/j.biochi.2010.01.002.

[8] Z. Sun, S.S. Guo, R. Fassler, Integrin-mediated mechanotransduction., J. Cell Biol. 215 (2016) 445–456. doi:10.1083/jcb.201609037.

[9] H.Y. Kueh, W.M. Brieher, T.J. Mitchison, Dynamic stabilization of actin filaments., Proc. Natl. Acad. Sci. U. S. A. 105 (2008) 16531–16536. doi:10.1073/pnas.0807394105.

[10] I. Nishimura, Genetic networks in osseointegration., J. Dent. Res. 92 (2013) 109S–18S. doi:10.1177/0022034513504928.

[11] V.I. Shubayev, R. Branemark, J. Steinauer, R.R. Myers, Titanium implants induce expression of matrix metalloproteinases in bone during osseointegration, J. Rehabil. Res. Dev. 41 (2004) 757. doi:10.1682/JRRD.2003.07.0107.

[12] H.K. Rooprai, A.J. Martin, A. King, U.D. Appadu, H. Jones, R.P. Selway, R.W. Gullan, G.J. Pilkington, Comparative gene expression profiling of ADAMs, MMPs, TIMPs, EMMPRIN, EGF-R and VEGFA in low grade meningioma., Int. J. Oncol. 49 (2016) 2309–2318. doi:10.3892/ijo.2016.3739.

[13] K.B.S. Paiva, J.M. Granjeiro, Bone tissue remodeling and development: focus on matrix metalloproteinase functions., Arch. Biochem. Biophys. 561 (2014) 74–87. doi:10.1016/j.abb.2014.07.034.

[14] W.F. Zambuzzi, C.L. Yano, A.D.M. Cavagis, M.P. Peppelenbosch, J.M. Granjeiro, C. V Ferreira, Ascorbate-induced osteoblast differentiation recruits distinct MMP-inhibitors: RECK and TIMP-2., Mol. Cell. Biochem. 322 (2009) 143–150. doi:10.1007/s11010-008-9951-x.

[15] M. Gottlander, C.B. Johansson, A. Wennerberg, T. Albrektsson, S. Radin, P. Ducheyne, Bone tissue reactions to an electrophoretically applied calcium phosphate coating., Biomaterials. 18 (1997) 551–557.

[16] L. Meirelles, A. Arvidsson, M. Andersson, P. Kjellin, T. Albrektsson, A. Wennerberg, Nano hydroxyapatite structures influence early bone formation., J. Biomed. Mater. Res. A. 87 (2008) 299–307. doi:10.1002/jbm.a.31744.

[17] F. Bezerra, M.R. Ferreira, G.N. Fontes, C.J. da Costa Fernandes, D.C. Andia, N.C. Cruz, R.A. da Silva, W.F. Zambuzzi, Nano hydroxyapatite-blasted titanium surface affects pre-osteoblast morphology by modulating critical intracellular pathways., Biotechnol. Bioeng. (2017). doi:10.1002/bit.26310.

[18] T. Accorsi-Mendonca, K.B. da S. Paiva, W.F. Zambuzzi, T.M. Cestari, V.S. Lara, M.C. Sogayar, R. Taga, J.M. Granjeiro, Expression of matrix metalloproteinases-2 and -9 and RECK during alveolar bone regeneration in rat., J. Mol. Histol. 39 (2008) 201–208. doi:10.1007/s10735-007-9152-z.

[19] W.F. Zambuzzi, A. Bruni-Cardoso, J.M. Granjeiro, M.P. Peppelenbosch, H.F. de Carvalho, H. Aoyama, C.V. Ferreira, On the road to understanding of the osteoblast adhesion: cytoskeleton organization is rearranged by distinct signaling pathways., J. Cell. Biochem. 108 (2009) 134–144. doi:10.1002/jcb.22236.

[20] C. Palumbo, M. Ferretti, A. De Pol, Apoptosis during intramembranous ossification, J. Anat. 203 (2003) 589–598. doi:10.1046/j.1469-7580.2003.00247.x.

[21] C.J. da Costa Fernandes, A.S. do Nascimento, R.A. da Silva, W.F. Zambuzzi, Fibroblast contributes for osteoblastic phenotype in a MAPK-ERK and sonic hedgehog signaling-independent manner., Mol. Cell. Biochem. (2017). doi:10.1007/s11010-017-3083-0.

[22] B.C.J. van der Eerden, A. Teti, W.F. Zambuzzi, Bone, a dynamic and integrating

tissue., Arch. Biochem. Biophys. 561 (2014) 1–2. doi:10.1016/j.abb.2014.08.012.

[23] M.C. Rossi, F.J.B. Bezerra, R.A. Silva, B.P. Crulhas, C.J.C. Fernandes, A.S. Nascimento, V.A. Pedrosa, P. Padilha, W.F. Zambuzzi, Titanium-released from dental implant enhances pre-osteoblast adhesion by ROS modulating crucial intracellular pathways., J. Biomed. Mater. Res. A. (2017). doi:10.1002/jbm.a.36150.

[24] W.F. Zambuzzi, G.V.O. Fernandes, F.G. Iano, M. da S. Fernandes, J.M. Granjeiro, R.C. Oliveira, Exploring anorganic bovine bone granules as osteoblast carriers for bone bioengineering: a study in rat critical-size calvarial defects., Braz. Dent. J. 23 (2012) 315–321.

[25] W.F. Zambuzzi, J.M. Granjeiro, K. Parikh, S. Yuvaraj, M.P. Peppelenbosch, C. V Ferreira, Modulation of Src activity by low molecular weight protein tyrosine phosphatase during osteoblast differentiation., Cell. Physiol. Biochem. 22 (2008) 497–506. doi:10.1159/000185506.

[26] G.V.O. Fernandes, A.D.M. Cavagis, C. V Ferreira, B. Olej, M. de S. Leao, C.L. Yano, M. Peppelenbosch, J.M. Granjeiro, W.F. Zambuzzi, Osteoblast adhesion dynamics: a possible role for ROS and LMW-PTP., J. Cell. Biochem. 115 (2014) 1063–1069. doi:10.1002/jcb.24691.

[27] S. Bertazzo, W.F. Zambuzzi, D.D.P. Campos, T.L. Ogeda, C. V Ferreira, C.A. Bertran, Hydroxyapatite surface solubility and effect on cell adhesion., Colloids Surf. B. Biointerfaces. 78 (2010) 177–184. doi:10.1016/j.colsurfb.2010.02.027.

[28] S. Gemini-Piperni, R. Milani, S. Bertazzo, M. Peppelenbosch, E.R. Takamori, J.M. Granjeiro, C. V Ferreira, A. Teti, W. Zambuzzi, Kinome profiling of osteoblasts on hydroxyapatite opens new avenues on biomaterial cell signaling., Biotechnol. Bioeng. 111 (2014) 1900–1905. doi:10.1002/bit.25246.

[29] A. Marumoto, R. Milani, R.A. da Silva, C.J. da Costa Fernandes, J.M. Granjeiro, C.V. Ferreira, M.P. Peppelenbosch, W.F. Zambuzzi, Phosphoproteome analysis reveals a critical role for hedgehog signalling in osteoblast morphological transitions., Bone. 103 (2017) 55-63. doi: 10.1016/j.bone.2017.06.012.

Capítulo 4

CoCr ENRICHED MEDIUM MODULATES INTEGRIN-BASED DOWNSTREAM SIGNALING AND REQUIRES A SET OF INFLAMMATORY GENES REPROGRAMING *IN VITRO*.

Célio J. C. FERNANDES*, Fabio BEZERRA*, Maiara das D. do CARMO*; Georgia FELTRAN; Mariana C. ROSSI; Rodrigo A. da SILVA; Pedro de M. PADILHA; Willian F. ZAMBUZZI‡

Dept. of Chemistry and Biochemistry, Bioscience Institute, State University of São Paulo – UNESP, *campus* Botucatu, Botucatu, São Paulo, Brazil.

Fernandes CJC, Bezerra F, do Carmo MDD, Feltran G, Rossi MC, da Silva RA, Padilha PM, Zambuzzi WF. CoCr enriched medium modulates integrin-based downstream signaling and requires a set of inflammatory genes reprograming *in vitro*. **J Biomed Mater Res A.** 2017 Sep 22. doi: 10.1002/jbm.a.36244.

ABSTRACT

Significant health concerns have been raised by the high levels of Cr and Co ions into whole blood as resulted of corrosion process released from biomedical implants, but very little is known about their biological behavior in governing cell metabolism. Thus, we prompted to address this issue by exploring the effects of CoCr enriched medium on both fibroblast and pre-osteoblast (pre-Ob) cells. Firstly, we showed there is a significant difference in Co and Cr releasing dependent on engineered surface, it being even more released in dual acid-etching treating surface (named w/DAE) than the machined surfaces (named wo/DAE). Thereafter, we showed CoCr affects pre-osteoblast and fibroblast metabolism by dynamically modulating integrin-based downstream signaling (FAK, Src, Rac1 and Cofilin). Specifically on this matter, we have shown there is dynamic ß1-integrin gene activation up 24 hours in both pre-osteoblast and fibroblast. Our analysis showed also that both pre-Ob and fibroblast are important resource of pro-inflammatory cytokines when responding to CoCr enriched medium. In addition, survival-related signaling pathway was also affected interfering on survival and proliferating signal, mainly affecting CDK2, mapk-Erk and mapk-p38 phosphorylations, while AKT/PKB-related gene remained active. In addition, during cell adhesion PP2A (an important Ser/Thr phosphatase) was inactive in both cell lineages and it seems be a CoCr's molecular fingerprint, regulating specific metabolic pathways involved with cytoskeleton rearrangement. Altogether, our results showed for the first time CoCr affects cellular performance in vitro by modulating integrin activation-based downstream signaling and requiring a reprograming of inflammatory genes activations in vitro.

Keywords: CoCr alloys; Fibroblast; Pre-osteoblast; Cell Signaling; Survival Signaling.

1. INTRODUCTION

Over the last decades a large number of search for metallic materials capable of satisfying physic-chemistry and biological properties have been achieve in order to propose novel biomedical materials. Since 1960s, when Prof. Per-Ingvar Brånemark presented positive results by using animal studies with screw-shaped titanium implants [1], researches on this field have intensified on purposing modifications on titanium alloys, particularly in terms of biotechnological modification on their surfaces able to enhance biological performance surrounding those implanted devices. Among metallic alloys applied on health, cobalt-chromium (CoCr) has been used over the last decades, but very little is known about its biological behavior, mainly regarding that circulating elements released on whole blood, since it has been determined that these devices release metal debris from corrosion [2, 3]. Importantly, most of the living organisms require small amounts of microelements as cofactor to a set of enzyme activities. Specifically to Cr and Co, it is known they are found in trace amounts in the humans regulating a very small number of specific.

It is well-known that an increasing of concerns have been raised by the toxic levels of Cr and Co released by metal-on-metal bearing surface used worldwide in dental and orthopedic surgerie [4]. In order to understand the biological responses to biomaterial's enriched medium, we have depth worked on evaluating intracellular signal transduction to understand the molecular fingerprint of the cells during mechanisms of adhesion and spreading, mainly in response to biomaterials. Still on this sense, we have proposed downstream signaling upon integrin activating as a very interesting biological parameter to be applied in order to predict, *in vitro*, the quality of cell/substrate interaction [5–9].

Furthermore, very few studies have addressed the biological effect of released CoCr on mammal's cells *in vitro*. On this end, some studies have reported the cytotoxicity of cobalt on fibroblast and the ability of cobalt-chromium particles to induce inflammatory mediators realizing from macrophages [10, 11]. Interestingly, Berstein demonstrated cobalt inhibits cell growth of gingival epithelial cells [12]. In addition, other studies have been published reporting the *in vitro* effects of cobalt on several cell lineages [13, 14]. In this way, there is a necessity to understand how CoCr interfere on cell behavior and this prompted us to address this issue by investigating

the biological effect of CoCr enriched medium on both fibroblast and pre-osteoblast cells, mainly focusing on intracellular signal transducers.

Since pre-osteoblast adhesion is an early and crucial step to promote osteointegration of implantable devices [15–17], we decided to investigate whether those CoCr enriched medium was able to modulate both fibroblast and pre-osteoblast adhesion and their possible relationship with the adverse tissue reaction.

Altogether, our analysis reveals several biological mechanisms triggered by CoCr enriched medium leading to interfere of on metabolism of both fibroblast and pre-osteoblast up to first 24 hours of adhesion. Among the signaling proteins evaluated, it seems be required downstream signaling upon integrin activation and culminating on cofilin inactivation (by phosphorylating Sero3), while PP2A was up-phosphorylated at Y307. In addition, we showed an increase of the activation of inflammatory-related genes in response to CoCr enriched medium.

2. MATERIAL AND METHODS

CoCr alloys and reagents

The metallic CoCr-based discs were gently donated by the S.I.N. (São Paulo, SP, Brazil). The following antibodies were purchased from Cell Signaling (Danvers, MA, USA): β1-Integrin (D6S1W) Rabbit mAb (#34971, 135 kDa); Rac1/Cdc42 Antibody (#4651, 21 kDa); Phospho-Rac1/Cdc42 Antibody (#4651, 21 kDa); Cofilin (D59) Antibody (#3318, 19 kDa); Phospho-Cofilin (Ser3) Antibody (#3311, 19 kDa); Phospho-CDK2 Antibody (#2561, 33 kDa); GAPDH (14C10) Rabbit mAb (#2118, 37 kDa); Akt Antibody (#9272, 69 kDa); Erk (42,44 kDa), p-ERK (42,44 kDa) and JNK (46,54 kDa) (Phospho-MAPK Family Antibody Sampler Kit #9910). From Abcam (Cambridge, MA, USA): Anti-P38 (ab7952); Anti-P38 [phospho-T180+Y182] (ab4822); Anti-FAK (ab61113); Anti-FAK [phospho-Y576+Y577] (ab76244); Anti-PP2A alpha + beta antibody (ab137849); Anti-PP2A alpha + beta antibody [phospho-Y119] (ab32141); Anti-p15 (INK4b) (ab53034); Anti-p16 [EP1551Y] (ab51243).

Cell lines and culture conditions

NIH-3T3-E1 fibroblasts and pre-osteoblasts cells [MC3T3-E1 (subclone 4)] were maintained in RPMI and α-MEM, respectively; both containing antibiotics (100U/mL

penicillin, 100mg/mL streptomycin). Ribonucleosides and Deoxyribonucleosides were added to α-MEM. Both media was added 10% (v/v) Bovine Fetal Serum (Nutricell, Campinas, SP, Brazil). Cells were maintained in an incubator at 37°C, 5% CO_2, and 95% humidity.

In order to establish the CoCr enriched medium, experimental alloys (n = 6) were incubated in cell culture media (α-MEM or RPMI) up to 24 h [0.2g/mL (w/v); ISO 10993:2016). CoCr enriched medium contains molecules/particles potentially released from the metallic alloys. Thereafter, CoCr enriched medium was used to treat the cells up to 24 hours in order to determine its cytotoxicity, influence on cell adhesion, and ability to modulate the activation of signaling proteins related with cell adhesion and survival.

Cell viability assay

Samples were prepared according to ISO10993-12:2016, as used previously [18, 19]. Briefly, metallic discs were transferred to conic tubes containing culture media at a ratio of 0.2g/mL (w/v) and maintained into an incubator up 24 hours. Thereafter, extracts were collected and tested to know its cytotoxicity, as follows. The cells were then sub-cultured on 96-well plates ($5x10^4$ cells/mL) and at semiconfluence treated with 100 µL/well of CoCr enriched medium (n=20), plus 20 µL 10% FBS. An internal control was assayed by keeping the cells exposed solely to conventional culture conditions. After 24 h of exposing, the cytotoxic effects of each sample (extracts) or controls were evaluated by a MTT reduction. Reduced MTT by viable cells was solubilized with absolute alcohol and the absorbance measured at 570 nm (Synergy II; BioTek Instruments, USA).

Cell adhesion assay

To determine viable the attached cell profile in response to CoCr enriched medium, the violet crystal approach was performed for the both fibroblast and pre-osteoblast, as described by Bezerra et al. (2017) for this end. First, cells were trypsinized, suspended in appropriate medium (CoCr enriched medium or not), and re-plated ($50x10^4$ cells/mL) in 96 well plates. Rigorously after 3, 6 or 24 hours, the cell adhesion profile was measured by Violet Crystal approach [23], when the adhered cell's nuclei are stained.

Thereafter, the staining was solubilized properly and later the absorbance measured at 590nm by using a microplate reader (Synergy II, BioTek Instruments, USA).

Quantification of CoCr by graphite furnace atomic absorption spectrometry (GFAAS)

To test, 10 µL of each sample was followed to analysis of metalomic CoCr in the medium. The CoCr determination was carried out by GFAAS using a SHIMADZU model AA-6800 atomic absorption spectrometer. This spectrometer was equipped with a background absorption corrector with a self-reverse system (SR), a pyrolytic graphite tube with an integrated platform and an ASC-6100 automatic sampler. A Shimadzu hollow cathode CoCr lamp was used and operated at a minimum current of 12 mA and a maximum current of 400 mA (current used in background correction – BG). The wavelengths used were 240,7 nm and 357,9 nm for cobalt and chromium, respectively, and the spectral resolution was 0.5 nm. Argon was used as the inert gas, and a constant flow of 1 L min^{-1} was maintained during the entire heating program except for the atomization stage, during which the gas flow was stopped. The absorbance measurements (based on the peak area) were carried out in triplicate. The graphite tube's heating program optimized for CoCr determinations was based on the procedure described by Silva et al. (2006) [22] for chromium determination with some modification and it is described in following: Drying temperature – 120/250 °C; Pyrolysis temperature – 900/1400°C; Atomization temperature – 2600°C and Cleanup temperature – 2800°C.

Gene expression analysis

The biological samples were collected respecting as it was detailed earlier. Quantitative polymerase chain reaction (qPCR) was performed using a *QuantStudio® 3* Real-Time PCR System to assess changes in mRNA expression in the following genes reported in **Table 1**. Total RNA was extracted from cells with Ambion TRIzol Reagent (Life Sciences - Fisher Scientific Inc, Walthan, MA, USA) and treated with DNase I (Invitrogen, Carlsband, CA, USA). cDNA synthesis was performed with High Capacity cDNA Reverse Transcription Kit (Applied Biosystems, Foster City, CA) according to the manufacturer's instructions. qPCR was carried out in a total of 10µl, containing PowerUp™ SYBR™ Green Master Mix 2x (5 µl) (Applied Biosystems, Foster City, CA), 0.4 µM of each primer,

50 ng of cDNA and nuclease free H_2O. Fold changes were analyzed using the comparative CT method (ΔΔCt) normalizing to ß-actin (housekeeping gene) expression and comparing to static conditions as a reference.

Immunoblot

Activated cells in response to CoCr enriched medium were re-plated and after 24 hours of adhesion process, the cells were lysed (50 mM Tris-HCl, pH 7.4, 1% Tween 20, 0.25% Sodium deoxycholate, 150 mM NaCl, 1 mM EGTA, 1 mM *O*-Vanadate, 1 mM NaF, and protease inhibitors [1 µg/ml aprotinin, 10 µg/ml leupeptin and 1 mM aminoethyl fluorosilicon 4-fluoride hydrochloride]). The samples were sonicated (1 pulse per second) - SONICS Vibra-Cell. The protein extracts were centrifuged and the protein concentration determined by the Lowry method. After, the protein extracts was added 1:1 sample buffer (Sample buffer: 2X sodium dodecyl sulfate (SDS), 100 mM Tris-HCl [pH 6.8], 200 mM Dithiothreitol (DTT), 4% SDS, 0.1% bromophenol blue and 20% glycerol. The proteins were resolved into a SDS-PAGE and transferred to the PVDF membranes. The membranes-containing proteins were blocked with either 1% fat-free dried milk or bovine serum albumin (2.5%) in Tris-buffered saline (TBS) – Tween 20 (0.05%) and incubated overnight at 4 °C with appropriate primary antibody at 1:1000 dilutions. After washing in TBS-Tween 20 (0.05%), membranes were incubated with appropriate secondary antibodies, at 1:5000 dilutions (in all immunoblotting assays), in blocking buffer for 1h. Then, the protein's detections were performed using Enhanced ChemiLuminescence (ECL).

Statistical Analysis

Results were represented as mean ± standard deviation (SD). The samples assumed a normal distribution and they were subjected to student's t-test (2-tailed) with $p < 0.05$ considered statistically significant and $p < 0.001$ considered highly significant. In the experiment where there were > 2 groups, we used one-way ANOVA with post-test of Bonferroni, in order to compare all pairs of groups. In this case, the significance level was considered when alpha=0.05 (95% confidence interval). The software used was GraphPad Prism 6.

3. RESULTS

Releasing of CoCr at nanomolar concentration

First, the CoCr enriched medium was prepared as detailed previously. Before treating the cells with, we evaluated any content of cobalt and chromium in the CoCr enriched medium and our results clearly showed there is a significant increase on the amount of these elements (**Fig.1**), quantified by graphite furnace as described earlier.

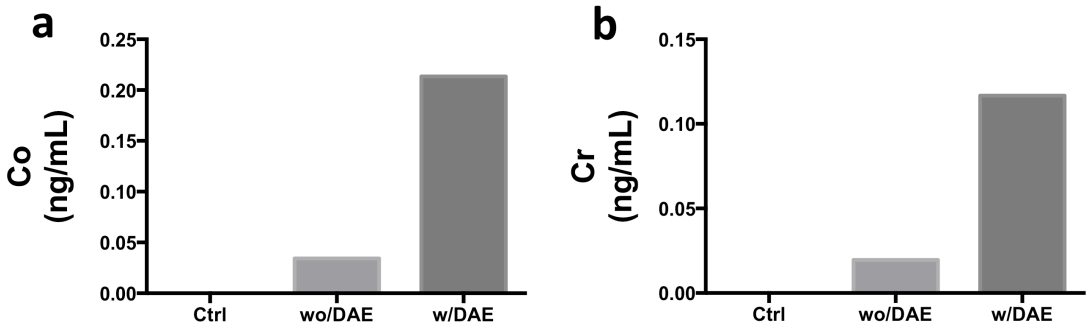

Fig. 1. Biomedical alloy releases Co- and Cr- at nanomolar concentration. The conditioned medium was taken for quantification of Co- and Cr- elements. Our results showed a significant increase of Co- and Cr- concentrations when considering its immediate control group. In addition, there was significance on Co- and Cr- releasing when 2 different surfaces were considered. Note: wo/DAE and w/DAE, without dual-acid etching and with dual-acid etching, respectively.

CoCr enriched medium affects pre-osteoblast adhesion by ß1-integrin molecular processing and signaling

Firstly, we have evaluated the effect of CoCr enriched medium on pre-osteoblast adhesion (**Fig. 2a-c**). We showed that CoCr enriched medium from alloy without DAE (wo/DAE) treatment significantly improved pre-osteoblast adhesion up to 24 hours (**Fig. 2c**). In this sense, any effect has been observed at 3 and 6 hours of adhesion time. In parallel, since ß1-integrin is required during osteoblast adhesion, we have checked ß1-integrin gene activation up to 24 hours. Our results showed there is a dynamic ß1-integrin gene activation during pre-osteoblast adhesion (**Fig. 2d-f**). Importantly, we have shown that w/DAE stimulates the gene activation earlier (6h) than wo/DAE (24h) and this genic processing is validated by using western blotting technology, when we have shown ß1-integrin protein amount was elevated in response to both kinds of CoCr alloys evaluated (**Fig. 2g-h**).

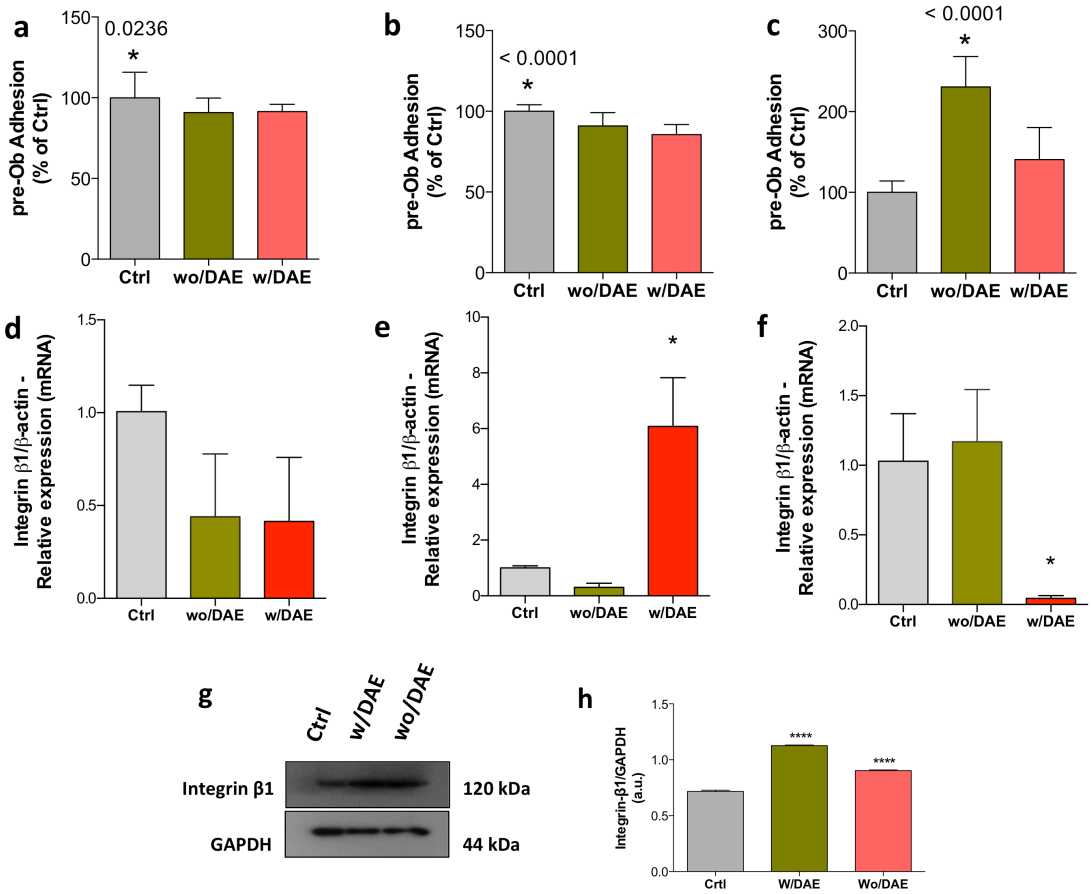

Fig. 2. ß1-integrin molecular processing during pre-osteoblast adhesion. Pre-Obs were maintained under classical culture conditions. In order to identify whether CoCr enriched medium interferes on pre-Ob adhesion, treated cells were trypsinized, counted and re-plated and the adherent cells were measured by using violet crystal at 3, 6 and 24 hours of adhesion time (**a-c**). Later, in order to evaluate the ß1-integrin molecular processing, we evaluated ß1-integrin gene activation by qPCR (**d-f**) and the protein profile by immunoblotting technology (**g-h**). GAPDH was used as an internal housekeeping control. Control group (Ctrl) was considered to be the cultured cells under normal conditions, without any treatment. Differences were considered significant when *p<0.05; ****p<0.0001.

Upon integrin activation, crucial signaling proteins are required: FAK and Src, triggering downstream signals culminating on cytoskeleton rearrangement (**Fig. 3a**). First on this regard, we have investigated whether both FAK and Src genes processing are required in response to CoCr enriched medium; FAK gene activating showed being down-regulated in response both w/DAE and wo/DAE up to 24 hours (**Fig. 3b**), while FAK protein was maintained active (**Fig. 3d,e**). Importantly, Src gene processing was

significantly up-expressed up to 24 hours (**Fig. 3c**). Src plays biphasic role in osteoblast metabolism during adhesion and differentiation (Zambuzzi et al., 2008).

In addition, immunoblots showed there is a downregulation on Rac1 phosphorylation and it being significant in response to wo/DAE (**Fig. 3f,g**). Also, a strong PP2A inactivation up to 24 hours of seeding in response to CoCr enriched medium was observed (**Fig. 3j,k**). In this meantime, cofilin, another cytoskeleton-related protein, was also evaluated, but any significant change was found (**Fig. 3h,i**).

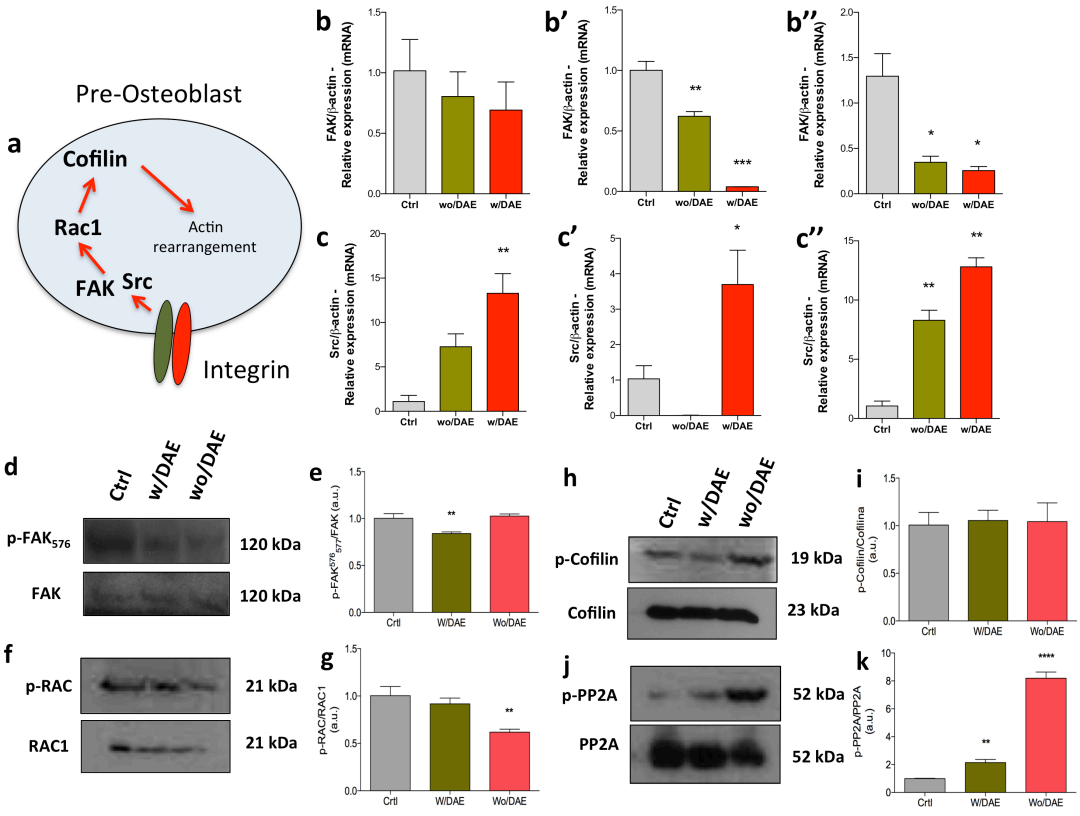

Fig. 3. Pre-osteoblast requires downstream signaling upon ß1-integrin activation in response to CoCr enriched medium. a. Schematization of the downstream signaling pathway upon integrin activation requiring sequentially phosphorylations of FAK, Src and Cofilin, culminating on cytoskeletal rearrangement-dependent cell adhesion. The graphs **b**, **b'**, **b''** bring the FAK gene activation during 3, 6 and 24 hours, respectively. In addition, the graphs **c**, **c'**, **c''** bring the Src gene activation during 3, 6 and 24 hours, respectively. Later, activation of FAK was also measured (**d,e**). Respecting the sequence of the downstream signaling pathway, Rac1 activation is shown (**f,g**), cofilin (**h,i**) and PP2A (**j,k**). GAPDH was used as an internal housekeeping control. Control group (Ctrl) was considered to be the cultured cells under normal conditions, without any treatment. Differences were considered significant when *p<0.05; **p<0.1906.

CoCr enriched medium up-modulates survival and proliferation pathways in pre-osteoblasts

Pre-osteoblasts were treated up to 24 hours with the CoCr enriched medium and any cytotoxic effects observed (**Fig.4a**). Thereafter, this previous result was tested by evaluating the expression of survival pathways transducers such as AKT (**Fig.4f,g**), JNK (**Fig.4f,i**) and MAPKs (**Fig.4b-e**) in response to CoCr enriched medium (**Fig.4d-g)**. All of them were up-modulated in response to both w/DAE and wo/DAE. Specific on regard MAPKs, our results showed both Mapk-38 and Mapk-ERK were significantly up-phosphorylated in response to wo/DAE. Importantly, at this fashion, we reported a significant CDK2 up-phosphorylation (**Fig.4f,h)**, while p15 was down-modulated (**Fig.4f,j)** and p16 was up-modulated in response to wo/DAE (**Fig.4f,k).**

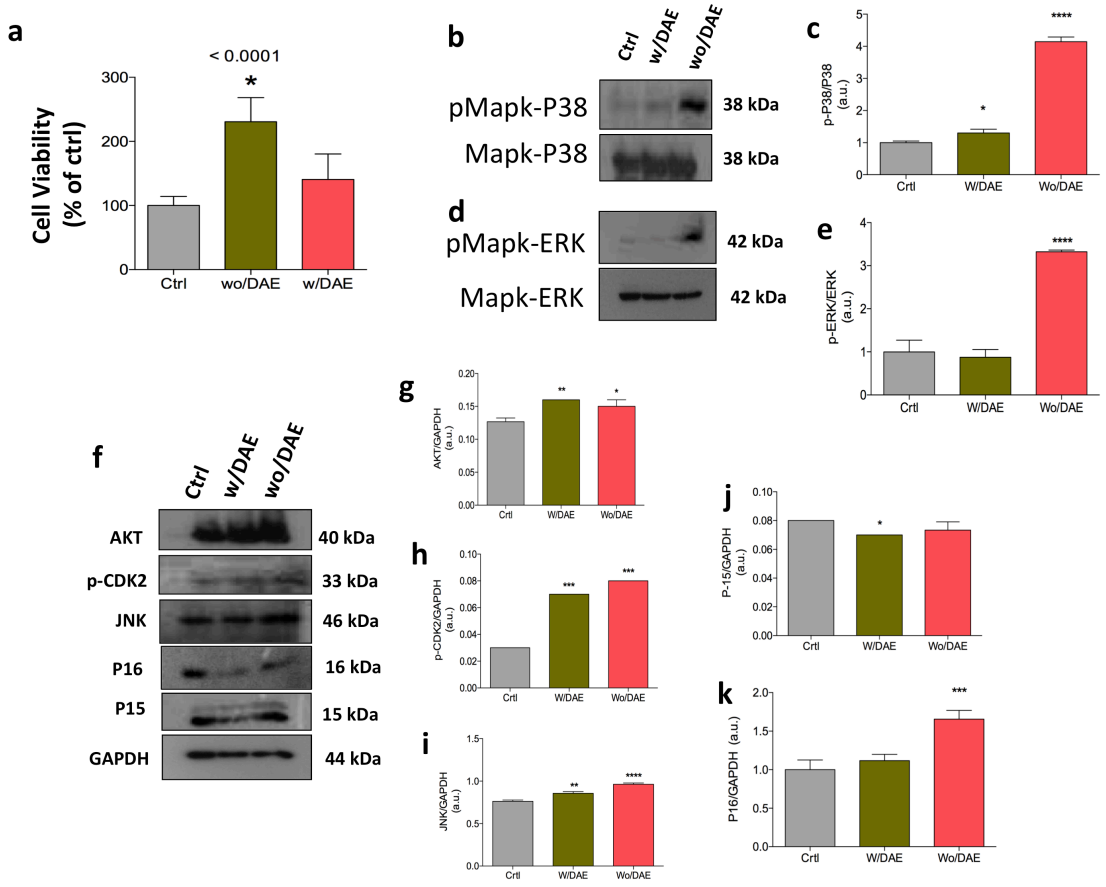

Fig. 4. CoCr modulates survival/proliferation intracellular pathways in pre-osteoblast. a. Firstly, CoCr enriched medium does not promote any cytotoxicity (**a**). At the same time, biological samples were collected to perform western blottings analysis for mapk-p38 (**b,c**), mapk-Erk (**d,e**), AKT (**f,g**), phospho-CDK2 (**f,h**), JNK (**f,i**), p16 (**f,j**), p15 (**f,k**), when representative blots were shown. Graphs show arbitrary values obtained from densitometric analysis of the specific bands normalized by the average values of the respective housekeeping-loading sample (GADPH). Control group (Ctrl) was considered to be the cultured cells under normal conditions, without any treatment. Differences were considered significant when *p<0.05; **p<0.1906; ***p<0.0002; ****p<0.0001.

CoCr enriched medium modulates fibroblast metabolism by guarantying cofilin phosphorylation

As fibroblast growth surrounding implanted devices is a key event to consider, we also investigated the effect of released CoCr on fibroblast phenotype. Firstly, our results showed significant decreased of fibroblast adhesion, estimated by a colorimetric assay (**Fig.5a-c).** Also, we evaluated the ß1-integrin gene activation by

quantifying its transcripts up to 24 hours. In general, it seems being a down regulation on its expression without any significance (**Fig.5d-f)**, except in response to wo/DAE at 6 hours (**Fig.5e),** when it was significantly down-expressed. However, it is important to consider that ß1-integrin protein was also investigated by immunoblotting technology and curiously it was up-expressed (**Fig.5g,h)**, suggesting there is a post-transcriptional processing of mRNA responsible to guarantee fibroblast adhesion.

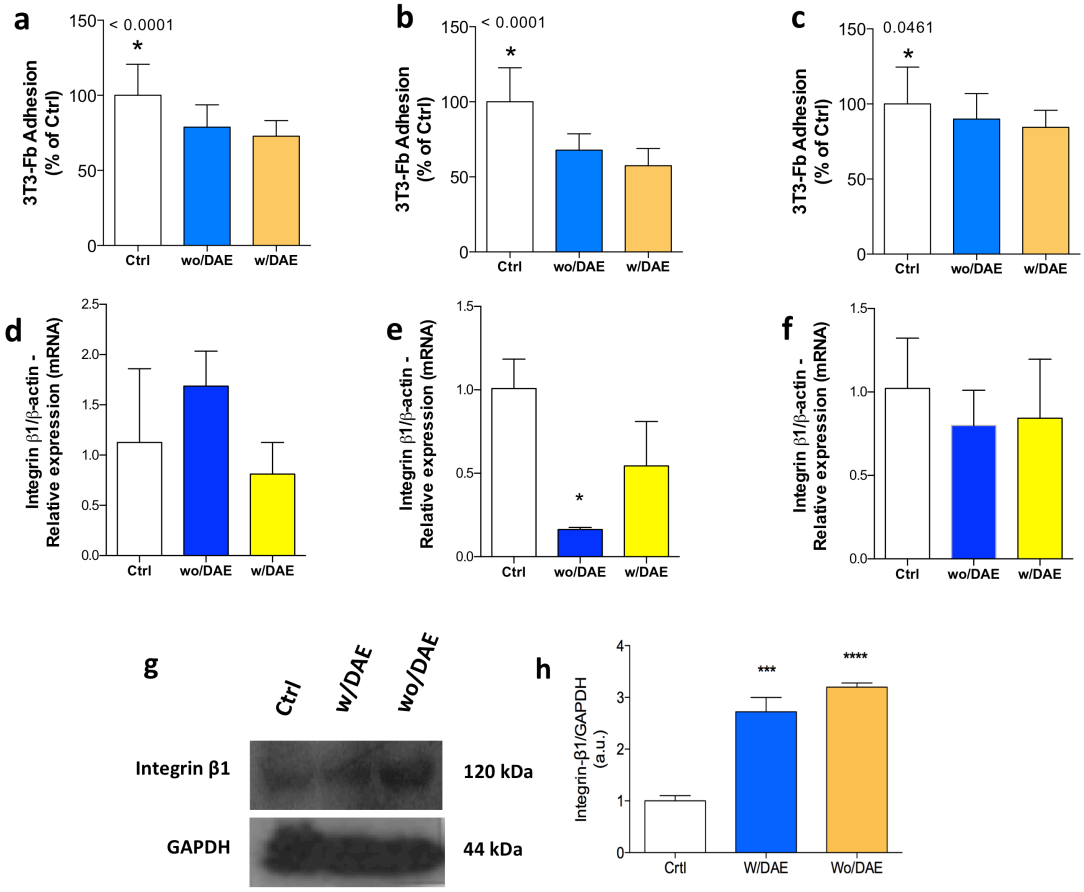

Fig. 5. CoCr enriched medium requiring a dynamic ß1-integrin molecular processing during fibroblast adhesion. Fibroblasts were maintained under classical culture conditions. In order to identify whether CoCr enriched medium interferes on Fibroblast adhesion, treated cells were trypsinized, counted and re-plated and the adherent cells were measured by using violet crystal at 3, 6 and 24 hours of adhesion time (**a-c)**. Later, in order to evaluate the ß1-integrin molecular processing, we evaluated ß1-integrin gene activation by qPCR (**d-f**) and the protein profile by immunoblotting technology (**g-h**). GAPDH was used as an internal housekeeping control. Control group (Ctrl) was considered to be the cultured cells under normal conditions, without any treatment. Differences were considered significant when *p<0.05; ***p<0.0002; ****p<0.0001.

Later, we evaluated the downstream signaling upon integrin activation (**Fig.6a).** Firstly on this matter, we showed there is an up-expression of FAK at 24 hours of seeding in response to wo/DAE condition (**Fig.6b).** In addition, Src showed being down-expressed in response to CoCr enriched medium, independently whether w/DAE or wo/DAE (**Fig.6c).** Thereafter, we also showed that FAK was up-phosphorylated in response to CoCr enriched medium (**Fig.6d,e)** and this profile of phosphorylation was maintained to Cofilin (**Fig.6f,g)** and PP2A (**Fig.6h,i).**

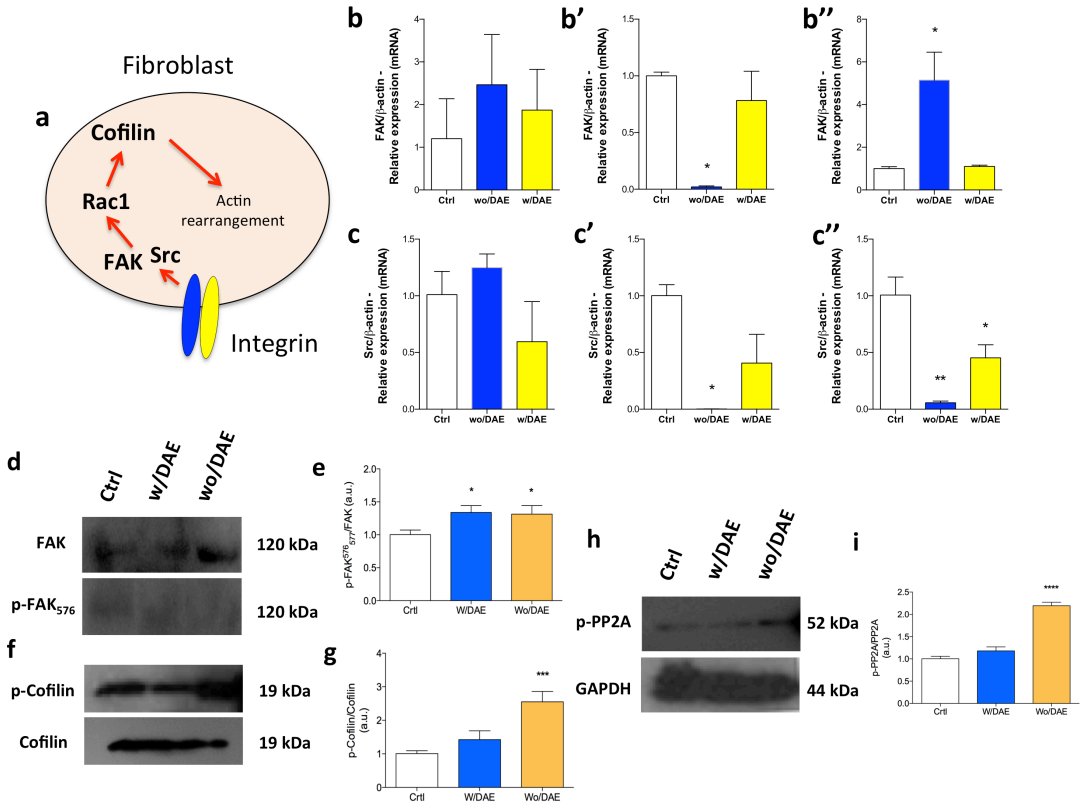

Fig. 6. Fibroblast dynamically requires downstream transducers upon ß1-integrin activation up to 24 hours of adhesion process. a. Schematization of the downstream signaling pathway upon integrin activation requiring sequentially phosphorylations of FAK, Src and Cofilin, culminating on cytoskeletal rearrangement-dependent cell adhesion. The graphs **b**, **b'**, **b''** bring the FAK gene activation during 3, 6 and 24 hours, respectively. In addition, the graphs **c**, **c'**, **c''** bring the Src gene activation during 3, 6 and 24 hours, respectively. Later, activation of FAK was also measured (**d,e**). Respecting the sequence of the downstream signaling pathway cofilin (**f,g**) and PP2A (**h,i**). GAPDH was used as an internal housekeeping control. Control group (Ctrl) was considered to be the cultured cells under normal conditions, without any treatment. Differences were considered significant when *p<0.05; **p<0.1906; ***p<0.0002; ****p<0.0001.

Finally, we have shown that CoCr enriched medium did not promote any cytotoxic effects of fibroblast (Supplemental data, **S1**), while phosphorylation of Mapk-p38 and expression of p15 were decreased in response to both CoCr enriched medium evaluated (Supplemental data, **S1**).

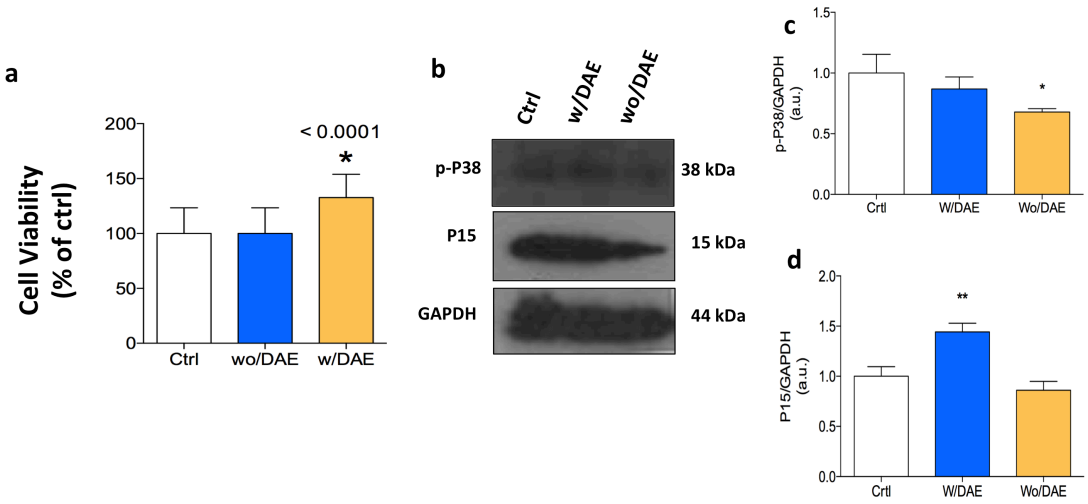

Fig. S1. CoCr enriched medium modulates survival profile in fibroblasts. a. Firstly, CoCr enriched medium does not promote any cytotoxicity. At the same time, biological samples were collected to perform western blottings analysis for mapk-p38 (**b,c**) and p15 (**b,d**), when representative blots were shown. Graphs show arbitrary values obtained from densitometric analysis of the specific bands normalized by the average values of the respective housekeeping-loading sample (GADPH). Control group (Ctrl) was considered to be the cultured cells under normal conditions, without any treatment. Differences were considered significant when *p<0.05; **p<0.1906.

Both pre-Osteoblast (pre-Ob) and fibroblast are sources of pro-inflammatory molecules in response to CoCr enriched medium

As inflammatory response is required for the first stages of healing process we decided to study TNFα and interleukins expression by both pre-Ob and fibroblasts in response to CoCr enriched medium. Our results showed both fibroblast and pre-Ob are important source of all molecules studied in a very dynamic processing up to 24 hours of seeding. Firstly, we showed pre-Ob significantly over-expressed TNFα (**Fig.7a)** at 24 hours (3 and 6 hours, see Supplemental data, **S2**) in response to w/DAE, also up-modulating the ILs-10 (**Fig.7c)**, -33 (**Fig.7d)**, -13 (**Fig.7f)** and 1ß (**Fig.7g)**, while ILs -18

(**Fig.7e)** and -16 (**Fig.7b)** were down-modulated.

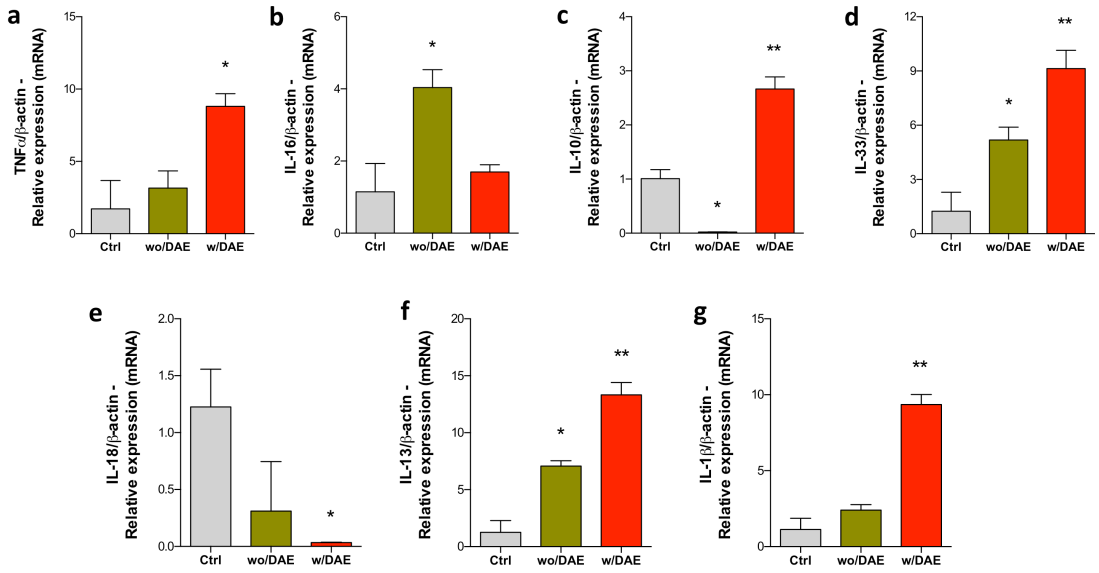

Fig. 7. CoCr enriched medium modulates the reprograming of inflammatory-related genes activation in pre-osteoblasts. As mentioned previously, the pre-Obs were maintained under classical culture routine. Pre-Obs were treated with CoCr enriched medium up to 24 hours, when the cells were harvested in TriZOL in order to purify mRNA used later to cDNA synthesis. We have investigated the quantification of TNF-α **(a)**, IL-16 **(b)**, IL-10 **(c)**, IL-33 **(d)**, IL18 **(e)**, IL-13 **(f)** and IL-1β **(g)**. Curiously, the most inflammatory genes evaluated were up-expressed; conversely, IL-18 was down-modulated in response to CoCr enriched medium. All analyzes were normalized by the internal control β-actin and *p<0.05; **p<0.1906.

In mechanism to promote paracrine and/or autocrine signaling during mechanism of tissue repair, we showed that fibroblasts up-expressed TNFα at 24 hours (3 and 6 hours, see Supplemental data, **S3**), also up-modulating ILs-16, -10, -33, -13, and -1ß (**Fig.8)**; conversely IL-18 was down-expressed (**Fig.8e).**

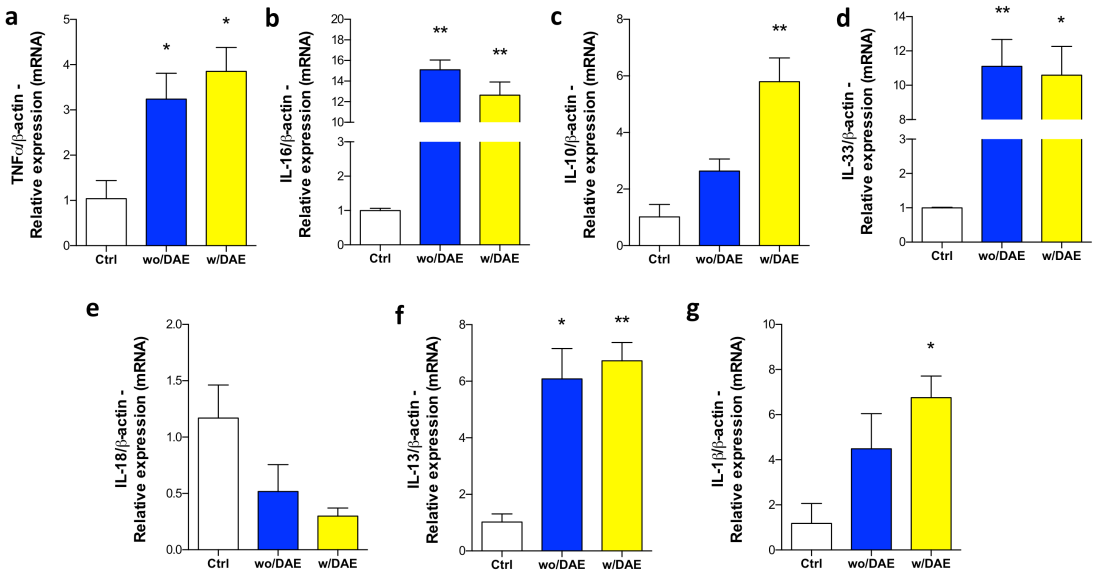

Fig. 8. Fibroblast seems being an important inflammatory cytokines source in response to CoCr enriched medium. Fibroblasts were treated with CoCr enriched medium up to 24 hours, when the cells were harvested in TriZOL in order to purify mRNA used later to cDNA synthesis, as detailed earlier. Likely to pre-Obs, we have investigated the quantification of TNF-α **(a)**, IL-16 **(b)**, IL-10 **(c)**, IL-33 **(d)**, IL18 **(e)**, IL-13 **(f)** and IL-1β **(g)**. Likely, IL-18 was not required in response to CoCr enriched medium. All analyzes were normalized by the internal control β-actin and *p<0.05; **p<0.1906.

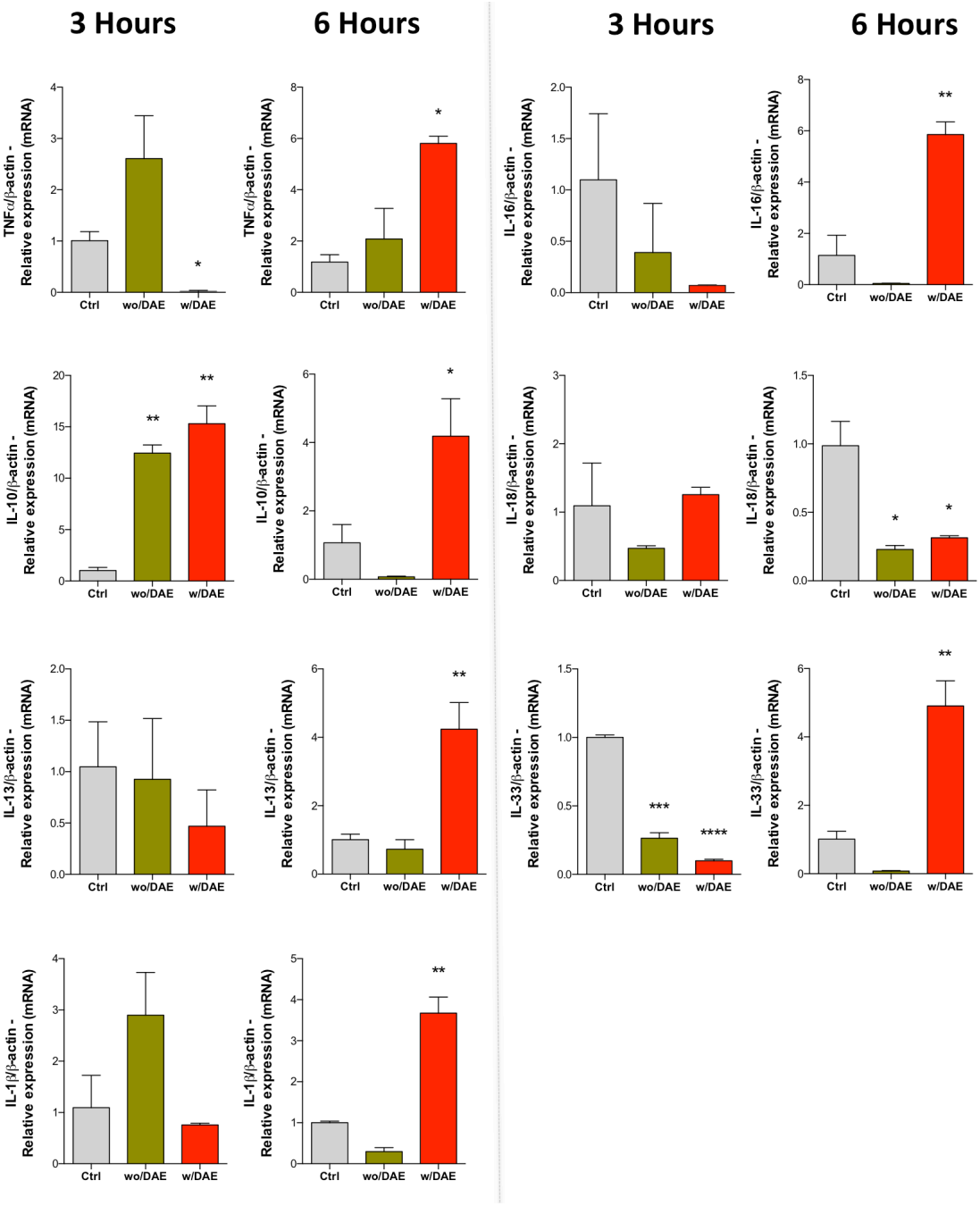

Fig. S2. CoCr enriched medium modulates the reprograming of inflammatory-related genes activation in the first 3 and 6 hours of pre-osteoblasts adhesion. As mentioned previously, the pre-Obs were maintained under classical culture routine. TNF-α, IL-16, IL-10, IL-33, IL18, IL-13 and IL-1β were here investigated. All analyzes were normalized by the internal control β-actin and *p<0.05; **p<0.1906.

4. DISCUSSION

Over the last years, the perfect harmony between implanted devices and surrounding tissues has been an important topic to be addressed, since metal-based implants continuously release micrometer and nanometer-sized wear debris, due to the tribocorrosion of the bearing surfaces [20]. These released debris are mostly colloidal CrCo alloys and likely some oxides (Cr_2O_3 and CoO). Thus, it is reasonable to purpose methodologies to better understand their biological outcomes.

In this scenario, *in vitro* approaches bring interesting methodological tools to investigate novel and potential biomaterials, serving as a preliminary screening to identify important biological responses as cytotoxicity and molecular processing. Exploring this topic, our group has suggested signaling pathways as an emerging field to be applied on biomaterials developmental for identifying biomarkers on cell behavior in response to them *in vitro* [9, 19, 18, 21] . Applying this reasonable experimental flow, we investigated the effect of chromium (Cr) and cobalt (Co) enriched medium on pre-osteoblast and fibroblast behavior by exploring signaling proteins related with intracellular pathways culminating on different cell fate, such as adhesion, proliferation, survival and capacity to activate inflammatory-related genes. There is interest in identifying CoCr effects on cellular metabolism their possible toxic effects because it is very known that arthroplasties are responsible to considerably increase levels of Co and Cr into circulating blood [22–29]. Thus, to develop methodologies to better understand the biological effect of CoCr enriched medium on mammal's cells is urgently required.

By exploring biological performance of the both pre-osteoblast and fibroblast in response to released factors from CoCr alloys, we showed there is a similarity on both cell lineages regarding mechanism of cell attachment, requiring downstream signaling upon integrin activation. Importantly, this biological event can be justified by differential ß1-integrin expression promoted by CoCr. As it is well-known, integrin family members are membrane-associated receptors reported with a variety of cell phenotype, ranging since adhesion to recognition in a variety of biological processes including embryogenesis and tissue repair [16]. Mechanistically, integrins are associated with cytoskeleton and extracellular matrix, maintaining a crosstalk between them [30–32]. In this scenario, we have previously showed integrins as important

receptors to governing the first hours of pre-osteoblast adhesion by culminating with a well-orchestrated cytoskeleton rearrangement, mainly upon FAK signaling [8, 9]. In this present work, we showed CoCr stimulates a similar mechanism since it promotes a rigorous downstream signaling culminating cofilin phosphorylation, a decisive protein governing actin rearrangement. Also on this hand, PP2A was inactive in response to CoCr, contributing to cofilin phosphorylation during pre-osteoblast adhesion, since PP2A is a Ser/Thr phosphatase able to hydrolyze phosphorylated Sero3 residue of Cofilin [33, 34], independent to the down-phosphorylation of Rac1.

We have showed over the last 10 years that both FAK and Src are relevant transducers required during osteoblast adhesion [5, 35, 36]. Here, we explored the both FAK and Src gene activations in response to CoCr enriched medium. Our analysis showed there is decrease of the gene expressions of both FAK and Src; disagreement, for pre-osteoblast, there was a decrease of FAK expression, while the Src expression was significantly up-expressed. Importantly to mention that Src plays well-known role during osteoblast differentiation [5, 6] and maybe this increase could be a prerequisite to osteoblastic maturation in response to CoCr enriched medium.

As a second mechanism, we showed CoCr promotes a differential requirement of protein-related cell survival/proliferating process. In this sense, our data showed that CoCr up-modulates activation of mapks-Erk and p38 in pre-osteoblast, culminating to up-activation of CDK2, a well-known protein related with cell cycle progression [37], when Akt was significantly up-expressed. It is very important to mention pre-osteoblast performance is required for bone-implanted devices [8], since osteoblasts form surrounding bone and positively impact their osteointegration.

As a third mechanism, our analysis showed that pro-inflammatory genes (TNFα, IL-16, IL-10, IL-33, IL-18, IL-13, IL-1ß) were up-activated in response to CoCr enriched medium in both pre-osteoblast and fibroblast, it being much more significant in fibroblast. [38] Caicedo et al (2009) showed that cobalt, molybdenum ions, and Co-Cr-Mo alloy particles similarly induce elevated secretion of IL-1β, TNFα, and IL-6, suggesting that metal-induced up-regulation of co-stimulatory molecules and pro-inflammatory cytokine production is necessary to induce lymphocyte activation/proliferation to metal implant debris. Likely, our results showed that fibroblast and pre-osteoblast contribute to this event as they being an important

resource to inflammatory cytokines. As IL-33 and IL-1ß are later processed by a inflammasome-dependent pathway [39] and they are significantly up-expressed in response to CoCr enriched medium, we can suggest the involvement of the inflammasome, however, a more detailed methodological approaches need to be applied to conclude on this matter.

Altogether, our analysis reveals several biological mechanisms triggered by CoCr enriched medium in both fibroblast and pre-osteoblast interfering on their attachment and capacity to express inflammatory cytokines. We can also suggest that these molecular mechanisms could affect cell phenotype surround to the implants, compromising their performance during mechanism of tissue repair.

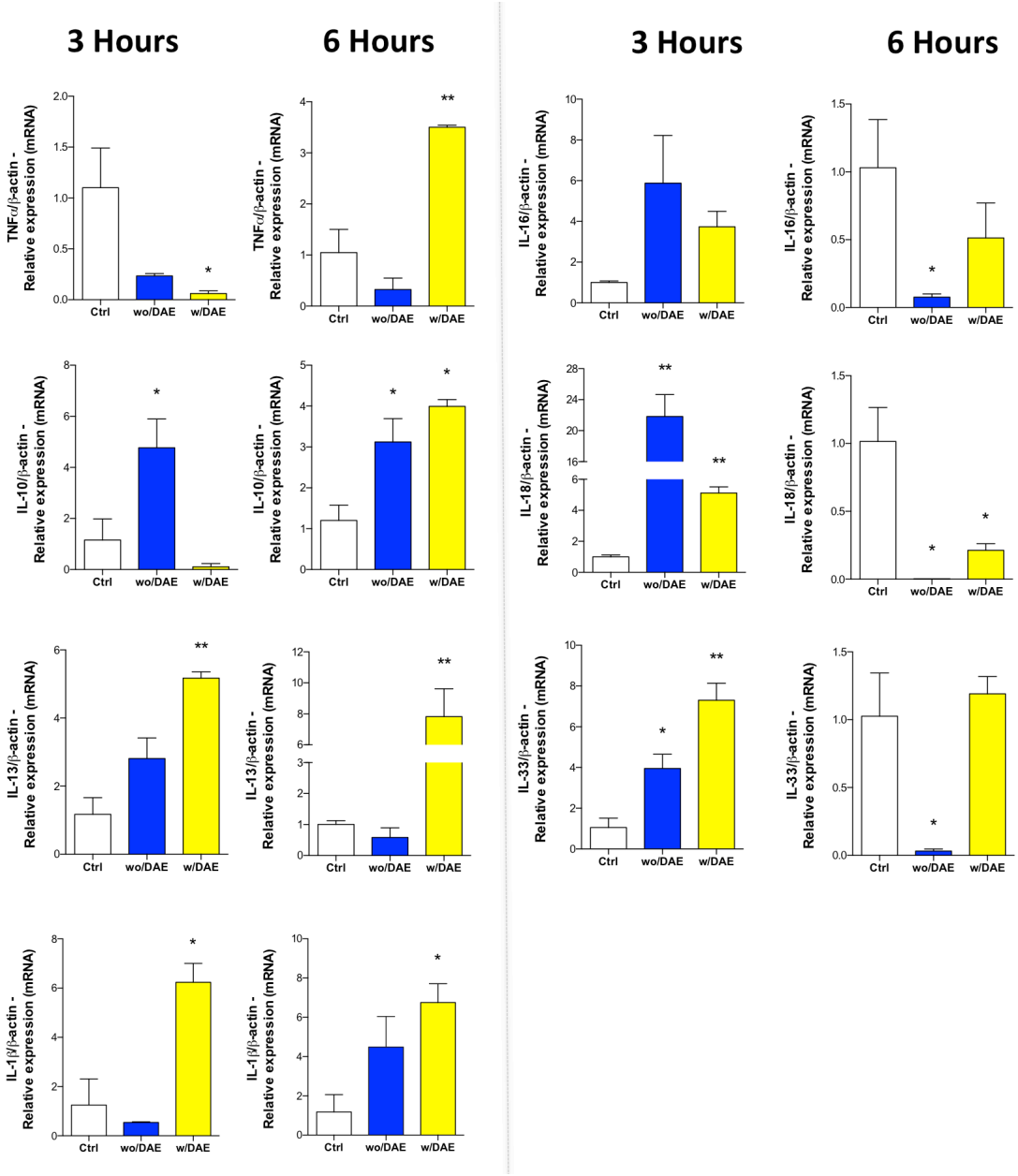

Fig. S3. CoCr enriched medium modulates the reprograming of inflammatory-related genes activation in the first 3 and 6 hours of fibroblast adhesion. As mentioned previously, the fibroblasts were maintained under classical culture routine. TNF-α, IL-16, IL-10, IL-33, IL18, IL-13 and IL-1β were here investigated. All analyzes were normalized by the internal control β-actin and *p<0.05; **p<0.1906.

ACKNOWLEDGEMENTS

The authors would like to thank FAPESP (2014/22689-3) and CNPq. Also we would like to thank S.I.N. – Brazilian Dental Implants Company (São Paulo, SP, Brazil) for gently donating the CoCr-based alloys assayed in this work. W.F.Z. is supported by fellowship at CNPq-PQ-2.

REFERENCES

1. Hamad K, Kon M, Hanawa T, et al (2002) Hydrothermal modification of titanium surface in calcium solutions. Biomaterials 23:2265–2272.

2. Huber M, Reinisch G, Trettenhahn G, et al (2009) Presence of corrosion products and hypersensitivity-associated reactions in periprosthetic tissue after aseptic loosening of total hip replacements with metal bearing surfaces. Acta Biomater 5:172–180. doi: 10.1016/j.actbio.2008.07.032

3. Higgs GB, Hanzlik JA, MacDonald DW, et al (2013) Is increased modularity associated with increased fretting and corrosion damage in metal-on-metal total hip arthroplasty devices?: a retrieval study. J Arthroplasty 28:2–6. doi: 10.1016/j.arth.2013.05.040

4. Bozic KJ, Kurtz S, Lau E, et al (2009) The epidemiology of bearing surface usage in total hip arthroplasty in the United States. J Bone Joint Surg Am 91:1614–1620. doi: 10.2106/JBJS.H.01220

5. Zambuzzi WF, Granjeiro JM, Parikh K, et al (2008) Modulation of Src activity by low molecular weight protein tyrosine phosphatase during osteoblast differentiation. Cell Physiol Biochem 22:497–506. doi: 10.1159/000185506

6. Zambuzzi WF, Milani R, Teti A (2010) Expanding the role of Src and protein-tyrosine phosphatases balance in modulating osteoblast metabolism: lessons from mice. Biochimie 92:327–332. doi: 10.1016/j.biochi.2010.01.002

7. Milani R, Ferreira C V, Granjeiro JM, et al (2010) Phosphoproteome reveals an atlas of protein signaling networks during osteoblast adhesion. J Cell Biochem 109:957–966. doi: 10.1002/jcb.22479

8. Gemini-Piperni S, Takamori ER, Sartoretto SC, et al (2014) Cellular behavior as a dynamic field for exploring bone bioengineering: a closer look at cell-biomaterial interface. Arch Biochem Biophys 561:88–98. doi: 10.1016/j.abb.2014.06.019

9. Gemini-Piperni S, Milani R, Bertazzo S, et al (2014) Kinome profiling of osteoblasts on hydroxyapatite opens new avenues on biomaterial cell signaling. Biotechnol Bioeng 111:1900–1905. doi: 10.1002/bit.25246

10. Arvidson K, Cottler-Fox M, Hammarlund E, Friberg U (1987) Cytotoxic effects of cobalt-chromium alloys on fibroblasts derived from human gingiva. Scand J Dent Res 95:356–363.

11. Howie DW, Rogers SD, McGee MA, Haynes DR (1996) Biologic effects of cobalt chrome in cell and animal models. Clin Orthop Relat Res S217-32.

12. Berstein A, Bernauer I, Marx R, Geurtsen W (1992) Human cell culture studies with dental metallic materials. Biomaterials 13:98–100.

13. Chen L, Shi K, Frary CE, et al (2015) Inhibiting actin depolymerization enhances osteoblast differentiation and bone formation in human stromal stem cells. Stem Cell Res 15:281–289. doi: 10.1016/j.scr.2015.06.009

14. Zheng Y, Zhao Y, Luo Q, et al (2016) Edaravone protects against cobalt chloride-induced dysfunctions in apoptosis and invasion in trophoblast cells. Mol Reprod Dev 83:576–587. doi: 10.1002/mrd.22652

15. Shirwaiker RA, Samberg ME, Cohen PH, et al (2013) Nanomaterials and synergistic low-intensity direct current (LIDC) stimulation technology for orthopedic implantable medical devices. Wiley Interdiscip Rev Nanomed Nanobiotechnol 5:191–204. doi: 10.1002/wnan.1201

16. Coelho PG, Jimbo R (2014) Osseointegration of metallic devices: current trends based on implant hardware design. Arch Biochem Biophys 561:99–108. doi: 10.1016/j.abb.2014.06.033

17. Soares Dos Santos MP, Marote A, Santos T, et al (2016) New cosurface capacitive stimulators for the development of active osseointegrative implantable devices. Sci Rep 6:30231. doi: 10.1038/srep30231

18. Rossi MC, Bezerra FJB, Silva RA, et al (2017) Titanium-released from dental implant enhances pre-osteoblast adhesion by ROS modulating crucial intracellular pathways. J Biomed Mater Res A. doi: 10.1002/jbm.a.36150

19. Bezerra F, Ferreira MR, Fontes GN, et al (2017) Nano hydroxyapatite-blasted titanium surface affects pre-osteoblast morphology by modulating critical intracellular pathways. Biotechnol Bioeng. doi: 10.1002/bit.26310

20. Bowsher JG, Hussain A, Williams PA, Shelton JC (2006) Metal-on-metal hip simulator study of increased wear particle surface area due to "severe" patient activity. Proc Inst Mech Eng H 220:279–287. doi: 10.1243/09544119JEIM93

21. da Costa Fernandes CJ, do Nascimento AS, da Silva RA, Zambuzzi WF (2017) Fibroblast contributes for osteoblastic phenotype in a MAPK-ERK and sonic hedgehog signaling-independent manner. Mol Cell Biochem. doi: 10.1007/s11010-017-3083-0

22. Merritt K, Brown SA (1996) Distribution of cobalt chromium wear and corrosion products and biologic reactions. Clin Orthop Relat Res S233-43.

23. Signorello LB, Ye W, Fryzek JP, et al (2001) Nationwide study of cancer risk among hip replacement patients in Sweden. J Natl Cancer Inst 93:1405–1410.

24. Anissian L, Stark A, Dahlstrand H, et al (2002) Cobalt ions influence proliferation and function of human osteoblast-like cells. Acta Orthop Scand 73:369–374. doi: 10.1080/00016470232015540

25. Shimmin AJ, Bare J, Back DL (2005) Complications associated with hip resurfacing arthroplasty. Orthop Clin North Am 36:187–93, ix. doi: 10.1016/j.ocl.2005.01.002

26. Willert H-G, Buchhorn GH, Fayyazi A, et al (2005) Metal-on-metal bearings and hypersensitivity in patients with artificial hip joints. A clinical and histomorphological study. J Bone Joint Surg Am 87:28–36. doi: 10.2106/JBJS.A.02039pp

27. Hart AJ, Hester T, Sinclair K, et al (2006) The association between metal ions from hip resurfacing and reduced T-cell counts. J Bone Joint Surg Br 88:449–454. doi: 10.1302/0301-620X.88B4.17216

28. Keegan GM, Learmonth ID, Case CP (2007) Orthopaedic metals and their potential toxicity in the arthroplasty patient: A review of current knowledge and future strategies. J Bone Joint Surg Br 89:567–573. doi: 10.1302/0301-620X.89B5.18903

29. Mabilleau G, Kwon Y-M, Pandit H, et al (2008) Metal-on-metal hip resurfacing arthroplasty: a review of periprosthetic biological reactions. Acta Orthop 79:734–747. doi: 10.1080/17453670810016795

30. Eich C, Manzo C, de Keijzer S, et al (2016) Changes in membrane sphingolipid composition modulate dynamics and adhesion of integrin nanoclusters. Sci Rep 6:20693. doi: 10.1038/srep20693

31. Sun Z, Guo SS, Fassler R (2016) Integrin-mediated mechanotransduction. J Cell Biol 215:445–456. doi: 10.1083/jcb.201609037

32. Beauchemin H, Shooshtarizadeh P, Vadnais C, et al (2017) Gfi1b controls integrin signaling-dependent cytoskeleton dynamics and organization in megakaryocytes. Haematologica. doi: 10.3324/haematol.2016.150375

33. Oleinik N V, Krupenko NI, Krupenko SA (2010) ALDH1L1 inhibits cell motility via dephosphorylation of cofilin by PP1 and PP2A. Oncogene 29:6233–6244. doi: 10.1038/onc.2010.356

34. Tomasella A, Blangy A, Brancolini C (2014) A receptor-interacting protein 1 (RIP1)-independent necrotic death under the control of protein phosphatase PP2A that involves the reorganization of actin cytoskeleton and the action of cofilin-1. J Biol Chem 289:25699–25710. doi: 10.1074/jbc.M114.575134

35. Deramaudt TB, Dujardin D, Noulet F, et al (2014) Altering FAK-paxillin interactions reduces adhesion, migration and invasion processes. PLoS One 9:e92059. doi: 10.1371/journal.pone.0092059

36. Sp N, Kang DY, Joung YH, et al (2017) Nobiletin Inhibits Angiogenesis by

Regulating Src/FAK/STAT3-Mediated Signaling through PXN in ER(+) Breast Cancer Cells. Int J Mol Sci. doi: 10.3390/ijms18050935

37. Ohtsuka S, Ogawa S, Wakamatsu E, Abe R (2016) Cell cycle arrest caused by MEK/ERK signaling is a mechanism for suppressing growth of antigen-hyperstimulated effector T cells. Int Immunol 28:547–557. doi: 10.1093/intimm/dxw037

38. Caicedo MS, Pennekamp PH, McAllister K, et al (2010) Soluble ions more than particulate cobalt-alloy implant debris induce monocyte costimulatory molecule expression and release of proinflammatory cytokines critical to metal-induced lymphocyte reactivity. J Biomed Mater Res A 93:1312–1321. doi: 10.1002/jbm.a.32627

39. Cayrol C, Girard J-P (2009) The IL-1-like cytokine IL-33 is inactivated after maturation by caspase-1. Proc Natl Acad Sci U S A 106:9021–9026. doi: 10.1073/pnas.0812690106

Capítulo 5

ZIRCONIA STIMULATES ECM-REMODELING AS A PREREQUISITE TO PRE-OSTEOBLAST ADHESION/PROLIFERATION BY POSSIBLE INTERFERENCE WITH CELLULAR ANCHORAGE

Celio J. da Costa FERNANDES[1], Marcel Rodrigues FERREIRA[1], Fábio J. B. BEZERRA[1], Willian F. ZAMBUZZI[1,*]

[1]Bioassays and Cell Dynamics Lab, Dept. of Chemistry and Biochemistry, Bioscience Institute, UNESP, Botucatu, Sao Paulo, Brazil.

Fernandes, CJC; Ferreira, MR; Bezerra, FJB; Zambuzzi, WF. ZrO2 enriched medium stimulates ecm-remodeling as a prerequisite to pre-osteoblast adhesion/proliferation by a possible interference on cellular anchoring. **Journal of Materials Science. Materials in Medicine.** (Accepted).

ABSTRACT

The biological response to zirconia (ZrO_2) is not completely understood, which prompted us to address its effect on pre-osteoblastic cells in both direct and indirect manner. Our results showed that zirconia triggers important intracellular signaling mainly by governing survival signals which leads to cell adhesion and proliferation by modulating signaling cascade responsible for dynamic cytoskeleton rearrangement, as observed by fluorescence microscopy. The phosphorylations of Focal Adhesion Kinase (FAK) and Rac1 decreased in response to ZrO_2 enriched medium. This corroborates the result of the crystal violet assay, which indicated a significant decrease of pre-osteoblast adhesion in responding to ZrO_2 enriched medium. However, we credit this decrease on pre-osteoblast adhesion to the need to govern intracellular repertory of intracellular pathways involved with cell cycle progression, because we found a significant up-phosphorylation of Mitogen-Activated Protein Kinase (MAPK)-p38 and Cyclin-dependent kinase 2 (CDK2), while p15 (a cell cycle suppressor) decreased. Importantly, Protein phosphatase 2A (PP2A) activity decreased, guaranteeing the significant up-phosphorylation of MAPK -p38 in response to ZrO_2 enriched medium. Complementarily, there was a regulation of Matrix Metalloproteinases (MMPs) in response to Zirconia and this remodeling could affect cell phenotype by interfering on cell anchorage. Altogether, our results show a repertory of signaling molecules, which suggests that ECM remodel as a pre-requisite to pre-osteoblast phenotype by affecting their anchoring in responding to zirconia.

Keywords: Biomaterials; Zirconia; Osteoblast; Proliferation; TIMP; ECM; MMP.

INTRODUCTION

Bone is a highly dynamic tissue capable of remodeling itself throughout life [1]. When damaged, its physiology allows regenerating of minor lesions. On the other hand, in cases of critical-sized bone defects, biomaterials must be used to guide tissue regeneration [2,3]. Ideally, a biomaterial should be able to recruit osteoprogenitor cells into the lesion region, subsequently stimulating their proliferation and consequent differentiation by well-orchestrated signaling involving cells and trophic molecules. Among the several properties to be considered for successful osseointegration, the biomaterial needs to have adequate physical-chemical composition and bioactivity on its surface [4]. Thus, titanium alloys are widely used for bone tissue regeneration, but in the last decade there has been growing interest in understanding the behavior of bioceramic materials as an implantable material, such as zirconium dioxide (ZrO_2), also known as zirconia [5,6].

Beyond its mechanical properties, zirconia devices have emerged as an alternative mainly due to aesthetic aspects; however, it has other important clinical properties [7]. Initially, zirconia was used in artificial dental crowns and abutments of implants, due to its very interesting physical and mechanical properties. Zirconia has low thermal conductivity and can withstand flexural stresses in the order of 1000 MPa and 2000 MPa of effective compression. Due to its great strength, zirconia is known as "ceramic steel", and is considered the second strongest material, only behind diamond [8,9]. Recently, zirconia has been used as for implants because of its biological response such as adequate biocompatibility with bone tissue cells. Many studies have demonstrated that zircon surfaces do not produce any cytotoxic effects by exploring in *in vitro* technologies, or any kind of systemic infection when implanted in mice or rabbits [8–10]. In addition, zirconia has been shown to be capable of inducing the proliferation of pre-osteoblast, as well as increasing the gene expression of type I collagen and osteopontin [10]. Although zirconia dental implants are receiving increasing attention, no papers have reported the molecular mechanisms governing cell adhesion on its surface.

Animal models are widely used in the research that evaluates biological behavior of novel biomaterials. Over the last decade, our group has proposed the use

of *in vitro* approaches by diagnostic intracellular signal transduction mechanisms, which have been proposed as important tools to predict biomaterial-cell interactions and are considered alternative approaches that reduce the use of experimental animals in biomedical materials research. To this end, biomarkers of cell metabolism, such as Focal Adhesion Kinase (FAK), Src, Paxilin, and Cofilin, among other kinases and phosphatases, appear as alternative tools to evaluate the biocompatibility of biomedical materials. In this work, we demonstrated for the first time part of the molecular mechanism involved with the biological response to zirconia, revealing a repertory of signaling molecules able to propose Extracellular Matrix (ECM) remodeling as a pre-requisite to contribute to pre-osteoblast phenotype by affecting their anchorage.

MATERIAL AND METHODS

Cell culture

Mouse pre-osteoblastic cells, MC3T3-E1 (subclone 4) (ATCC CRL-2593), were culture in αMEM supplemented with 10% of Fetal Bovine Serum (FBS) at 37 °C and 5% CO_2. For all experiments, cells were tripsinized at subconfluent passages when they were used.

Cell viability assay

For the cell viability assay, αMEM was conditioned with zirconia (ZrO_2) discs (0.01 mg/mL, with 0.6 cm diameter) for 24 h and then the ZrO_2 enriched medium was used to treat the pre-osteoblast for additional 24 h in semiconfluence (around 100×10^3 cells/ml). Thereafter, the medium was replaced by a vital dye MTT (1 mg/mL) [11] and incubated for an additional 4 h. Then, the MTT medium was removed and the blue precipitate dye diluted in 100 µL/well of absolute alcohol. In the end, the cell viability was estimated by measuring the absorbance in a microplate reader (SYNERGY-HTX multi-mode reader, Biotek, USA) at 570 nm wavelength.

Cell adhesion assay

ZrO_2 enriched medium was also used to measure its influence on cell adhesion by using crystal violet as the approach (Rossi et al., 2017; Bezerra et al., 2017). Previously, the cells were challenged with ZrO_2 enriched medium up to 24 hours when the cells were trypsinized, and reseeded on 96-well microplate at 100×10^3 cells/ml. A control group was considered by reseeding the cells with conventional cell culture conditions. After 24 h of seeding, cell adhesion was estimated by incorporating the crystal violet, as detailed somewhere. The absorbance was measured at 540 nm using a microplate reader (SYNERGY-HTX multi-mode reader, Biotek, USA), which was used to estimate the profile of adherent cells.

Scanning Electron Microscopy (SEM)

Pre-osteoblasts were plated onto zirconia discs at the density of 50×10^3 cells/disc, and after 24 h were fixed with 2.5% of glutaraldehyde in 0.1 M phosphate buffer pH 7.3 for 24 h. After the dehydration steps, they were sent to the critical point, assembled in the "stubs" and then metallized. The SEM analyses were performed on a Quanta 200—FEI Company scanning electron microscope at an accelerating voltage of 12.5 kV.

Western Blotting (WB)

Semiconfluent pre-osteoblasts were treated in ZrO_2 enriched medium up to 24 h, then they were lysed on ice for 2 h with Lysis Cocktail (50 mM Tris [tris(hydroxymethyl)aminomethane]–HCl [pH 7.4], 1% Tween 20, 0.25% sodium deoxycholate, 150 mM NaCl, 1 mM EGTA (ethylene glycol tetraacetic acid), 1 mM O-Vanadate, 1 mM NaF, and protease inhibitors [1 µg/mL aprotinin, 10 µg/mL leupeptin, and 1 mM 4-(2-amino-ethyl)-benzolsulfonyl-fluorid-hydrochloride]) to obtain the pool of protein. After being lysed, the samples were sonicated (1 pulse per second; SONICS Vibra-Cell, USA) and maintained for an additional 1 h on ice. The protein extracts were clarified and the protein concentration determined by the Lowry method [12]. Proteins extracts were resolved by SDS-PAGE (10 or 12%) and transferred to PVDF membranes (Bio-Rad, Hercules, CA, USA). Immediately, the membranes were blocked with either 1% fat-free dried milk or bovine serum albumin (2.5%) in Tris-buffered saline (TBS)–Tween 20 (0.05%) and incubated overnight at 4 °C with appropriate primary antibody

at 1:1,000 dilutions overnight. After washing in TBS-Tween 20 (0.05%), the membranes were incubated with horseradish peroxidase-conjugated anti-rabbit, anti-goat, or anti-mouse IgGs secondary antibodies, at 1:5,000 dilutions, in blocking buffer for 1 h at room temperature. Thereafter, Enhance Chemiluminescence (ECL, Pierce, USA) was used to detect the bands.

RT-qPCR

To collect samples for qPCR, the pre-osteoblasts were plated in a petri dish (100 mm diameter) for adhesion. At semiconfluence, they were treated with ZrO_2 enriched medium (indirect model) or grown on zirconia (direct model) for 24 h, when the culture medium was removed and TriZOL and treated with DNase I (Invitrogen, Carlsband, CA, USA). cDNA synthesis was performed with High Capacity cDNA Reverse Transcription Kit (Applied Biosystems, Foster City, CA) according to the manufacturer's instructions. qPCR was carried out in a total of 10 µl, containing PowerUp™ SYBR™ Green Master Mix 2x (5 µl) (Applied Biosystems, Foster City, CA), 0.4 µM of each primer, 50 ng of cDNA and nuclease free H_2O. Fold changes were analyzed using the comparative Ct method (ΔΔCt) normalizing to GAPDH expression and comparing to static conditions as a reference. qPCR was performed using a QuantStudio® 3 Real-Time PCR System to assess changes in mRNA expression in the genes (**Table 1**).

Table 1. Expression primers sequences and PCR cycle conditions.

Gene	Primer	5'-3' Sequence	Reactions Condition
MMP2	Forward	AACTTTGAGAAGGATGGCAAGT	95°C - 3s; 55°C - 8s; 72°C - 20s
	Reverse	TGCCACCCATGGTAAACAA	
MMP9	Forward	TGTGCCCTGGAACTCACACGAC	95°C - 3s; 55°C - 8s; 72°C - 20s
	Reverse	ACGTCGTCCACCTGGTTCACCT	
TIMP1	Forward	ATCCTCTTGTTGCTATCACTG	95°C - 5s; 56°C - 10s; 72°C - 15s
	Reverse	GGTCTCGTTGATTTCTGGG	
TIMP2	Forward	GCAACAGGCGTTTTGCAATG	95°C - 3s; 55°C - 8s; 72°C - 20s
	Reverse	CGGAATCCACCTCCTTCTCG	
RECK	Forward	CCTCAGTGAGCACAGTTCAGA	95°C - 3s; 55°C - 8s; 72°C - 20s
	Reverse	CCTGTGGCATCCACGAAACT	
Integrin-β1	Forward	CTGATTGGCTGGAGGAATGT	95°C - 3s; 60°C - 8s; 72°C - 20s
	Reverse	TGAGCAATTGAAGGATAATCATAG	
Src	Forward	TCGTGAGGGAGAGTGAGAC	95°C - 3s; 60°C - 8s; 72°C - 20s
	Reverse	GCGGGAGGTGATGTAGAAAC	
PP2A	Forward	ATGGGCCTCTCTCCCATTCT	95°C - 3s; 60°C - 8s; 72°C - 20s
	Reverse	CATGCACAGGGAGTGACAGT	
FAK	Forward	TCCACCAAAGAAACCACCTC	95°C - 3s; 60°C - 8s; 72°C - 20s
	Reverse	ACGGCTTGACACCCTCATT	
Cofilin	Forward	CAGACAAGGACTGCCGCTAT	95°C - 3s; 60°C - 8s; 72°C - 20s
	Reverse	TTGCTCTTGAGGGGTGCATT	
CDK2	Forward	TACCCAGTACTGCCATCCGA	95°C - 3s; 60°C - 8s; 72°C - 20s
	Reverse	CGGGTCACCATTTCAGCAAA	
CDK4	Forward	TCGATATGAACCCGTGGCTG	95°C - 3s; 60°C - 8s; 72°C - 20s
	Reverse	TTCTCACTCTGCGTCGCTTT	
CDK6	Forward	CGCCGATCAGCAGTATGAGT	95°C - 3s; 60°C - 8s; 72°C - 20s
	Reverse	GCCGGGCTCTGGAACTTTAT	
P21	Forward	CGCCGATCAGCAGTATGAGT	95°C - 3s; 60°C - 8s; 72°C - 20s
	Reverse	GCCGGGCTCTGGAACTTTAT	
GAPDH	Forward	AGGCCGGTGCTGAGTATGTC	95°C - 3s; 60°C - 8s; 72°C - 20s
	Reverse	TGCCTGCTTC ACCACCTTCT	

Matrix Metalloproteinase activities

After identifying the involvement of matrix remodeling marker gene in response to ZrO_2 enriched medium, we decided to investigate whether there were MMP activities by exploring the Zymography approach. The pre-osteoblast cultures were treated as detailed previously when the conditioned medium was collected. The gelatinolytic activities of the samples were evaluated by resolving the sample from cell culture supernatants, and SDS-PAGE was performed on gels containing 0.1% gelatin and 10% polyacrylamide [13]. Samples, previously mixed with loading buffer (2% SDS and 0.1% bromophenol blue), were electrophoresed under nonreducing conditions. After electrophoresis, gels were washed in 2% Triton X-100 and immersed in buffer containing 50 mM Tris-HCl (pH 7.6), 200 mM NaCl, and 10 mM CaCl2 for 18 h at 37°C. The gels were stained with 0.5% Coomassie Blue G-250 in acetic acid/methanol/water (1:4:5 vol/vol/vol) [14] and distained in acetic acid/methanol/water (1:2:7 vol/vol/vol).

Statistical analysis

The results were plotted as mean ± standard deviation (SD) and significances were verified using One-Way ANOVA (non-parametric) with Tukey test powders. In this case, $p<0.05$ was considered statistically significant and $p<0.0001$ considered highly significant. For the statistical analysis, the groups were standardized by the percentage of control.

RESULTS

Zirconia compromises pre-osteoblast adhesion by down-regulating FAK and RAC1 activations

To verify whether zirconia is able to modulate osteoblast performance, we explored 2 biological models: direct and indirect contact. For the direct model the cells were seeded on the zirconia, and for the indirect model, the zirconia was incubated in cell culture medium up to 24 hours in order to enrich previously the medium (ZrO_2-enriched medium) to treat the cells, in agreement to ISO 10993:2016. First, we found that ZrO_2-enriched medium influenced pre-osteoblast performance. Using violet crystal, it was verified that ZrO_2 enriched medium decreased the cellular adhesion of

pre-osteoblasts compared to the control (**Fig.1a**). To understand this event, we investigated the balance of the crucial proteins involved with the intracellular cascade triggered upon integrin activation (signaling pathway proposed in **Fig.1b**), culminating in cytoskeleton rearrangement; thus, ß1-integrin, FAK, Rac1 and Cofilin were analyzed (**Fig.1c-j**), while GADPH as used a housekeeping control.

The activation of FAK was analyzed by investigating its three possible phosphorylated residues, Y397 (**Fig.1c,e)**, Y576/577 (**Fig.1c,f),** and Y925 (**Fig.1c,g)**, all involved with cell adhesion and governing cytoskeleton rearrangement culminating in the transitionally cofilin phosphorylation. Phosphorylations at residues Y576/577 and Y925 did not present any change, while the residue Y397 showed significant decrease ($p = 0.0060$) in response to ZrO_2 enriched medium. Concomitantly, we also found an important effect on ß1-integrin expression (**Fig.1c,d**), while Rac1 activation was down-modulated ($p=0.0001$; **Fig.1h,i**). For cytoskeleton-based cell adhesion, cofilin phosphorylation presented the same profile as the control (**Fig. 1h,j**). To validate this biological effect, we investigated the actin-based cytoskeleton rearrangement by using fluorescence microscopy and found that ZrO_2 promotes significant changes in actin organization (**Fig.1k-p**). As these large bundles of actin, called stress fibers, appear preferentially in response to ZrO_2, our model provides a mechanism for stress fiber formation and stiffness sensing in ZrO_2-responding cells.

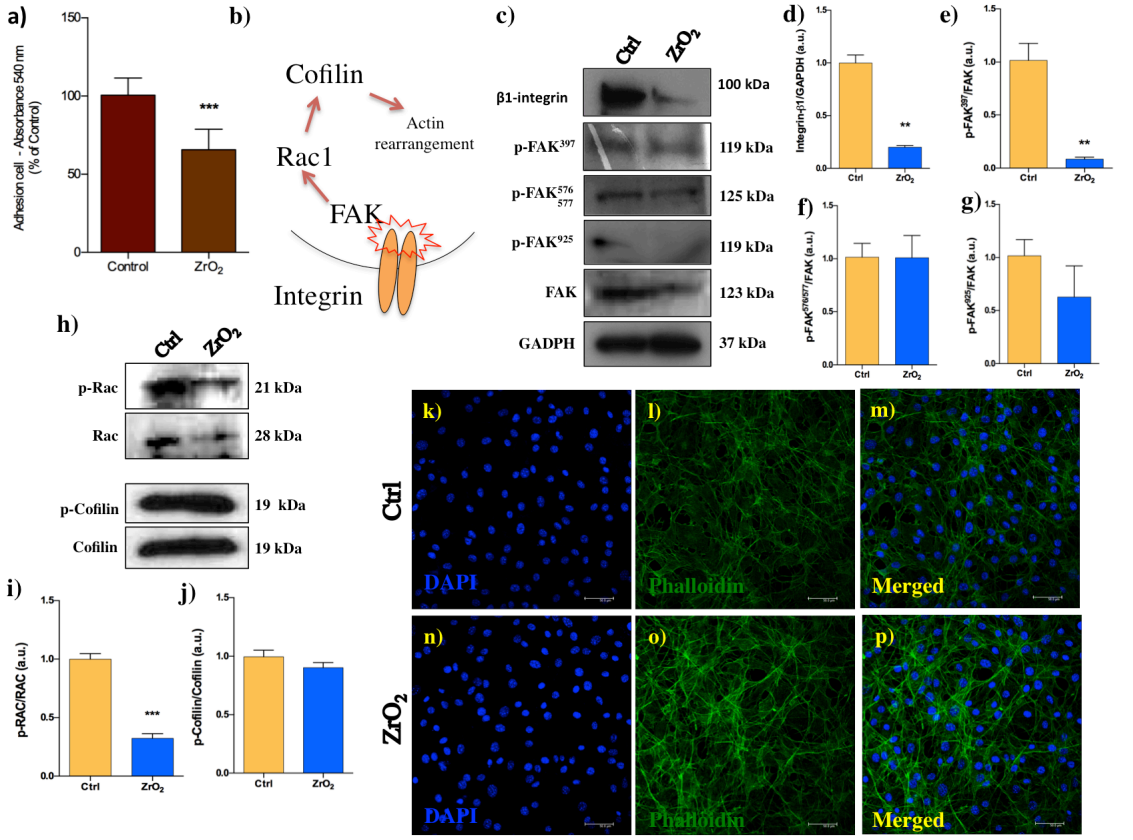

Fig.1 – ZrO_2 enriched medium modulates the activation of important proteins during the adhesion of pre-osteoblasts. (a) adhesion was evaluated when pre-osteoblasts were challenged with to ZrO2 enriched medium up to 24 hours. To understand the intracellular signaling responsible for governing the adhesion, we first proposed the general scheme presented in **(b).** The cascade of the activation involves FAK, Rac, and Cofilin upon integrin activation culminating in the cytoskeleton rearrangement and later governing cell adhesion. FAK was evaluated **(c-g),** and it is possible to observe its phosphorylations at several residues (Y397, Y576/577, and Y925), as well as the pan Rac1 and Cofilin, and their phosphorylated residues **(h-j).** All of these proteins were resolved by immunoblotting technology and the GAPDH used as the housekeeping gene. In the images **(k-p),** cells were challenged with ZrO_2-enriched media and then evaluated for cytoskeletal rearrangement. Significances were considered when **p<0.0015; ***p<0.0007.

Using a direct contact model, we later evaluated the morphological changes of pre-osteoblasts grown on the zirconia surface for 24 hours using SEM, when adhered cells showed advanced spreading, indicating modulation of signaling pathways responsible for governing cytoskeleton rearrangement (**Fig.2a**). In addition, we investigated expression of genes related with cell adaptation on the substrate and

showed *ß1-integrin* (**Fig.2b**) and *Src* (**Fig.2d**) were significantly down-modulated, but *FAK* (**Fig.2c**), *cofilin* (**Fig.2e**), and *PP2A* (**Fig.2f**) were significantly up-modulated.

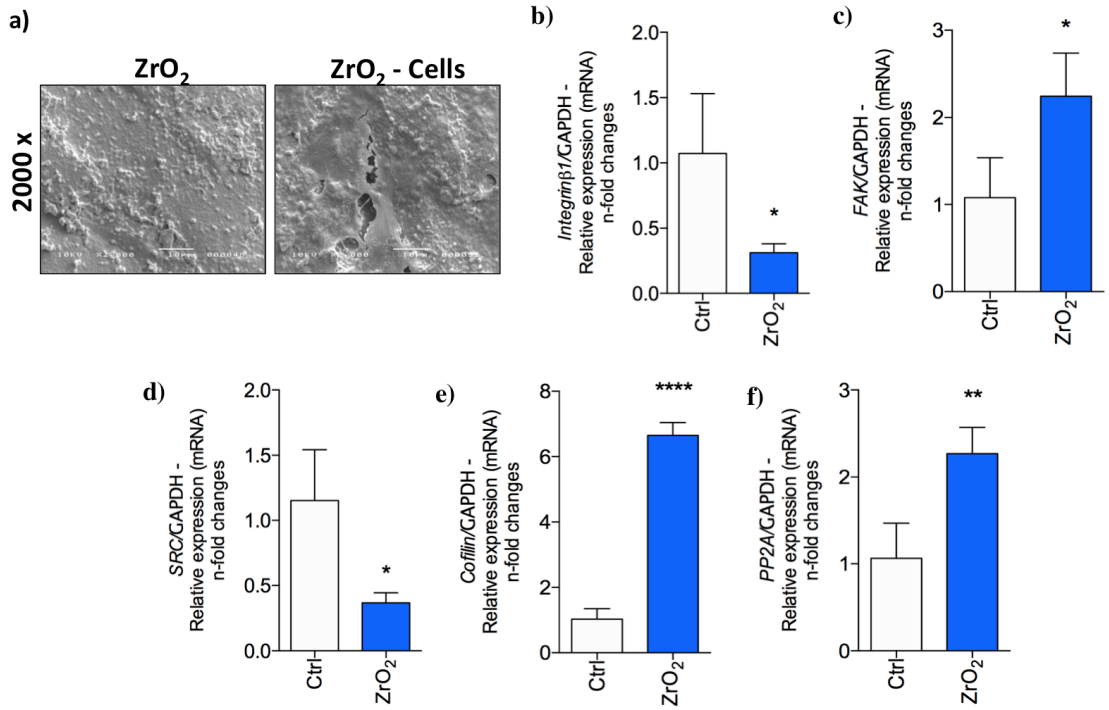

Fig. 2 - Zirconia modulates the expression of adhesion genes and cytoskeletal rearrangement of pre-osteoblasts in direct contact. The electronmicrography **(a)** shows pre-osteoblast adhesion in direct contact with ZrO_2 devices, where the cells are seeded on the disc up to 24 hours and later evaluated by Scanning Electron Microscopy. The same biological model was explored to collect the samples for the qPCR analysis, when previously the samples were harvested in TriZOL to evaluate an expression of adhesion and cytoskeleton rearrangement-related genes **(b-f).** Significances were considered when *p<0.02, **p<0.0057 and ****p<0.0001.

Zirconia enhances survival signaling-related transducers

First, we evaluated the cell viability of pre-osteoblast subjected to ZrO_2 enriched medium by using classical MTT assay. Ferreira et al. using MTT estimated cell viability and proliferation [15]. Our results showed that ZrO_2-enriched medium enhances pre-osteoblasts viability (**Fig. 3a**), which suggests an increased cell cycle. For a better understanding, the signaling pathway was addressed by evaluating protein-related cell cycle and survival signaling transducers. Thus, we evaluated the involvement of important signaling transducers for cell survival and found an important AKT requirement (**Fig. 3b,c**). In addition, mitogen-activated protein kinases (MAPKs)

were significantly up-activated, as follows: p38 (**Fig. 3d,e**), ERK (**Fig. 3f,g**), and JNK (**Fig. 3h,i**). In order to evaluate whether those survival signaling culminate in proliferation fashion, we reported a significant increase of CDK2 phosphorylation (**Fig. 3j,k**), while p15 expression presented a slight down-regulation (**Fig. 3l,m**). The balance on CDK2 and p15 is known to be involved in cell cycle progression. At this point, it seems the Ser/Thr phosphorylation balance is an important biomarker of zirconia-related response. Thus, we decided to investigate the potential involvement of PP2A, a Ser/Thr phosphatase able to hydrolyze phosphoryl moiety from phosphorylated Ser/Thr sites. Our results showed PP2A was significantly up-phosphorylated at Y307 ($p = 0.0431$) in response to ZrO_2-enriched medium (**Fig. 3n,o**), indicating its inhibition.

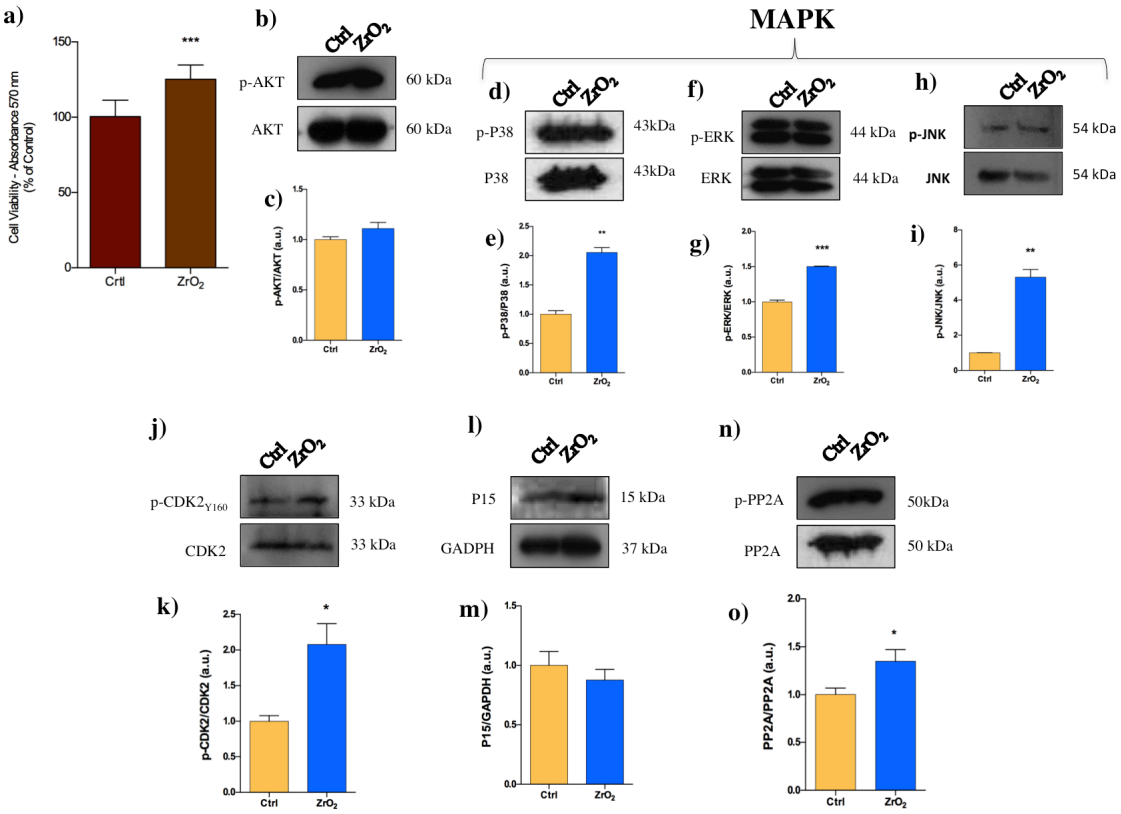

Fig. 3 - ZrO_2 enriched medium modulates pre-osteoblast survival and proliferating processes. The effect on the pre-osteoblast viability was measured by classical MTT approach **(a)** and by revealing key proteins in these processes through immunoblotting, where we evaluated the phosphorylations of AKT **(b-c)** and a set of MAPKs (p38 and p-p38; ERK and p-ERK; JNK and p-JNK) **(d-i)**. The proliferation events were estimated by evaluating CDK2 and p15, as well as PP2A **(j-o)** up to 24 hours in response to ZrO_2 enriched media. GAPDH was used as a housekeeping gene. Significances were considered when *p<0.04; **p<0.0057.

In parallel, considering the direct effect of the zirconia on pre-osteoblast viability, we found a singular cell phenotype that stimulates cell proliferation, as *CDK4* gene was significant up-activated (**Fig. 4a**), while *CDK2* (**Fig. 4b**) and *CDK6* (**Fig. 4c**) remained unchanged, as well as *p21* (**Fig. 4d**), a well-documented gene suppressor. Thus, it is clear zirconia-based cell signaling promotes cell cycle progression in both the direct and indirect model.

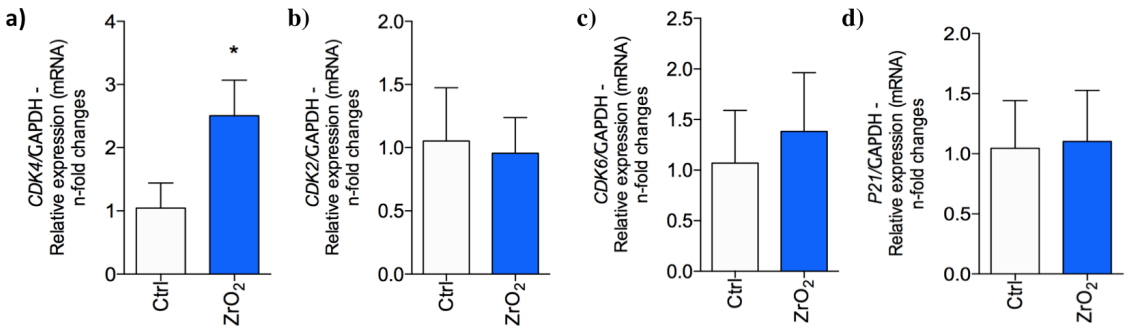

Fig. 4 – Zirconia modulates directly pre-osteoblast cell cycle. Previously the cells were marinated up to 24 hours directly in contact with zirconia, when the RNA was extracted and provided condition for cDNA synthesis. We evaluated the expression profile of the CDK-2, CDK-4, and CDK-6 **(a-c)** and p21 **(d)**, all of them related with cell cycle progression. Significances were considered when *p<0.05.

Zirconia stimulates a fine ECM remodeling-related protein processing

To understand whether zirconia enriched medium affects ECM-remodeling, we investigated the capacity of challenged pre-osteoblast to process MMP-2, MMP-9, and their tissue inhibitors, TIMP1, TIMP2 and reversion-inducing-cysteine-rich protein with kazal motifs (RECK). First, the ZrO_2-enriched medium (indirect manner) caused a considerable ECM remodeling controlled by the challenged pre-osteoblast. Both *MMPs-2* and *-9* genes were significantly up-activated (**Figs.5a,b**), while both *TIMPs-1* and *-2* genes were down-activated (**Figs.5c,d**). Later, we measured the activity of the conditioned medium by challenged pre-osteoblast (**Fig.5e**) and found an increase of their activities (**Figs.5f-k**). In addition, a very similar profile was obtained on the machinery of ECM remodeling-related genes when cells were grown directly on the zirconia devices.

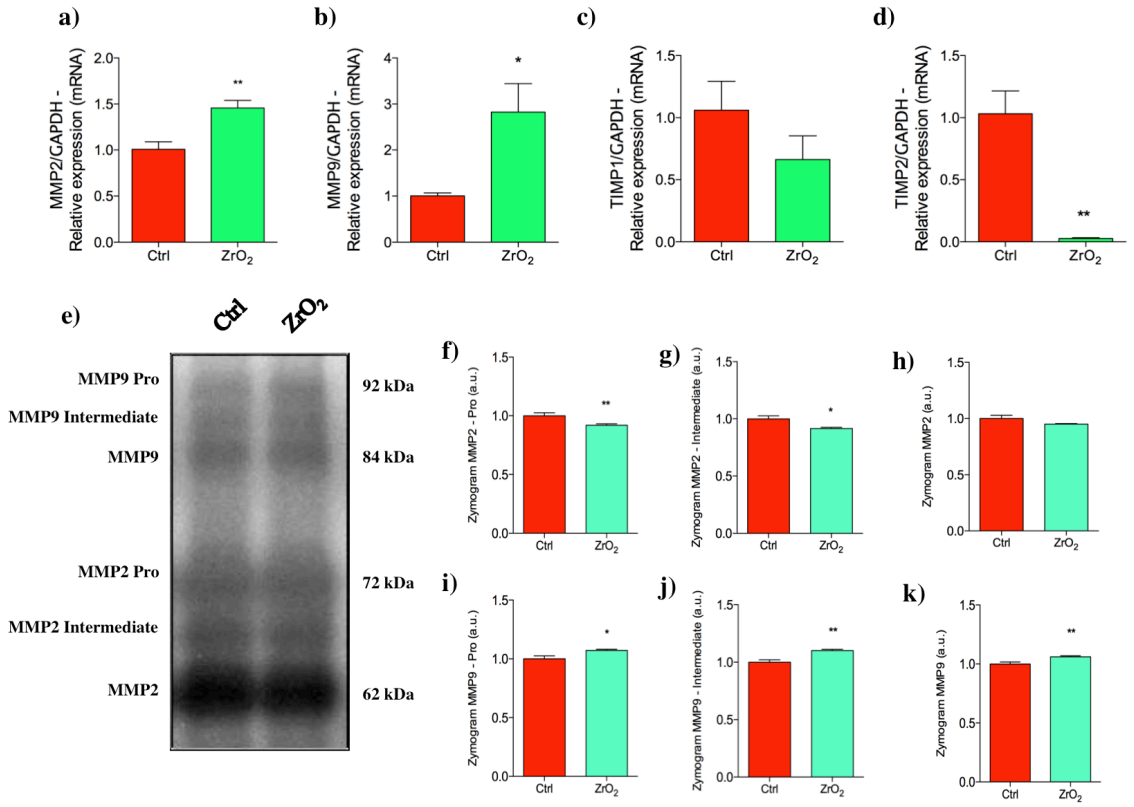

Fig. 5 - MMPs molecular processing in response to ZrO_2 enriched medium. Here we evaluated the expression profile of MMP2 and MMP9 **(a-b)** and their tissue inhibitors (TIMPs): TIMP1 and TIMP2 **(c-d)**. In addition, MMPs activities were measured by the Zymography technology **(e)** and the analysis of those activities of both MMP9 and MMP2 are presented **(f-k)**. Significances were considered when *p<0.02 and **p<0.0027.

Thus, **Fig.6a** illustrates significant *MMP-2* gene activation, while *MMP-9* gene was unchanged (**Fig.6b**). Importantly, MMP inhibitors *TIMP-1* and *RECK* were up-expressed (approximately 15-fold changes and 3.5-fold changes, respectively; **Fig. 6c,d**), while *TIMP-2* remained unchanged (**Fig.6e**)

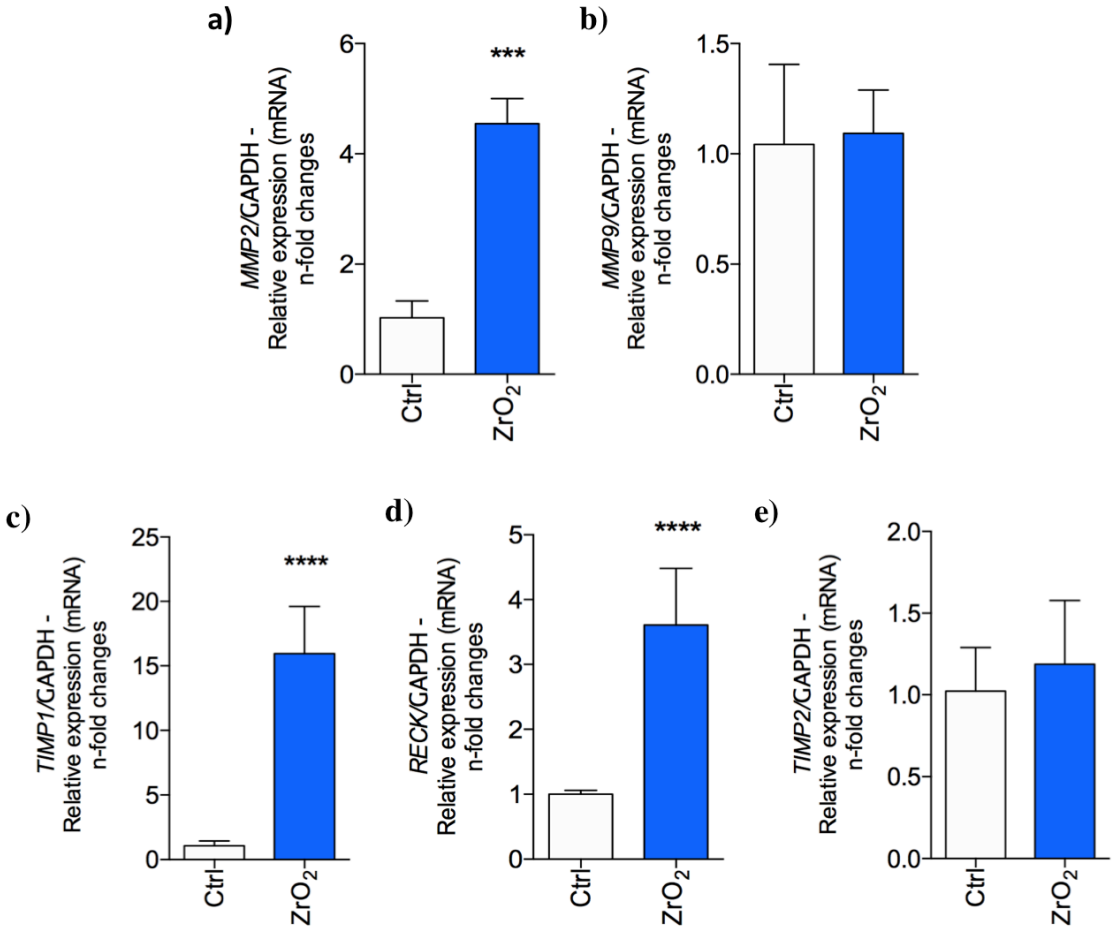

Fig. 6 - MMPs genes are reprogrammed in response directly to Zirconia. The biological model was explored by seeding the cells directly on the zirconia discs and after 24 hours the RNA was extracted. To estimate the ECM remodeling-related genes, we evaluated the expression profile of MMP2 and MMP9 **(a-b)** and their tissue inhibitors: TIMPs and RECK **(c-e)**. Significances were considered when ***p<0.0007 and ****p<0.0001.

DISCUSSION

There is now a growing search for alternative methods to animal experimentation and also to understand the molecular mechanism involved with biomaterial response. Hence, we have been working to this end by exploring molecular pathways of the cell/biomaterial interaction responses to prioritize *in vitro* over *in vivo* tests. Many *in vitro* tests have indicated zirconia as a biocompatible material. However, it is necessary to understand the intracellular signaling responsible for governing its biological response, because Josset et al. [16] showed that zirconia surface allowed adhesion and spreading of human osteoblasts and the cells preserved their capacity to

proliferate and differentiate. To address this issue, we investigated signaling pathways that govern crucial cell fates such as adhesion and proliferation by considering 2 biological models: an indirect, where the pre-osteoblasts were challenged with zirconia-enriched medium, and a direct, where the osteoblasts were grown directly on the zirconia surface. Our data strongly suggest zirconia interacts with the surrounding tissue, considering both direct and indirect model.

Previously, we considered Focal Adhesion Kinase (FAK) activation as a very interesting biomarker of cell adhesion upon integrin activation when interacting with substrates [17]. It is very known that FAK has three independent tyrosine-residues (Y) that undergo phosphorylations, which are classically related to cell adhesion, Y397, Y576/577, and Y925 [18,19]. Mechanistically, the autophosphorylation at residue Y397 activates FAK and allows its interaction with Src, a protein tyrosine kinase also involved with cell adhesion process and cell survival pathways [20,21]. Consequently, when phosphorylated at residue Y576/577, FAK initiates a cascade responsible for the rearrangement of the actin-based cytoskeleton [18,22]. Lastly, the phosphorylation of the Y925 residue is related to adhesion, differentiation, and motile processes, among others by activating the MAPK pathway [23,24]. In this work, the phosphorylation at Y397 site was decreased in response to ZrO_2 enriched medium, but Y576/577 and Y925 sites remain unchanged. The phosphorylation at Y397 provoked FAK tridimensional changes providing interaction with SH2 domains as well as phosphorylation of residues Y576/577 and Y925 [20,25]. Thus, our results suggest that the decrease of cell adhesion in response to ZrO_2 enriched medium, proposed by the violet crystal approach, is related to the decrease of Y397 phosphorylation and this molecular mechanism could be a prerequisite to start cell proliferation.

In addition on this scenario, a decrease of Rac1 phosphorylation in response to ZrO_2 enriched medium was also observed. Rac1, which is related to the cytoskeleton adaptations during the cellular attachment on substrate, migration, and adhesion process [26,27], is regulated by FAK, Src, and others Rho GPTases members upstream [28]. The self-regulation of Rho GTPases is responsible, among others, for the formation and alteration of lamellipodial protrusion in the cell, and is very necessary during the cell migration process [28]. In conjunction, these signaling pathway can explain the different actin-related cytoskeleton rearrangement in response to zirconia,

mainly because Rac1 also acts in the regulation of Cofilin [2], which is highly responsible for the reorganization of actin filaments during cell adhesion and spreading [29]. In agreement, our results found no significance in cofilin phosphorylation (S03) in response to ZrO_2 enriched medium, when compared to the control group. This result can be reported both by the performance of other Rho GTPases [30], because Rac1 activation was decreased, as well as by the increased MAPK-p38 phosphorylation, observed in response to ZrO_2 enriched medium.

In this scenario, we also investigated the Ser/Thr phosphatase 2A (PP2A). When phosphorylated by Src at its Y307 residue, PP2A is inactivated by decreasing its activity in hydrolyzing phospho-serine and phospho-threonine residues [31]. This may be an explanation for the increased phosphorylation of P38 [32], in turn for the compensation mechanism for phosphorylation of Cofilin, since the residue S03 remains phosphorylated [33]. Combining these results, it is possible to suggest an extensive performance of Src in the mechanisms of adhesion and survival of cells in contact with zirconia surface. The involvement of other members of the Rho GTPase family (such as ROCK1, RhoA, RhoC, among others) may also explain the adhesion mechanisms in response to zirconia [34].

Additionally, we also reported an increase of MTT result by pre-osteoblast in response to ZrO_2 enriched medium when compared to control. This can be interpreted as an increase in the energy demand of cells, by increasing the demand of dehydrogenases, or enhancing the number of cells as the ZrO_2 enriched medium stimulates pre-osteoblast proliferation. To identify whether this treatment interferes in cell cycle progression as suggested earlier, we decided to investigate CDK2 and p15. The significant up-phosphorylation of CDK2 (Y160) suggests its involvement in progressing the cell cycle [35,36]. On the other hand, the expression of p15, a cellular inhibitor for CDK2, remained unchanged in response to ZrO_2 enriched medium, obviously evidencing the greater involvement of CDK2 in mechanisms of cell cycle modulation.

Later, to see whether ZrO_2 enriched medium could interfere in ECM remodeling, we investigated the balance of MMPs and their inhibitors. In our cell culture model, we observed *MMP-2* and *-9* expression by qPCR technology and the

presence of pro-MMP-2 gelatinolytic activity by zymography. *TIMP2* expression was reduced while *MMP2* and *MMP9* expressions significantly increased and this balance is in agreement, since TIMP2 is a metalloproteinase inhibitor [13]. Additionally, the expression of *MMP9* by qPCR was found to be highly significant in response to ZrO_2 enriched medium. MMP9 seems to play an important and functional role for pre-osteoblast behavior in response to ZrO_2 enriched medium, because its activity also significantly increased while MMP2 activity decreased. Our results are consistent with other works that demonstrated the influence of this biomaterial on MMP production in osteoblasts [37,38]. These data are in agreement with results provided by *in vitro* and *in vivo* experiments and suggest that MMPs and TIMPs produced by bone cells are important in the balance between bone formation and resorption.

The down-regulation of MMP2 could explain the low phosphorylation of FAK at residue Y379, found in the response to ZrO_2 enriched medium, since the activation of the FAK / Src / PI3K / AKT pathway is required for remodeling of the extracellular medium by MMP2 action [39,40]. Another hypothesis for low MMP2 activity would be a low production of collagen by the cell [41]. The interactions between osteoblasts and biomaterials, such as zirconia, alter both MMP-2, -9 and TIMP-1 expression indicating that biomaterials may influence bone remodeling-required integration of biomedical devices.

Altogether, our results showed for the first time the molecular mechanisms triggered by zirconia on pre-osteoblasts. Specifically, our results showed that there is a stimulus for ECM remodeling as a prerequisite to promote cell cycle progression by finely orchestrating multisite FAK phophorylations and culminating in cytoskeleton rearrangement. In addition, our proposal is able to recognize mechanisms involved with cell/biomaterial interaction, promoting a necessary stage of refinement of technologies used during new biomaterial development, consequently reducing the animal experimentation during the process, which is absolutely in accordance with the 3 R's principle proposed as an international ethical parameter for animal experimentation.

ACKNOWLEDGEMENTS

The authors are grateful to Fundação de Amparo a Pesquisa do Estado de São Paulo (FAPESP) for the financial support (grants: #2015/03639-8, 2016/08888-9, 2014/22689-3).

REFERENCES

1. van der Eerden BCJ, Teti A, Zambuzzi WF. Bone, a dynamic and integrating tissue. Arch. Biochem. Biophys. United States; 2014. p. 1–2.

2. Zambuzzi WF, Ferreira C V, Granjeiro JM, Aoyama H. Biological behavior of pre-osteoblasts on natural hydroxyapatite: a study of signaling molecules from attachment to differentiation. J. Biomed. Mater. Res. A. United States; 2011;97:193–200.

3. Coelho PG, Jimbo R. Osseointegration of metallic devices: current trends based on implant hardware design. Arch. Biochem. Biophys. United States; 2014;561:99–108.

4. Bezerra F, Ferreira MR, Fontes GN, da Costa Fernandes CJ, Andia DC, Cruz NC, et al. Nano hydroxyapatite-blasted titanium surface affects pre-osteoblast morphology by modulating critical intracellular pathways. Biotechnol. Bioeng. United States; 2017;

5. Pasold J, Markhoff J, Tillmann J, Krogull M, Pisowocki P, Bader R. Direct influence of titanium and zirconia particles on the morphology and functionality of mature human osteoclasts. J. Biomed. Mater. Res. A. 2017;

6. Parmigiani-Izquierdo JM, Cabaña-Muñoz ME, Merino JJ, Sánchez-Pérez A. Zirconia implants and peek restorations for the replacement of upper molars. Int. J. Implant Dent. International Journal of Implant Dentistry; 2017;3:5.

7. Hafezeqoran A, Koodaryan R. Effect of Zirconia Dental Implant Surfaces on Bone Integration: A Systematic Review and Meta-Analysis. Biomed Res. Int. 2017.

8. Gautam C, Joyner J, Gautam A, Rao J, Vajtai R. Zirconia based dental ceramics: structure, mechanical properties, biocompatibility and applications. Dalt. Trans. Royal Society of Chemistry; 2016;45:19194–215.

9. Cionca N, Hashim D, Mombelli A. Zirconia dental implants: where are we now, and where are we heading? Periodontol. 2000. 2017;73:241–58.

10. Gapski R, Martinez EF. Behavior of MC3T3-E1 Osteoblastic Cells Cultured on Titanium and Zirconia Surfaces. Implant Dent. 2017;1.

11. Mosmann T. Rapid colorimetric assay for cellular growth and survival: application to proliferation and cytotoxicity assays. J. Immunol. Methods. Netherlands; 1983;65:55–63.

12. LOWRY OH, ROSEBROUGH NJ, FARR AL, RANDALL RJ. Protein measurement with the Folin phenol reagent. J. Biol. Chem. United States; 1951;193:265–75.

13. Zambuzzi WF, Yano CL, Cavagis ADM, Peppelenbosch MP, Granjeiro JM, Ferreira C V. Ascorbate-induced osteoblast differentiation recruits distinct MMP-inhibitors: RECK and TIMP-2. Mol. Cell. Biochem. Netherlands; 2009;322:143–50.

14. Lefebvre V, Peeters-Joris C, Vaes G. Production of gelatin-degrading matrix metalloproteinases ('type IV collagenases') and inhibitors by articular chondrocytes during their dedifferentiation by serial subcultures and under stimulation by interleukin-1 and tumor necrosis factor alpha. Biochim. Biophys. Acta. Netherlands; 1991;1094:8–18.

15. Ferreira CF, Carriel Gomes MC, Filho JS, Granjeiro JM, Oliveira Simoes CM, Magini R de S. Platelet-rich plasma influence on human osteoblasts growth. Clin. Oral Implants Res. Denmark; 2005;16:456–60.

16. Josset Y, Oum'Hamed Z, Zarrinpour A, Lorenzato M, Adnet JJ, Laurent-Maquin D. In vitro reactions of human osteoblasts in culture with zirconia and alumina ceramics. J. Biomed. Mater. Res. United States; 1999;47:481–93.

17. Zambuzzi WF, Bruni-Cardoso A, Granjeiro JM, Peppelenbosch MP, de Carvalho HF, Aoyama H, et al. On the road to understanding of the osteoblast adhesion: cytoskeleton organization is rearranged by distinct signaling pathways. J. Cell. Biochem. United States; 2009;108:134–44.

18. Cavagis A, Takamori E, Granjeiro J, Oliveira R, Ferreira C, Peppelenbosch M, et al. TNFalpha contributes for attenuating both Y397FAK and Y416Src phosphorylations in osteoblasts. Oral Dis. Denmark; 2014;20:780–6.

19. Fang X-Q, Liu X-F, Yao L, Chen C-Q, Lin J-F, Gu Z-D, et al. Focal adhesion kinase regulates the phosphorylation protein tyrosine phosphatase-alpha at Tyr789 in breast cancer cells. Mol. Med. Rep. Greece; 2015;11:4303–8.

20. Thiyagarajan V, Lin S, Chia Y, Weng C. Biochimica et Biophysica Acta the autophosphorylation site of focal adhesion kinase (Y397) by molecular docking. BBA - Gen. Subj. Elsevier B.V.; 2013;1830:4091–101.

21. Dixon RDS, Chen Y, Ding F, Khare SD, Prutzman KC, Schaller MD, et al. New Insights into FAK Signaling and Localization Based on Detection of a FAT Domain Folding Intermediate University of North Carolina at Chapel Hill. 2004;12:2161–71.

22. Blangy A, Touaitahuata H, Cres G, Pawlak G. Cofilin activation during podosome belt formation in osteoclasts. PLoS One. United States; 2012;7:e45909.

23. Mitra SK, Mikolon D, Molina JE, Hsia DA, Hanson DA, Chi A, et al. Intrinsic FAK activity and Y925 phosphorylation facilitate an angiogenic switch in tumors. 2006;5969–84.

24. da Costa Fernandes CJ, do Nascimento AS, da Silva RA, Zambuzzi WF. Fibroblast contributes for osteoblastic phenotype in a MAPK-ERK and sonic hedgehog signaling-independent manner. Mol. Cell. Biochem. Netherlands; 2017;

25. Fang X, Liu X, Yao L, Chen C, Lin J, Ni P, et al. New Insights into FAK Phosphorylation Based on a FAT Domain-Defective Mutation. 2014;9:1–10.

26. Wolfenson H, Lavelin I, Geiger B. Dynamic Regulation of the Structure and

Functions of Integrin Adhesions. Dev. Cell. Elsevier Inc.; 2013;24:447–58.

27. Wehrle-Haller B, Imhof BA. The inner lives of focal adhesions. Trends Cell Biol. 2002;12:382–9.

28. Parsons JT, Horwitz AR, Schwartz MA. Cell adhesion: integrating cytoskeletal dynamics and cellular tension. Nat. Rev. Mol. Cell Biol. England; 2010;11:633–43.

29. Kueh HY, Brieher WM, Mitchison TJ. Dynamic stabilization of actin filaments. Proc. Natl. Acad. Sci. U. S. A. United States; 2008;105:16531–6.

30. Martín-Villar E, Borda-d'Agua B, Carrasco-Ramirez P, Renart J, Parsons M, Quintanilla M, et al. Podoplanin mediates ECM degradation by squamous carcinoma cells through control of invadopodia stability. Oncogene. 2015;34:4531–44.

31. Barisic S, Schmidt C, Walczak H, Kulms D. Tyrosine phosphatase inhibition triggers sustained canonical serine-dependent NFκB activation via Src-dependent blockade of PP2A. Biochem. Pharmacol. Elsevier Inc.; 2010;80:439–47.

32. Avdi NJ, Malcolm KC, Nick JA, Worthen GS. A Role for Protein Phosphatase-2A in p38 Mitogen-activated Protein Kinase-mediated Regulation of the c-Jun NH2-terminal Kinase Pathway in Human Neutrophils. J. Biol. Chem. 2002;277:40687–96.

33. Oleinik N V, Krupenko NI, Krupenko SA. ALDH1L1 inhibits cell motility via dephosphorylation of cofilin by PP1 and PP2A. Oncogene. England; 2010;29:6233–44.

34. Bertazzo S, Zambuzzi WF, Campos DDP, Ferreira C V, Bertran CA. A simple method for enhancing cell adhesion to hydroxyapatite surface. Clin. Oral Implants Res. Denmark; 2010;21:1411–3.

35. Hughes BT, Sidorova J, Swanger J, Monnat RJ, Clurman BE. Essential role for Cdk2 inhibitory phosphorylation during replication stress revealed by a human Cdk2 knockin mutation. Proc. Natl. Acad. Sci. 2013;110:8954–9.

36. Ayaydin F, Vissi E, Mészáros T, Miskolczi P, Kovács I, Fehér A, et al. Inhibition of serine/threonine-specific protein phosphatases causes premature activation of cdc2MsF kinase at G2/M transition and early mitotic microtubule organisation in alfalfa. Plant J. 2000;23:85–96.

37. Haynes DR, Hay SJ, Rogers SD, Ohta S, Howie DW, Graves SE. Regulation of bone cells by particle-activated mononuclear phagocytes. J. Bone Joint Surg. Br. England; 1997;79:988–94.

38. Panagakos FS, Kumar S. Differentiation of human osteoblastic cells in culture: modulation of proteases by extracellular matrix and tumor necrosis factor-alpha. Inflammation. United States; 1995;19:423–43.

39. Wang R, Wang W, Ao L, Wang Z, Hao X, Zhang H. Benzo[a]pyrene-7,8-diol-9,10-epoxide suppresses the migration and invasion of human extravillous trophoblast HTR-8/SVneo cells by down-regulating MMP2 through inhibition of FAK/SRC/PI3K/AKT pathway. Toxicology. Elsevier; 2017;386:72–83.

40. Dang D, Bamburg JR, Ramos DM. ??v??3 integrin and cofilin modulate K1735 melanoma cell invasion. Exp. Cell Res. 2006;312:468–77.

41. Oum'hamed Z, Garnotel R, Josset Y, Trenteseaux C, Laurent-Maquin D. Matrix metalloproteinases MMP-2, -9 and tissue inhibitors TIMP-1, -2 expression and secretion by primary human osteoblast cells in response to titanium, zirconia, and alumina ceramics. J. Biomed. Mater. Res. A. United States; 2004;68:114–22.

Capítulo 6

DISCUSSÃO

Estudos na área de biotecnologia voltada para o campo de implantes dentários têm apontado para estratégias que possam reduzir o tempo da reabilitação de pacientes que sofrem de edentulismo (Dang et al., 2016; Sohrabi et al., 2012). Neste contexto, o desenvolvimento de novas superfícies biofuncionais de titânio, e ou o desenvolvimneto de novos materiais, tem provado ser fundamental para a estimular a performance de células osteoprogenitoras e assim acelerar a neoformação óssea ao redor de dispositivos implantáveis, impactando positivamente o processo de Osseointegração (Kulkarni et al., 2015; Longo et al., 2016). Assim sendo, nosso grupo tem investigado os mecanismos de sinalização celular envolvidos nas respostas a diferentes biomateriais (Gemini-Piperni et al., 2014a; Gemini-Piperni et al., 2014b; Zambuzzi et al., 2014; Rossi et al., 2017; Bezerra et al., 2017)) com o intuito de identificar biomarcadores intracelulares relacionados a este cenário. Neste contexto, temos proposto a importância do envolvimento de Src e FAK como proteínas sinalizadoras que identificam a texturização de superfície dos substratos (Zambuzzi et al., 2009; Zambuzzi et al., 2010).

Temos discutido também que o ataque celular é um evento biológico precoce responsável pela integração de dispositivos implantáveis ao tecido ósseo. Além disto, temos considerado o recobrimento proteico sobre os implantes como um evento que ocorre previamente a chegada das células. Para enfocar este tópico temos demonstrado que diferentes texturizações de superfícies de titânio promovem respostas distintas na adsorção proteica, principalmente relacionada a rugosidade de superfície (Zambuzzi et al., 2014) e que o titânio liberado por implantes dentais aumentam a adesão pré-osteoblástica através da modulação de ROS (Rossi et al., 2017).

As propriedades físico-químicas da superfície, como a molhabilidade (avaliada através do ângulo de contato com a água) e a topografia de superfície (avaliada por microscopia de força atômica) interferem profundamente na adesão, espraiamento, proliferação e diferenciação tardia celular. Seguindo uma sequência hierárquica de eventos biológicos ao redor dos dispositivos implantáveis, a molhabilidade dá início a uma linha do tempo complexa que favorecerá ou não o reparo tecidual. A molhabilidade da superfície direciona a adsorção de proteínas, estabelecendo um recobrimento biológico e impactando na interação celular tardia. Os resultados deste estudo demonstraram que há uma diferença significativa na topografia das superfícies de titânio avaliadas e isto se refletiu na molhabilidade. Usualmente é relatado que a adesão celular requer uma hidrofilia moderada, mas a performance celular é negativamente modulada quando o material se torna muito hidrofílico.

Deve-se notar que durante a adesão de células eucarióticas, tanto FAK quanto Src são proteínas responsáveis pela modulação de mecanismos intracelulares para controlar a interação celular através da ativação de integrinas (Barkarmo et al., 2014b; Zambuzzi et al., 2014). Demonstramos recentemente que os mecanismos intracelulares através das vias de integrinas/FAK/Src promovem um rearranjo do citoesqueleto e isto parece ser decisivo para a adaptação celular sobre superfícies com diferentes rugosidades, determinando a morfologia celular. Neste trabalho foi demonstrado que o cultivo de pré-osteoblastos em superfícies de titânio com diferentes texturizações promoveram modificações profundas, aqui analisadas por microscopia eletrônica de varredura. De maneira sucinta, as micrografias eletrônicas demonstraram que os pré-osteoblastos cultivados sobre a nHA apresentaram um espraiamento precoce quando comparada a superfícies maquinadas (superfície controle). Este achado está de acordo com Gaviria et al. (2014) que propôs que superfícies rugosas produzem orientação celular e guiam sua locomoção afetando a forma e função celular. Além disto, este trabalho também validou estes resultados com o EDX co-localizando carbono e titânio. Importante observar que as mudanças morfológicas foram acompanhadas pela ativação de FAK e Src, analisada aqui por sítios de fosforilação de ambas proteínas sinalizadoras.

Assim, acreditamos que estas mudanças morfológicas durante a adaptação celular são dependentes da ativação de FAK e Src, como demonstrado previamente na

adesão de osteoblastos em superfícies de poliestireno (Zambuzzi et al., 2009). Neste ponto acreditamos que FAK e Src reconhecem as propriedades físico-químicas das superfícies e são considerados importantes biomarcadores da interação célula-superfície.

Outro ponto importante, demonstrado aqui, foi que a mecanismo de transdução de sinal que coordenam a sobrevivência celular (Ras/Raf /MEK/Erk) foi requerida em culturas de pré-osteoblastos em superfícies texturizadas de titânio por 4 horas de adesão, nos materiais avaliados.

Outro ponto importante a ser discutido foi a influência da nHA em promover a diferenciação osteoblástica pelo aumento significante de biomarcadores clássicos como a RUNX2 e a atividade da Fosfatase Alcalina quando os pré-osteoblastos cresceram diretamente nos discos de titânio. Estas características influenciam a resposta biológica a aparelhos implantáveis pela aceleração da reparo tecidual e posterior osseointegração (Dang et al., 2016; Longo et al., 2016). Em relação a biofuncionalidade da superfície nHA, a íntima mistura dos componentes do revestimento permite um processamento em temperaturas mais baixas prevenindo transições de fase indesejáveis a uma alta homogeneidade do revestimento é esperado (Gottlander et al., 1997; Meirelles et al., 2008).

Capítulo 7

CONSTATAÇÕES

Os resultados obtidos durante a execução deste projeto nos permitiram constatar que:

1. As mudanças morfológicas dos pré-osteoblastos são dependentes da texturização de superfície do titânio;
2. A sinalização da adesão dos osteoblastos é finamente modulada pela superfície modificada pela nHA;
3. A superfície de titânio com nHA promove uma sinalização anti-apoptótica;
4. Superfícies texturizadas de titânio promovem uma sinalização de sobrevivência e proliferação osteoblástica;
5. Superfícies texturizadas de titânio promovem uma diferenciação tardia de osteoblastos.
6. Biointerface entre superfícies modificadas de titânio e osteoblastos requer uma reprogramação dinâmica de genes relacionados à adesão;
7. As superfícies modificadas com titânio diferencialmente orquestram os genes relacionados à remodelação ECM;
8. Os genes relacionados à remodelação de Src e ECM são características dos efeitos diretos e indiretos das superfícies modificadas com titânio sobre o comportamento pré-osteoblastos durante o fenótipo osteogênico;
9. O meio enriquecido de CoCr afeta a adesão pré-osteoblástica pelo processamento e sinalização molecular ß1-integrina;
10. CoCr modula as vias de sobrevivência e proliferação em pré-osteoblastos;
11. CoCr modula o metabolismo dos fibroblastos garantindo a fosforilação da cofilina;Tanto o pre-Osteoblastos (pré-Ob) quanto o fibroblastos são fontes de moléculas pró-inflamatórias em resposta ao meio enriquecido com CoCr;
12. Zircônia compromete a adesão pré-osteoblástica por regulação negativa das ativações FAK e RAC1;

13. O meio enriquecido com ZrO_2 aumenta proteínas relacionadas à sinalização de sobrevivência;
14. Pré-osteoblastos são modulados por ZrO2 ativando vias que levam ao remodelamento da ECM.

Capítulo 8

CONCLUSÃO

Concluimos que o entendimento dos mecanismos intracelulares de sinalização envolvidos na adesão, proliferação e diferenciação de osteoblastos em dispositivos implantáveis odontológicos é fundamental para compreender eventos que regem biocompatibilidade e osseointegração, contribuindo para o desenvolvimento de *Smart-Materials*. Esta compreensão colabora, ainda, para uma proposta racional de metodologias alternativas, capazes de diminuir o uso de animais de experimentação, além de viabilizar, acelerando sua apresentação ao setor produtivo.

Capítulo 9

PERSPECTIVAS FUTURAS

Os resultados aqui encontrados nos encorajam a prosseguir com estudos clínicos que possam comprovar a maior efetividade da superfície de titânio texturizada pelo duplo ataque ácido térmico e recoberta com hidroxiapatita em escala nanométrica para obtenção da Osseointegração, sendo que o desenvolvimento de biomateriais ou superfícies inteligentes e específicas poderão compensar deficiências cicatriciais sistêmicas ou locais, aumentando a previsibilidade dos tratamentos odontológicos com implantes dentários.

Por se tratar de uma análise preditiva com alto grau de precisão e confiabilidade, a transdução de sinal pode aferir a resposta molecular do hospedeiro ao biomaterial implantado, através de interações positivas ou negativas sinalizadas através de fosforilações em cadeia. Este método poderá gerar um banco de dados de biomarcadores que demonstrarão em escala molecular *in vitro* a viabilidade de novas propostas de superfícies ou biomateriais, evitando ou minimizando a necessidade de realização de estudos animais em fases iniciais de desenvolvimento de produtos inovadores.

Por fim, o maior conhecimento biológico da resposta cicatricial em seus estágios iniciais, em nível molecular, poderá servir de alicerce para o desenvolvimento de novas superfícies com nano-ativadores que sejam catalisadores do processo de osseointegração.

Capítulo 10

REFERÊNCIAS BIBLIOGRÁFICAS

1. Agarwal R, García AJ. 2015. Biomaterial strategies for engineering implants for enhanced osseointegration and bone repair. *Adv Drug Deliv Rev.* Nov (1); 94: 53-62.
2. Asati V, Mahapatra DK, Bharti SK. 2016. PI3K/Akt/mTOR and Ras/Raf/MEK/ERK signaling pathways inhibitors as anticancer agents: Structural and pharmacological perspectives. Journal Article. *Eur. J. Med. Chem.* **109**:314–341.
3. Barkarmo S, Andersson M, Currie F, Kjellin P, Jimbo R, Johansson CB, Stenport V. 2014a. Enhanced bone healing around nanohydroxyapatite-coated polyetheretherketone implants: An experimental study in rabbit bone. *J. Biomater. Appl.* **29**:737–47.
4. Barkarmo S, Andersson M, Currie F, Kjellin P, Jimbo R, Johansson CB, Stenport V. 2014b. Enhanced bone healing around nanohydroxyapatite-coated polyetheretherketone implants: An experimental study in rabbit bone. Journal Article, Research Support, Non-U.S. Gov't. *J. Biomater. Appl.* **29**:737–747.
5. Bergeron JJM, Di Guglielmo GM, Dahan S, Dominguez M, Posner BI. 2016. Spatial and Temporal Regulation of Receptor Tyrosine Kinase Activation and Intracellular Signal Transduction. JOURNAL ARTICLE. *Annu. Rev. Biochem.*
6. Bertazzo S, Zambuzzi WF, Campos DDP, Ferreira C V, Bertran CA. 2010a. A simple method for enhancing cell adhesion to hydroxyapatite surface. Journal Article, Research Support, Non-U.S. Gov't. *Clin. Oral Implants Res.* **21**:1411–1413.
7. Bertazzo S, Zambuzzi WF, Campos DDP, Ogeda TL, Ferreira C V, Bertran CA. 2010b. Hydroxyapatite surface solubility and effect on cell adhesion. *Colloids Surfaces BBiointerfaces***78**:177184.http://www.sciencedirect.com/science/article/pii/S0927776510001153.
8. Bezerra F, Ferreira MR, Fontes GN, da Costa Fernandes CJ, Andia DC, Cruz NC,

da Silva RA, Zambuzzi WF. 2017. Nano-hydroxiapatite-blasted titanium surface affects pre-osteoblast morphology by modulating critical intracellular pathways. *Biotechnol Bioeng.* Aug; 114(8): 1888-1898.

9. Cavagis A, Takamori E, Granjeiro J, Oliveira R, Ferreira C, Peppelenbosch M, Zambuzzi W. 2014. TNFalpha contributes for attenuating both Y397FAK and Y416Src phosphorylations in osteoblasts. Journal Article, Research Support, Non-U.S. Gov't. *Oral Dis.* **20**:780–786.
10. Dang Y, Zhang L, Song W, Chang B, Han T, Zhang Y, Zhao L. 2016. In vivo osseointegration of Ti implants with a strontium-containing nanotubular coating. Journal Article. *Int. J. Nanomedicine* **11**:1003–1011.
11. Di Liddo R, Paganin P, Lora S, Dalzoppo D, Giraudo C, Miotto D, Tasso A, Barbon S, Artico M, Bianchi E, Parnigotto PP, Conconi MT, Grandi C. 2014. Poly-epsilon-caprolactone composite scaffolds for bone repair. Journal Article. *Int. J. Mol. Med.* **34**:1537–1546.
12. Fernandes CJC, Bezerra F, do Carmo MDD, Feltran G, Rossi MC, da Silva RA, Padilha PM, Zambuzzi WF. 2017. CoCr enriched medium modulates integrin-based downstream signaling and requires a set of inflamatory genes reprograming in vitro. *J Biomed Mater Res A*. Sep 22. doi: 10.1002/jbm.a.36244. (Epub ahead of print)
13. Fernandes GVO, Cavagis ADM, Ferreira C V, Olej B, Leao M de S, Yano CL, Peppelenbosch M, Granjeiro JM, Zambuzzi WF. 2014. Osteoblast adhesion dynamics: a possible role for ROS and LMW-PTP. Journal Article, Research Support, Non-U.S. Gov't. *J. Cell. Biochem.* **115**:1063–1069.
14. Gaviria L, Salcido JP, Guda T, Ong JL. 2014. Current trends in dental implants. Journal Article, Review. *J. Korean Assoc. Oral Maxillofac. Surg.* **40**:50–60.
15. Gemini-Piperni S, Milani R, Bertazzo S, Peppelenbosch M, Takamori ER, Granjeiro JM, Ferreira C V, Teti A, Zambuzzi W. 2014a. Kinome profiling of osteoblasts on hydroxyapatite opens new avenues on biomaterial cell signaling. Journal Article, Research Support, Non-U.S. Gov't. *Biotechnol. Bioeng.* **111**:1900–1905.
16. Gemini-Piperni S, Takamori ER, Sartoretto SC, Paiva KBS, Granjeiro JM, de Oliveira RC, Zambuzzi WF. 2014b. Cellular behavior as a dynamic field for

exploring bone bioengineering: a closer look at cell-biomaterial interface. Journal Article, Research Support, Non-U.S. Gov't, Review. *Arch. Biochem. Biophys.* **561**:88–98.

17. Gottlander M, Johansson CB, Wennerberg A, Albrektsson T, Radin S, Ducheyne P. 1997. Bone tissue reactions to an electrophor- etically applied calcium phosphate coating. *Biomaterials*. **18**:551–557.
18. Henkel J, Woodruff M, Epari D, Steck R, Glatt V, Dickinson I, Choong P, Schuetz M, Hutmacher D. 2013. Bone Regeneration Based on Tissue Engineering Conceptions – A 21st Century Perspective. *Bone Res.* **1**:216–248. http://dx.doi.org/10.4248/BR201303002.
19. Hu N, Feng C, Jiang Y, Miao Q, Liu H. 2015. Regulative Effect of Mir-205 on Osteogenic Differentiation of Bone Mesenchymal Stem Cells (BMSCs): Possible Role of SATB2/Runx2 and ERK/MAPK Pathway. Journal Article, Research Support, Non-U.S. Gov't. *Int. J. Mol. Sci.* **16**:10491–10506.
20. Jiang T, Guo L, Ni S, Zhao Y. 2015. Upregulation of cell proliferation via Shc and ERK1/2 MAPK signaling in SaOS-2 osteoblasts grown on magnesium alloy surface coating with tricalcium phosphate. Journal Article, Research Support, Non-U.S. Gov't. *J. Mater. Sci. Mater. Med.* **26**:158.
21. Jimbo R, Coelho PG, Bryington M, Baldassarri M, Tovar N, Currie F, Hayashi M, Janal MN, Andersson M, Ono D, Vandeweghe S, Wennerberg A. 2012. Nano hydroxyapatite-coated implants improve bone nanomechanical properties. Comparative Study, Journal Article, Research Support, Non-U.S. Gov't. *J. Dent. Res.* **91**:1172–1177.
22. Kulkarni M, Mazare A, Gongadze E, Perutkova \v{S}., Kralj-Igli\v{c} V, Milo\v{s}ev I, Schmuki P, Igli\v{c} A, Mozeti\v{c} M. 2015. Titanium nanostructures for biomedical applications. *Nanotechnology* **26**:62002 (1-18).
23. Kjellin P, Andersson M. 2006. SE-0401524-4, assignee. Synthetic nano-sized crystalline calcium phosphate and method of production patent SE527610.
24. Longo G, Ioannidu CA, Scotto d'Abusco A, Superti F, Misiano C, Zanoni R, Politi L, Mazzola L, Iosi F, Mura F, Scandurra R. 2016. Improving Osteoblast Response In Vitro by a Nanostructured Thin Film with Titanium Carbide and Titanium Oxides Clustered around Graphitic Carbon. Journal Article. *PLoS One*

11:e0152566.

25. Martinez EF, Ishikawa GJ, de Lemos AB, Barbosa Bezerra FJ, Sperandio M, Napimoga MH. 2017. Evaluation of a titanium surface treated with hydroxiapatite nanocrystals on osteogenic cell behavior: An in vitro study. *Int J Oral Maxillofac Implants.* Sep22. doi: 10.11607/jomi. 5887 (Epub ahead of print).
26. Meirelles L, Arvidsson A, Andersson M, Kjellin P, Albrektsson T, Wennerberg A. 2008. Nano hydroxyapatite structures influence early bone formation. *J. Biomed. Mater. Res. A*. **87**:299-307.
27. Rosa MB, Albrektsson T, Francischone CE, Filho HO, Wennerberg A. 2013. Micrometric characterization of the implant surfaces from the five largest companies in Brazil, the second largest worldwide implant market. *Int J Oral Maxillofac Implants* Mar-Apr; 28(2): 358-365,
28. Rossi MC, Bezerra FJB, Silva RA, Crulhas BP, Fernandes CJC, Nascimento AS, Pedrosa VA, Padilha P, Zambuzzi WF. 2017. Titanium-released from dental implant enhances pre-osteoblast adhesion by ROS modulating crucial intracellular pathways. *J Biomed Mater Res A*. Nove; 105 (11): 2968-2976.
29. Salou L, Hoornaert A, Stanovici J, Briand S, Louarn G, Layrolle P. 2015. Comparative bone tissue integration of nanostructured and microroughened dental implants. Journal Article, Research Support, Non-U.S. Gov't. *Nanomedicine (Lond).* **10**:741–751.
30. Sohrabi K, Mushantat A, Esfandiari S, Feine J. 2012. How successful are small-diameter implants ? A literature review.
31. Wennerberg A, Albrektsson T. Effects of titanium surface topography on bone integration: A systematic review. *Clin Oral Implants Res* 2009; 20(suppl 4): 172-184.
32. Zambuzzi WF, Fernandes GVO, Iano FG, Fernandes M da S, Granjeiro JM, Oliveira RC. 2012. Exploring anorganic bovine bone granules as osteoblast carriers for bone bioengineering: A study in rat critical-size calvarial defects. *Braz. Dent. J.* **23**:315–321.
33. Zambuzzi WF, Milani R, Teti A. 2010. Expanding the role of Src and protein-tyrosine phosphatases balance in modulating osteoblast metabolism: Lessons from mice. *Biochimie* **92**:327–332.

http://dx.doi.org/10.1016/j.biochi.2010.01.002.

34. Zambuzzi WF, Bonfante EA, Jimbo R, Hayashi M, Andersson M, Alves G, Takamori ER, Beltrao PJ, Coelho PG, Granjeiro JM. 2014. Nanometer scale titanium surface texturing are detected by signaling pathways involving transient FAK and Src activations. Journal Article, Research Support, Non-U.S. Gov't. *PLoS One* **9**:e95662.
35. Zambuzzi WF, Coelho PG, Alves GG, Granjeiro JM. 2011a. Intracellular signal transduction as a factor in the development of "smart" biomaterials for bone tissue engineering. Journal Article, Review. *Biotechnol. Bioeng.* **108**:1246–1250.
36. Zambuzzi WF, Ferreira C V, Granjeiro JM, Aoyama H. 2011b. Biological behavior of pre-osteoblasts on natural hydroxyapatite: a study of signaling molecules from attachment to differentiation. Journal Article, Research Support, Non-U.S. Gov't. *J. Biomed. Mater. Res. A* **97**:193–200.
37. Zambuzzi WF, Bruni-Cardoso A, Granjeiro JM, Peppelenbosch MP, De Carvalho HF, Aoyama H, Ferreira CV. 2009. On the road to understanding of the osteoblast adhesion: Cytoskeleton organization is rearranged by distinct signaling pathways. *J. Cell. Biochem.* **108**:134–144.